ECOLE DOCTORALE VIE-AGRO-SANTE présentée par Dynamical behaviour of the human red blood cell ionic channels

Agnieszka Dyrda

N°d'ordre
4062

ANNÉE 2009

UNIVERSITÉ DE RENNES 1

THÈSE / UNIVERSITÉ DE RENNES 1
sous le sceau de l'Université Européenne de Bretagne

pour le grade de
DOCTEUR DE L'UNIVERSITÉ DE RENNES 1
Mention : Biologie
ECOLE DOCTORALE VIE-AGRO-SANTE

présentée par

Agnieszka DYRDA

préparée dans l'unité de recherche Mer et Santé UMR 7150
Equipe Physiologie Comparée des Erythrocytes
Sciences de la Vie et de l'Environnement

Dynamical behaviour of the human red blood cell ionic channels.

Thèse soutenue à Roscoff, France
le 17. 12. 2009

devant le jury composé de:

M. Daniel THOMAS,
DR CNRS - Université Rennes 1 / *président*

M. Brian J. HARVEY,
Professeur, RCSI (Irlande) / *rapporteur*

M. Gordon LANGSLEY,
DR CNRS Institut Cochin / *rapporteur*

M. François TIAHO,
MCF, Université Rennes 1 / *examinateur*

M. Serge THOMAS,
DR, CNRS - Université Pierre et Marie Curie / *directeur de thèse*

M. Stéphane EGEE,
MCF, Université Pierre et Marie Curie / *co-directeur de thèse*

ACKNOWLEDGEMENTS.

"None of us has gotten where we are solely by pulling ourselves up from our own bootstraps.
We got here because somebody bent down and helped us."
Thurgood Marshall

First of all I am extremely grateful to Professor Małgorzata Komorowska from Wroclaw University of Technology, Poland. It is she who told me about the place on Earth called Roscoff and encouraged me to come to France without fluent command of French!

Next I would like to thanks all of people engaged in organization of Marie Curie Action in the Station Biologiqe de Roscoff. I appreciate a lot the time and energy you invested in preparation of ESTeam training programme.

Then I thanks to Doctor Serge Thomas, my supervisor. It is he who welcomed me very warmly in France as well as in the lab and led my work during this 3-year-long stay there. I will never forget his kindness, support, helpful advices and that whatever he is doing is done with the passion. I will also remember that Serge's soft spot is a cup (or two) of good coffee.
Under his supervision I heard 329 times "You will be punished for this" but none of these threats have been realized.

I would like to thank all the Doctor Virgilio Lew's team from University of Cambridge, UK for their engagement in measurement of the volume-fraction of RBC cytosol lost by Ca^{2+}-induced exovesiculation and their boss especially – for the effort put in OFC paper preparation and valuable hints about RBCs in general.

I thank Doctor Poul Bennekou and Doctor Karen Eskesen from University of Copenhagen, Denmark for valuable comments and tips which helped in better understanding of Gardos channel behaviour and electrophysiology rules.

I would like also to say thanks to my colleges from whole UMR 7150 “Mer&Santé” for their help and friendliness. In particular I am grateful to staff from “Physiologie Comparée des Erythrocytes” in general for an incredible positive atmosphere of work and in particular:

- Anne Cueff for her invaluable help in experiments. It has been a great pleasure to share the lab bench as well as the office with her.
- Guillame Bouyer and Stéphane Egée for their marvellous advises, indispensable technical support, interesting discussions and plenty, plenty, plenty, plenty, plenty of patience.
- So called Polish connection: Edyciak/Hryderyka, Cytlakowa, AniaC, AgaLi, Justyna i Grażka. Niezmiernie cieszę się dziewczyny, że skusiłyście się na przyjazd. Dzięki Wam rozłąka z Polską nie była tak dokuczliwa. Poza tym miałam z kimś wspólny język ;-) na tym krańcu świata (!), żeby pogadać, pożartować no i ponarzekać (chociażby na ....pogodę i drogie piwo w pubie)! Dziękuję Wam również za te hektogodziny spędzone przed patchem i za to, że mogłam wykorzystać Waszą prace w moim doktoracie. Uściski!!!!!! (Edyta – dzięki kochana!)
- Celine Ollivaux for your positive energy, help and nice conversations.

I am thankful to all people from SBR for your openness, help and good time I have spent with you (after work too)!

Of course I am extremely grateful for help in blood collation to the personnel of the Centre de Perharidy. I was surprised that blood donation can be painless. You have got gold hands (and patient friendly needles) there!

Chciałabym również podziękować mojej rodzinie za wsparcie. Dobrze jest mieć poczucie, że ktoś czeka, martwi się o ciebie, ale i cieszy z twoich sukcesów. Wielki ukłon w Wasza stronę kochani!

Również nie mogę pominąć i nie podziękować AdzeB, AsiJ, TomkowiW i Gosze (Matko Boska! Goha, jak poprawnie odmienia się Twoje pseudo?!) conajmniej i aż za to, że zawsze można na Was liczyć i godzinami swobodnie rozmawiać o wszystkim.

Je dois également un grand merci à tous les membres de la famille Maron. Merci pour votre hospitalité, et tous ces moments merveilleux passés à vos côtés. Je me rappelle particulièrement ces réunions familiales où se succèdent les plats traditionnels bretons, les fruits de mer, accompagnés de vins français sans oublier l'inévitable fromage. Je me suis sentie si bien en votre compagnie.

Gilles – I am extremely happy that 23rd March 2006 Darth Vader opened for me THIS bottle of beer. Thanks for your big hart and goodness and support and open mind and that I can count on you and…. for many, many other things which I cannot list here because additional 10^7 pages would be needed. Bisou!

CONTENTS.

ACKNOWLEDGMENTS. 3

ABBREVIATIONS. 13

LIST OF FIGURES. 19

LIST OF TABLES. 21

I. IN BRIEF. 23
I. 1. Aims. 23
I. 2. Summary of results. 29
I. 3. Scientific communication. 31
I. 3. 1. Publications. 31
I. 3. 2. Oral communications. 33
I. 4. IN BRIEF en Fraçais. 37
I. 5. IN BRIEF po polsku. 39

II. GENERAL CONTEXT. 41
II. 1. Oxygen. 41
II. 2. Haemoglobin. 41
II. 3. Erythrocytes. 43
II. 4. Human red blood cell. 43
II. 5. RBC membrane transporters. 45
II. 5. 1. Pumps, exchangers, cotransporters. 45
II. 5 .2. Aquaporins. 47
II. 5. 3. Ionic channels. 49
II. 5. 3. 1. Cationic channels. 49
II. 5. 3. 2. Anionic channels. 55
II. 5. 3. 3. Physiological role of ionic channels. 63

III. MATERIALS AND METHODS. 71
III. 1. Contribution of ionic channels in dehydration-elicited rehydration: lysis curves and osmotic fragility data acquisition. 71

III. 1. 1. Experimental design. 71
III. 1. 2. Solutions. 77
III. 1. 3. Preparation of red blood cells. 79
III. 1. 4. The biphasic OFC protocol. 79
III. 1. 5. Measurement of the volume-fraction of RBC cytosol lost by Ca^{2+}-induced exovesiculation*. 81
III. 1. 5. 1. Processing of vesicle samples for transmission and scanning electronmicroscopy. 83
III. 2. Electrophysiology. 85
III. 2. 1. Preparation of cells. 85
III. 2. 2. Solutions. 85
III. 2. 3. Current recordings. 87
III. 3. Chemicals. 93
III. 4. Red blood cell model. 95

IV. RESULTS. 97
IV. 1. First question: Are RBC's membrane channels involved in rehydration elicited by isosmotic dehydration? 97
IV. 1. 1. Results. 97
IV. 1. 2. Discussion. 121
IV. 2. Second question: Does membrane deformation induce channel activity? 125
IV. 2. 1. Results. 125
IV. 2. 1. 1. Evidence for spontaneous channel activity following seal formation. 129
IV. 2. 1. 2. Transient nature of recorded currents. 133
IV. 2. 1. 3. Identification of Gardos channels. 137
IV. 2. 1. 4. Simulation by mathematical RBC model. 145
IV. 2. 1. 5. Evidence for anionic channel activation. 151
IV. 2. 2. Discussion. 155
IV. 2. 2. 1. Activation of Gardos channels. 155
IV. 2. 2. 2. Activation of anionic channels. 165
IV. 2. 2. 3. Transient nature of Gardos channel activity. 167
IV. 2. 2. 4. Fast transitions. 169

* The paragraph III. 1. 5 was realized by the collaborators in: Physiological Laboratory, Department of Physiology, Development and Neuroscience, University of Cambridge, UK as well as Laser Analytics Group, Department of Chemical Engineering and Biotechnology, University of Cambridge, UK, under Dr V. L. Lew supervision.

IV. 3. Third question: What is the molecular identity of anionic channels present in RBC membrane? 171

V. GENERAL CONCLUTIONS AND PROSPECTS. 193

ANNEX #1. 203

ANNEX #2. 205

ANNEX #3. 207

ANNEX #4. 209

ANNEX #5. 213

REFERENCES. 215

ABBREVIATIONS.

2-CMNQ	2-chloromethyl-1,4-naphthoquinone
2,3-CMNQ	2,3-bis(chloromethyl)-1,4-naphthoquinone
7-CMNQ	7-chloromethyl-1,4-naphthoquinone
9-AC	9-aminocamptothecin
[X]	concentration of ion X
A	membrane area of erythrocyte
A/V	area-to-volume ratio
A23187	calcium (divalent cation) ionophore
ABC	ATP binding cassette
$\overline{A}_c$	mean area of erythrocyte membrane
ADP	adenosine 5′-diphosphate
AE1	anion exchanger, band 3 protein
AMP	adenosine 5′-monophosphate
AQP(1;3)	aquaporin, water channel (isoforms: 1 or 3)
ATP	adenosine triphosphate
C-A	cell-attached configuration of patch clamp technique
CA II	carbonic anhydrase type II
CaM	calmodulin
cAMP	cyclic adenosine 3′,5′-cyclophosphate
cDNA	complementary DNA
CFTR	cystic fibrosis transmembrane conductance regulator
CLT	clotrimazole
ChTX	charybdotoxin
CHV	critical haemolytic volume

C_{iso}	constant that defines isotonicity with plasma
ClC-2	chloride channel type 2
$\overline{d}$	mean vesicle diameter
Da	dalton
deoxy-RBC	ceoxygenated erythrocyte
DIOA	(2-n-butyl-6,7-dichloro-2-cyclopentyl-2,3-dihydro-1-oxo-1H-inden-5-yl)oxy]acetic acid
DIDS	4,4'-diiosothiocyanatostilbene-2,2'-disulfonate
DIW	deionised water
DMSO	methyl sulfoxide
DPC	1,5-diphenylcarbohydrazide
EDTA	ethylene diamine tetraacetique acid
EGTA	ethylene glycol tetraacetic acid
EIPA	5-(N-ethyl-N-isopropyl) amiloride
EM	electron microscopy
E_m	resting membrane potential
E_X	equilibrium potential for ion X
f_A	vesicle area-fraction
f_V	vesicle volume-fraction
γ	conductance of the channel
γ_X	conductance of the ion X
Hct	haematocrit
HEPES	4-(2-hydroxyethyl)-1-piperazineethanesulfonic acid
HMW-28 kDa	N-glycosylated form of 28 kDa form of aquaporin
hRBC	human erythrocyte
hSK4	Ca^{2+}-dependent K^+ channel, Gardos channel
I	current amplitude
IBMX	3-isobutyl-1-methylxantine
IK1	Ca^{2+}-sensitive K^+ channel, Gardos channel
Index:	
i	intracellular
o	extracellular
I-O	inside-out configuration of patch clamp technique
IRC	inwardly rectifying channel
KCa 3.1	Ca^{2+}-dependent K^+ channel, Gardos channel
l_{cw}	litre of cell water
l_{oc}	litter of originally packed cells
MDR	multidrug resistance associated protein, ATP-binding cassette, sub-family B, member 1B
MRP1	multidrug resistance associated protein, ATP-binding cassette, sub-family C, member 1
NS309	3-oxime-6,7-dichloro-1H-indole-2,3-dione
NS(VD)C	non-selective (voltage-dependent) cationic channel
NMDG	N-methyl-D-glucamine
NPPB	5-nitro-2-(phenylpropylamino)-benzoate
NPPs	new permeation pathways
OFC	osmotic fragility curve
O-O	outside-out configuration of patch clamp technique
ORC	outwardly rectifying channel
ORCC	outwardly rectified chloride channel
oxy-RBC	oxygenated erythrocyte
P-gp	P-glycoprotein
Panx1	pannexin 1

pCa	$-\log[Ca^{2+}]$
pCO_2	carbon dioxide partial pressure
P_{cat}	cation permeability channel
P_d	diffusional water permeability
P_f	osmotic water permeability
PGE2	prostaglandin E2
pH	$-\log[H^+]$
PIPES	1,4-piperazinediethanesulfonic acid
PKA	protein kinase A
PMCA	plasma membrane calcium pump
P_o	open probability of the channel
pO_2	oxygen partial pressure
Prefix:	
G	10^9
M	10^6
k	10^3
m	10^{-3}
µ	10^{-6}
n	10^{-9}
p	10^{-12}
Prx 2	peroxiredoxin 2
PSAC	plasmodial surface anionic channel
P_{sickle}	the electrodifutional pathway for ions which leads to cell dehydration
PTH	parathyroid hormone
P_X	permeability of ion X
P_X^G	electrodiffusional permeability for X ion
Q	osmotically active solute
RBC	red blood cell
RCM	red cell mathematical model
RPMI	the acronym of place, Roswell Park Memorial Institute, were the culture medium was developed,
RT	relative tonicity
RT_{50}	value of relative tonicity where 50% of cells are lysied
RTL	maximal pre-lytic swelling
SCC	small conductance channel
SEM	scanning electron microscopy
T	temperature in Kelvin
TEA	tetraethylammonium
TEM	transmission electron microscopy
TRAM-34	1-[(2-chlorophenyl)diphenylmethyl]-1H-pyrazole
V	volume
$\overline{V_C}$	mean erythrocyte volume
VDAC	voltage-dependent anionic channel
V_H	volume occupied by haemoglobin molecules
V_m	membrane potential
V_P	potential of pipette
VRAC	volume-regulated anionic channel
V_W	water content of the cell
W-C	whole-cell configuration of patch clamp technique

LIST OF FIGURES.

Figure II. 1.	Haematopoiesis.	62
Figure III. 1.	Osmotic fragility curve (OFC).	73
Figure III. 2.	Modes of patch clamp configurations.	89
Figure IV. 1.	Changes in osmotic fragility, spontaneous haemolysis and water content of RBCs during Ca^{2+}-induced biphasic dehydration-hydration protocol.	99
Figure IV. 2.	Effects of a sustained Ca^{2+} load on the time-dependent changes in osmotic fragility and water content of RBCs in conditions that prevent Ca^{2+}-induced dehydration.	103
Figure IV. 3.	Effects of RBC dehydration without elevated $[Ca^{2+}]_i$ on the osmotic fragility of the red cells.	105
Figure IV. 4.	Effect of the magnitude of the A23187-mediated Ca^{2+} load on osmotic fragility, spontaneous lysis and water content of the red cells as a function of time.	109
Figure IV. 5.	The participation of different ion transport systems of the RBC membrane on the osmotic fragility effects elicited by elevated $[Ca2+]_i$.	111
Figure IV. 6.	Effects of vanadate on the time-dependent changes in osmotic fragility, water content and spontaneous haemolysis of RBCs.	113
Figure IV. 7.	Effects of Na^+ substitution by choline chloride on the time-dependent changes in osmotic fragility, water content and spontaneous haemolysis of RBCs.	115
Figure IV. 8.	Ca^{2+}-induced exovesiculation.	117
Figure IV. 9.	Effects of membrane area loss by exovesiculation on the osmotic fragility of Ca^{2+}-loaded RBCs.	123
Figure IV. 10.	Evidence for spontaneous channel activity following seal formation.	131
Figure IV. 11.	Transient nature of recorded currents.	135
Figure IV. 12.	Fast transitions.	139
Figure IV. 13.	Identification of Gardos channels.	141
Figure IV. 14.	Inhibition of calcium extrusion by plasma membrane calcium pump (PMCA).	145
Figure IV. 15.	Simulation by mathematical RBC model.	149
Figure IV. 16.	Evidence for anionic channel activation (a).	153
Figure IV. 17.	Evidence for anionic channel activation (b).	157
Figure IV. 18.	Membrane transporters that participate in the observed events.	159
Figure IV. 19.	Schematic representation of the expected time course of changes in $[Ca^{2+}]_i$.	163

.

Figure IV. 20. Anionic channel activity following seal formation. 176
Figure IV. 21. Anionic channel activity in steady state. 179
Figure IV. 22. Effect of SCN^- ions. 183
Figure IV. 23. Effect of 0.5% serum. 183
Figure IV. 24. I/V plot corresponding to Fig. IV. 22 and Fig. IV. 23 pooled together. 184
Figure IV. 25. Recording of higher conductance levels (1/3). 186
Figure IV. 26. Recording of higher conductance levels (2/3). 187
Figure IV. 27. Recording of higher conductance levels (3/3). 187
Figure IV. 28. I/V plot of high conductance levels. 188
Figure IV. 29. Inhibition by 1 µM NPPB. 189

LIST OF TABLES.

Table III. 1. The composition of the solutions used in OFC experiments. 77
Table III. 2. The composition of the solutions used in patch clamp experiments. 85
Table III. 3. The list of chemical compounds used in OFCs and patch clamp experiments. 95
Annex #4. Activators and modulators of Gardos channel. 209
Annex #5. Formulation of RPMI medium 1640 213

I. IN BRIEF.

"I didn't think; I experimented."

Wilhelm Roentgen

I. 1. Aims.

Erythrocytes appear amongst the most frequently studied biological models on membrane transport (for a review see "Red cell membrane transport in health and disease" (Bernhardt and Ellory 2003)). To date, however, the number of works aimed at description of conductive pathways (channels) existing in red blood cells (RBCs), in general, remain paradoxically very limited due to technical difficulties. In particular, the fragility and small size of the mammalian RBCs makes this approach difficult. Therefore, little is known of the conductive pathways present in the human RBC membrane.

Following the invention of the "patch clamp" technique of electrophysiology allowing continuous recording of channel activity at the single level (Hamill et al. 1981), two different cation channels have been characterized, an intermediate conductance Ca^{2+}-activated K^+ channel, known as the Gardos channel (Hamill 1981; Grygorczyk et al. 1984; Grygorczyk and Schwarz 1985; Shields et al. 1985; Alvarez and Garcia-Sancho 1987; Grygorczyk 1987; Fehlau et al. 1989; Bennekou and Christophersen 1990; Christophersen 1991; Leinders et al. 1992; Leinders et al. 1992; Romero and Rojas 1992; Pellegrino and Pellegrini 1998; Pellegrino et al. 1998; Del Carlo et al. 2003), and a non-selective cation channel (Christophersen and Bennekou 1991; Bennekou 1993; Kaestner et al. 1999; Kaestner and Bernhardt 2002). Concerning anions, except an early study by Schwarz et al. (Schwarz et al. 1989) reporting small electrophysiological events most likely carried by anions, no real description of anion channel was available in the literature until recently, although there was some biochemical evidence that anion channel are probably present in the red cell membrane

(Hardy et al. 1995; Dawson et al. 1999).

The electrophysiological study of RBCs, using the patch clamp technique, has been going through a renaissance with the recent discovery of novel channel activity in the host plasma membrane of Plasmodium falciparum-infected human RBCs (Desai et al. 2000; Egee et al. 2002; Thomas and Lew 2004; Bouyer et al. 2006; Bouyer et al. 2007; Merckx et al. 2008; Merckx et al. 2009) but the questions of whether this activity is host- or parasite-derived and its molecular nature have not been resolved yet. This renaissance arose from the finding that infected RBCs have altered permeability characteristics due to the induction of new permeation pathways (NPPs), which are defined, using non-electrophysiological techniques, as having the general characteristics of anion channels (i.e. high anion permeability, linear concentration-dependence, inability to distinguish between stereo-isomers of permeant solutes), while still able to transport a range of other solutes at reduced rates (Ginsburg et al. 1983; Ginsburg 1994; Kirk 2001).

Since 1999, the team “Physiologie Comparée des Erythrocytes” have spent (75 – 85) % of its activity at describing the identity, nature, regulation and physiological role of ionic channels present in human red cell membrane in health and disease. This lab shares now the leadership in this field with a small number of other labs worldwide and 4 PhD thesis have been presented between 2000 and 2009, documenting the presence of three types of anionic channels identified in uninfected and infected RBCs: a small (~5 pS, SCC) and a medium (~15 pS, IRC) linear conductance channels induced via two modes of activation (PKA/ATP and membrane deformation) and visible in more than 80% of membrane patches and an outwardly rectifying anion channel ((75 – 85) pS at positive membrane potentials, ORC) that is present in less than 5% of cell patches (Egee et al. 2002; Decherf et al. 2004; Bouyer et al. 2006; Bouyer et al. 2007; Merckx et al. 2008; Merckx et al. 2009).

The present work follows on to these studies with the specific intention to address 1/ the physiological role played by cationic and anionic channels in cell volume regulation and 2/ their possible activation by membrane deformation and with the 3rd/ intention to bring further clues on the dynamical behavior, electrophysiological characterization and molecular identity of anionic channels. Hence, the three chapters of this document were aimed at providing answers to the three following questions:

First question:

Are RBC's membrane channels involved in rehydration elicited by isosmotic dehydration?

High throughput methodologies that measure the distribution of osmotic fragilities in red blood cell populations have enabled the investigation of dynamic changes in red cell homeostasis and membrane permeability in health and disease (Lew et al. 1995; Raftos et al. 1996; Lew et al. 2003; Lew et al. 2005; Tiffert et al. 2005). The common assumption in the interpretation of dynamic changes in osmotic fragility curves is that left or right shifts reflect a decreased or increased hydration state of the cells, respectively, allowing direct inferences on membrane transport from osmotic fragility measurements. However, the assumed correlation between shifts in osmotic fragility and hydration state has never been directly explored, and the role played by ionic channels in this process has never been clearly established even though the involvement of a cationic conductance (P_{cat}) was frequently suggested (Bookchin et al. 2000; Lew et al. 2007).

Second question:

Does membrane deformation induce channel activity?

Red blood cells possess elastic properties allowing bending and flowing through the narrowest of capillaries where they are submitted to considerable shear stress and membrane deformation (Skalak and Branemark 1969; Chien 1987; Kikuchi 1992; Discher and Mohandas 1996; Svetina et al. 2004). Whether physiological or experimental membrane deformation may trigger channel activity and particularly enhanced calcium permeability with subsequent Gardos channel activity with immediate consequences on blood viscosity remained an open

question.

Third question:

What is the molecular identity of anionic channels present in RBC membrane?

In 2000, Desai and co-workers (Desai et al. 2000) reported an inward rectifying channel in malaria infected cells, with a conductance of less than 10 pS at physiological salt concentration and with rectification due to voltage dependent gating. From then on, a number of apparently different anion channels have been reported in the human red cell membrane (Egee et al. 2002; Huber et al. 2002; Staines et al. 2003; Huber et al. 2004; Huber et al. 2005; Bouyer et al. 2006), leading to great confusion. This part of thesis work is an in-depth analysis of recordings obtained using the cell-attached and excised inside-out configurations of the patch clamp technique aimed at clarifying and explaining early confusing results and interpretations in the literature.

I. 2. Summary of results.

Contribution of ionic channels in dehydration-elicited rehydration (Question 1).

We investigated whether the correlation between osmotic fragility and cell volume holds for red cells exposed to isosmotic dehydration and whether cell volume recovery results from activation of conductive pathways. Contrary to our expectations, but very interestingly, the results showed that progressive increase in osmotic fragility following dehydration is not caused by cell hydration which remained a minimal contribution (< 8%) but rather by elevated cell calcium. Loss of membrane area by the release of (160 ± 40) nm diameter (mean ± SD) vesicles is shown to be a major contributor, but may not account for the full non-hydration component. The rest must reflect a specific calcium-induced lytic vulnerability of the membrane causing rupture before the cells attain their maximal spherical volumes.

Gardos (and anionic) channels activation induced by local membrane deformation in intact human red blood cells (Question 2).

The experiments reported here were designed to test to what extent membrane deformation of human RBC could induce channel activity. Deformation was obtained by depression of 10 mmHg applied for less than 5 s in glass microelectrode brought in contact with the intention of generating a very electrically resistive seal around the edge of the tip allowing recordings of single channel activity using the cell-attached configuration of the patch clamp technique. We present here electrophysiological evidence that Ca^{2+}-sensitive K^+ channel are transiently activated when seal formation induces membrane deformation and that this phenomenon can result only from activation of a permeability pathway with a finite Ca^{2+} conductance (P_{Ca}). This transient activity generates secondary transient anionic channel activity.

Further clues on the identity of the anion channels in human red blood cells in health and disease (Question 3).

This study demonstrates that the diversity of anionic channel activities recorded in normal human erythrocytes, as well as in P.falciparum-infected erythrocytes, corresponds to different kinetic modalities of a unique type of maxi anion channel with multiple conductance levels, gating properties and pharmacology, depending on conditions.

I. 3. Scientific communication.

I. 3. 1. Publication.

Effects of elevated intracellular calcium on the osmotic fragility of human red blood cells. Submitted to *Cell Calcium.*

Anne Cueff, Rachel Seear, Agnieszka Dyrda, Guillaume Bouyer, Stéphane Egée, Alessandro Esposito, Jeremy Skepper, Teresa Tiffert, Virgilio L. Lew and Serge L.Y. Thomas.

Contribution: SLYT and VLL conceived and designed project and experiments, contributed to their performance, analyzed data and wrote the manuscript; TT conceived and designed project and experiments, revised and edited the manuscript; AC, RS, AD, GB and SE contri-

buted to experimental design and performed experiments; AE contributed to data analysis; JS performed experiments and analysed data.

Gardos (and anionic) channels activation induced by local membrane deformation in intact human red blood cells (Blood Cells, Molecules and Diseases, in press)

Agnieszka Dyrda, Urszula Cytlak, Anna Ciuraszkiewicz, Agnieszka Lipińska, Anne Cueff, Guillaume Bouyer, Stéphane Egée, Poul Bennekou, Virgilio L. Lew and Serge L.Y. Thomas

Contribution: SLYT conceived and designed project and experiments, contributed to their performance, analyzed data and wrote the manuscript; VLL and PB contributed to data analysis, revised and edited the manuscript; AD performed the majority of experiments and analysed data; UC, AC, AL, AC performed experiments , GB and SE contributed to experimental design.

Further clues on the identity of the anion channels in human red blood cells in health and disease (Blood Cells, Molecules and Diseases, in press)

Edyta Głogowska, Agnieszka Dyrda, Anne Cueff, Guillaume Bouyer, Stéphane Egée, Poul Bennekou, Virgilio L. Lew and Serge L.Y. Thomas

Contribution: SLYT conceived and designed project and experiments, contributed to their performance, analyzed data and wrote the manuscript; VLL and PB contributed to data analysis, revised and edited the manuscript; EG and AD contributed equally to the majority of experiments and analysed data; AC, GB and SE performed experiments and contributed to experimental design.

I. 3. 2. Oral communication.

As a speaker:

► XVII meeting of European Association for Red Cell Research in Truggio, Italy (23 – 27 April 2009). ‘Gardos and anionic channels activation induced by local membrane deformation in intact human red blood cells’.

► XVI meeting of European Association for Red Cell Research in Oxford, United Kingdom (15 – 20 March 2007). ‘Activation of channels by near infrared radiation in human erythrocytes’.

As a contributor:

► Red Cell Club Meeting, American Society for Hematology, New-Haven Yale, USA (16 – 17 October 2009). ‘Further clues on the identity and dynamical behaviour of ionic channels in human red blood cell’. (SLY. Thomas)

► BioMalPar annual meeting, EMBL Heidelberg, Germany (May 18 – 20 2009). ‘Further clues on the identity of the permeation pathway activated in Plasmodium falciparum-infected erythrocytes’. (SLY. Thomas)

► XVII meeting of European Association for Red Cell Research in Truggio, Italy (23 – 27 April 2009). Analysis of the relation between water content and osmotic fragility of human red blood cells. (SLY. Thomas)

I. 4. IN BRIEF en Français.

« Etude du comportement dynamique des canaux ioniques de la membrane du globule rouge humain. »

Les globules rouges ont toujours été l'un des modèles biologiques les plus utilisés en recherche, en particulier pour l'étude des transporteurs membranaires. La membrane de l'érythrocyte contient de nombreux systèmes de transport qui ont, pour la plupart, été caractérisés sur le plan fonctionnel et dont la cinétique et la pharmacologie est parfaitement décrite. Alors donc qu'il y a pléthore de publications scientifiques sur les protéines de transport du globule rouge humain, il n'existe que très peu d'informations sur ses canaux ioniques membranaires. Ceci tient à la très petite taille et à la grande déformabilité de ce type cellulaire. La plupart des données disponibles sur les mouvements ioniques transmembranaires des globules rouges ont été obtenues par des mesures de flux isotopiques, de lyse osmotique, de fluorescence ou d'analyse d'ions, seules méthodes pratiquées jusqu'aux années 80, époque à laquelle est apparue la technique du «patch clamp» qui permet l'enregistrement des courants unitaires résultant du passage des ions au travers des canaux ioniques (Hamill et al. 1981). Cette invention rendait possible la caractérisation directe des canaux présents dans les membranes des globules rouges. Les premiers travaux ont permis la description du « Gardos channel » des globules rouges humains, canal potassique activé par le calcium intracellulaire (Hamill 1981; Grygorczyk and Schwarz 1983). Ils ont été suivis de quelques études démontrant l'existence d'un canal cationique non sélectif (Christophersen and Bennekou 1991; Bennekou 1993; Kaestner et al. 1999; Huber et al. 2001; Duranton et al. 2002; Kaestner et al. 2004). Malgré ces quelques approches électrophysiologiques, le rôle de ces canaux n'a jamais pu être clairement défini et l'activité dans ce domaine a rapidement décliné (une trentaine de publications, tous modèles confondus, parues en 20 ans, une douzaine seulement sur les globules rouges humains). Aucune information substantielle n'était disponible jusqu'en 2000 sur la présence éventuelle de canaux anioniques dans la membrane du globule rouge humain. Seule une étude électrophysiologique sommaire menée par Schwartz et collaborateurs

(Schwarz et al. 1989) présentait des enregistrements qui en suggéraient l'existence, tandis que plusieurs approches biochimiques en renforçaient l'idée. Ces indications étaient particulièrement importantes dans le cas du paludisme (malaria) et de l'anémie falciforme (drépanocytose) où des études non électrophysiologiques (flux isotopiques et hémolyse) indiquaient que des canaux anioniques étaient impliqués dans le transport accru de divers substrats au travers de la membrane du globule rouge. Depuis 1999 les difficultés techniques du patch clamp des globules rouges humains ont été surmontées et l'équipe de « Physiologie comparée des érythrocytes » de la Station Biologique de Roscoff consacre 75 à 80% de son activité à la description et à l'étude du rôle physiologique des canaux de la membrane; elle figure actuellement parmi les 3 ou 4 équipes qui, au niveau mondial, animent la recherche dans ce domaine. Des canaux anioniques insoupçonnés jusqu'à présent dans la membrane du globule rouge humain ont pu être mis en évidence. Ces canaux sont peu actifs dans la membrane du globule rouge non stimulé et non déformé et leur rôle physiologique reste à déterminer. Ils sont par contre très actifs après l'invasion de la cellule par le parasite de la malaria (Plasmodium falciparum). Ces travaux ont fait l'objet entre 2000 et 2009 de quatre thèses qui font apparaître une grande diversité des conductances et des cinétiques selon les conditions expérimentales.

I. 5. IN BRIEF po polsku.

”Dynamiczne zachowanie kanałów jonowych w błonie czerwonych komórek krwi”.

Czerwone komórki krwi (RBC) od dawna służą badaczom za model i punkt odniesienia dla zrozumienia procesów zachodzących w bardziej złożonych komórkach. Jednakże dotychczas co najmniej dwa z ogólnie przyjętych założeń nie zostały sprawdzone. Mianowicie, że:

1) hemoliza czerwonych komórek krwi jest ściśle związana z ich stanem hydratacyjnym;

2) w zdrowych, nie wystawionych na działanie bodźców zewnętrznych krwinkach, kanały jonowe są nieaktywne. W niniejszej pracy zrewidowano oba te poglądy.

W pierwszej części pracy zbadano zmiany w oporności osmotycznej krwinek w czasie. Równocześnie z krzywą hemolizy monitorowano ilość wewnątrzkomórkowej wody. Analiza wyników pozwoliła skorygować powszechnie panującą opinię – w warunkach, gdy stężenie jonów wapniowych w erytrocytach przewyższa stężenie fizjologiczne, obserwowane zwiększenie odporności osmotycznej krwinek wynika z 1) zmniejszenia objętości komórki (w wyniku exovesiculation), 2) ze zmian właściwości błony/cytoszkieletu, 3) lub jest suma obu powyższych czynników, nie jest natomiast skutkiem pęcznienia krwinek (nie stwierdzono wpływu wody). Ponieważ istnieje kilka sposobów aktywacji kanałów Gardosa (w tym przypadku wybrano jonofor A23187), rodzi się pytanie czy w pozostałych przypadkach otrzymane wyniki potwierdzą te zamieszczone w niniejszej pracy.

W drugiej części pracy studiowano na ile deformacja błony, mająca miejsce przy formowaniu ‘seala’ w technice patch clampu, jest w stanie aktywować kanały jonowe. Z danych eksperymentalych wynika, że w wyniku deformacji błony czerwonej komórki krwi następuje aktywacja kanałów potasowych wapniowo-zależnych. Stąd, wniosek pośredni – wpływ jonów wapniowych ma miejsce za pośrednictwem kanałów (mechanozależnych bądź nieselektywnych kationowych). Dalsze doświadczenia dały dowody na towarzyszący wypływowi jonów potasowych wpływ anionów. Obserwowany efekt jest czasowo zależny (we

wszystkich studiowanych przypadkach zanikał po ok. 20 min.), co zostało zinterpretowane jako ustalenie sie nowego, bądź jako powrót do wyjściowego stanu homeostazy.

Trzecia cześć pracy jest kontynuacją części drugiej. W niej uwaga została skupiona na kanałach anionowych towarzyszących efektowi Gardosa. Analiza wyników pozwoliła wyodrębnić co najmniej trzy konduktancje należące do kanałów anionowych: małą, średnią i dużą. Oznaczałoby to iż trzy różne kanały chlorowe biorą udział w opisywanym efekcie. Jednakże na podstawie analizy przeprowadzonej przez Poula Bennekou podejrzewa się, iż mamy do czynienia z aktywacją nie kilku, ale jednego typu kanału anionowego o różnych podstanach. Dalsze badania są niezbędne, aby potwierdzić tę możliwość.

II. GENERAL CONTEXT.

"The life of a creature is in the blood".

Leviticus 17:11

II. 1. Oxygen....

Unlike plants, animals are unable to use inorganic matter to build organic compounds. Instead, most of them find energy through the oxidation of organic substrates which they obtain by eating plants or other animals. When Lavoisier and Laplace claimed in 1780 that "Life is combustion", they simply characterized respiration as consumption of oxygen (O_2) and production of carbon dioxide (CO_2) with liberation of heat. However, in contrast to combustion of a piece of charcoal which produces carbon dioxide by oxygen binding to carbon, in the process of animal respiration oxygen does not bind to carbon to produce carbon dioxide. Rather, in intracellular energy-yielding reactions, the oxidation of organic compounds liberates electrons and oxygen supplied by respiration is used as an acceptor of this electrons, oxygen fixes them in parallel with formation of the usual end-products of oxidation of organic substrates in animals: carbon dioxide and water.

II. 2. ....haemoglobin....

In unicellular organisms and many small metazoa, oxygen is transferred exclusively in solution, but in most complex metazoa oxygen fixing pigments are necessary vehicles for transferring these molecules by diffusion or by convection through various structures and compartments between the ambient media, air or water, to the cells. Oxygen-fixing pigments have a very long evolutionary history (for a review, see (Scott 1966; Glomski and Tamburlin 1989; Glomski and Tamburlin 1990). Among them, haemoglobin (Hb) molecules appeared more than 1000 million years ago and have become established as

the dominant universal respiratory pigment of vertebrates. In this metalloprotein, the haeme moiety of the molecule can be considered evolutionary stable and is responsible for the reversible binding of oxygen, while the globin moiety is structurally variable and, through this variability, determines the conditions under which oxygen binding and release can be favoured. Hb molecules are therefore specifically adapted for species and for environmental or temporal requisites.

II. 3. ....erythrocytes....

In vertebrates, Hb molecules are enclosed in circulating erythrocytes which offer the important advantage to separate the chemical intraerythrocytic environment from the plasma and then a better control of factors affecting oxygen binding and release such as organic phosphates and inorganic ions. RBCs have then evolved to optimize two functions: (1) the transport of oxygen from lungs or gills to tissues, and (2) removal of waste such as carbon dioxide. This job is done by two specialized molecular machines: Hb and an anion exchange carrier (AE1) in the RBC membrane. RBCs from most species are richly endowed with these two components (Annex #1). All the other components are geared to maintain the constancy of volume and elastic properties that allow RBCs to bend and flow through the narrowest of capillaries (Annex #2 and #3).

II. 4. ....human red blood cell....

Human erythrocytes are the most abundant morphotic element of blood. One microliter of this tissue contains (4 – 6) x 10^6 RBCs. Human RBCs are small (~8 µm in diameter and ~2 µm in thickness which gives ~90 fl of cell volume) and biconcave in form. This characteristic shape is a consequence of cell maturation. In this process, the nucleus is extruded, mitochondria, endoplasmic reticulum, ribosomes, Golgi apparatus and lysosomes are degraded. Thus circulating human RBCs are devoid of intracellular organelles. This increases both capacity of transported O_2, because there is more space for Hb molecules and the area-to-volume ratio (A/V), which is ~40% higher if compared to a sphere of the same diameter. There are ~270 millions of Hb molecules in one RBC,

which is equal to 340g/l_{oc} or 5 mM of this metalloprotein.

II. 5. ....RBC membrane transporters....

As a consequence of haemoglobin encapsulation, the transport of O_2 and CO_2 within the blood is intricately related to the electrolytes and acid-base status of the RBCs, which are themselves strongly dependent on the permeability properties of the membrane. Indeed, whereas O_2 and CO_2 are able to cross the cell membranes by solubility/diffusion processes according to their gradients of partial pressure, the organic and inorganic substances influencing the electrolytes and acid-base status diffuse very slowly across the lipid bilayer of the membrane and therefore must follow specific pathways. There are eventually a limited number of means by which solutes move across the RBC membrane and thus influence the gaseous exchanges. This work focuses on electrodiffusional ionic movements through RBC membrane exclusively and is aimed to underline the main characteristics of conductive pathways in human RBC and to address some of the more controversial and poorly understood aspects of their regulation and physiological role. These aspects are considered in the double standpoint i/ of the implication of ionic movements in upholding the electrolytic and acid-base steady-state corresponding to intracellular homeostasis, and ii/ of their participation in the processes of regulation activated as soon as this steady-state is disrupted.

II. 5. 1. ....pumps, exchangers, cotransporters....

Among the different types of ion transports known in animal cells, those documented up to now in RBCs result from the activity of transporters belonging to two major families: 1/ the primary active and energy consuming Na^+/K^+ ATPase and Ca^{2+} ATPase and 2/ the secondary active transporters, labelled as exchangers (or antiports) and cotransports (or symports) according to the relative direction of the solutes. The Na^+/K^+ ATPase is an electrogenic pump whilst the transport processes of the second family (Na^+/H^+ exchanger, Cl^-/HCO_3^- exchanger and K^+-Cl^- cotransporter) are electrically silent. Most of the above ion pathways have been observed in all vertebrates with few exceptions

and are shared by both anucleated and nucleated RBCs. However, many other ion pathways exist and have been described in many vertebrates, particularly ionic channels are present in human, avian, batracian and fish RBCs (Thomas and Egee 1998; Shindo et al. 2000; Lapaix et al. 2002; Hamill 2006; Lapaix et al. 2008).

II. 5. 2. ....aquaporins....

In RBCs water exchange is ~4 ms what is equal to diffusional water permeability (P_d) 4 x 10^{-3} cm/s. But the ratio of osmotic (P_f) to diffusional water permeability is P_f:P_d = 6. "The discovery of aquaporin water channels (AQP) in the early 1990s (Denker et al. 1988; Smith and Agre 1991) has, to a great extent, solved the paradoxes surrounding water permeability in a variety of eukaryotic cell types. AQP1, the first water channel to be identified at the molecular level from RBCs, is 28 kDa protein. It was shown that it is an integral membrane protein and present in erythrocytes at a high copy number (typically (12000 – 160000) copies/cell). Furthermore two forms of the protein, 28 kDa and (35 – 60) kDa (HMW-28 kDa) were detected and this second one was shown to be an N-glycosylated form of 28 kDa.

Erythrocytes express at least two isoforms of AQP, namely 1 and 3. Of these, AQP1 is by far most abundant. AQP3 is resistant to the action of mercurial agents and this, therefore, explains the small mercury-insensitive component of erythrocyte water permeability. Although AQP3 demonstrates a high permeability to glycerol and urea, it must, however, be remembered that specific, facilitative urea transporters exist in erythrocyte membranes which also contribute to the high urea permeability of this cell type.

Opinions vary as to why RBCs require such a high permeability to water. First – cirucalting RBCs encounter region of higher than 1 M osmolality (the renal medulla area). So the rapid unload and load water is desired. Second – recent studies demonstrated that AQP1, in common with certain other water channels, is additionally permeable to CO_2. But individuals lacking AQP1 expression (Colton group-null individuals) demonstrate no clinical abnormalities and no significant erythrocytes abnormality, apart

from a significantly reduced osmotic water permeability (~80%) nor are significant changes in CO_2 gas transport noticeable. So the physiological role of AQP is not clear." (Browning and Wilkins 2003).

II. 5. 3. ....ionic channels....

The information available when this work was undertaken on ion movements in human RBCs were provided mostly by tracer flux studies and were therefore limited for giving molecular details on the nature of the ion pathways. The technique of extracellular patch clamp has little been used in human RBCs, even though the pioneer works of (Hamill 1981) have shown that its high temporal and spatial resolution provide a unique opportunity to extend the knowledge of RBC permeabilities to the molecular level. The patch clamp electrophysiological technique represents the best method available to investigate channel-mediated transport of charged solutes through the red cell membrane. By measuring the electrical current across a membrane (produced by the charged solutes) in relation to a known applied potential difference, it is possible to obtain a detailed characterisation of ion transporting channels at both cellular and single level. However, until recently, electrophysiological studies on human RBCs have been difficult due to the fragility and small size of the cells, and little is known of the anionic conductive pathways present in the RBC membrane in health and disease. The work on human red cell is in marked contrast to early studies on nucleated, e.g. amphibian (Hamill 1983) and more recently fish (Egee et al. 1998; Lapaix et al. 2002) and avian (Drew et al. 2002; Lapaix et al. 2008) red cells where patch clamping proved easy and productive. The difference was attributed to the size of these cells.

II. 5. 3. 1. ....cationic channels....

During the past two decades, electrophysiological studies on human RBCs revealed two different cationic channels: an intermediate conductance Ca^{2+}-activated K^+ channel, known as the Gardos channel from the name of this Hungarian scientist who first showed that metabolic depletion/arrest induces K^+ efflux when Ca^{2+} ions are present in the extra-

cellular medium (Gardos 1958), and a non-selective cationic (NSC) channel. Many attempts have been made to characterise Ca^{2+}-gated K^+ channels in human erythrocytes. It has been shown that metabolic depletion (Gardos 1958) is not the only activator of Gardos channels. Many others activators as well as modulators have been reported to impact this conductive pathway (Annex #4). Having various modes of action, these compounds alter the hIK1 channels directly or indirectly. The action of three compounds should be underlined: clotrimazole (CLT), charibdotoxin (ChTX) and apamine. The two first, CLT and ChTX, are potent Gardos channel inhibitors whereas apamine is not. Because of this pharmacological characteristic, intermediate Ca^{2+}-dependent K^+ channels can be distinguished form small Ca^{2+}-gated K^+ channels. Based on patch clamp measurements, mainly in excised I-O configuration, Gardos channel has been classified as a highly-K^+ selective, inwardly rectified, voltage-independent (Tharp and Bowles 2009), with a conductance of ~20 pS. To activate this channel, requirement of one (Leinders et al. 1992) or two (Grygorczyk and Schwarz 1983; Schwarz and Passow 1983; Grygorczyk and Schwarz 1985) Ca^{2+} ions have been reported. But it should be kept in mind that Ca^{2+} ions do not interact with the channels' protein directly but through camodulin (CaM). CaM is a small (~16 kDa), acidic protein possessing high affinity motifs for Ca^{2+} binding. In Gardos channels CaM is prebound to the cytoplasmic C-tail of the channel and mediates Ca^{2+}-dependent gating of these channels. As Fanger and co-workers demonstrated, four calmodulin molecules are associated with the channel and Ca^{2+} ions must be bound to all four CaM proteins to induced conformational changes for the channel to open (Fanger et al. 1999). Thus, not 1 or 2 but 4 Ca^{2+} ions are required to activate KCa 3.1. As shown by Stampe and Vestergaard-Bogind (Stampe and Vestergaard-Bogind 1985), the KCa 3.1 sensitivity to intracellular ionized Ca^{2+} changes with the intracellular pH (pH_i) variation. In their experimental conditions half-maximal K^+ efflux was observed at pH_i 6.1. However, this pH_i value was shifted to higher pH_i at lower ionized Ca^{2+} concentration (Stampe and Vestergaard-Bogind 1985). Furthermore Gardos channel's open probability (P_o) seems to be dependent on tempe-

rature (increases with temperature reduction) (Grygorczyk 1987) and $[Ca^{2+}]_i$ (increasing with $[Ca^{2+}]_i$ increase) (Leinders et al. 1992) but P_o is membrane potential-independent (Leinders et al. 1992). For interpretation of recordings presented in the results section, it is important to keep in mind that in most cases extinction of Gardos channel activity is manifested by P_o decline rather than by current amplitude reduction (exception – inhibition by TEA) (Dunn 1998). According to different authors the number of channels per red cell have been estimated to be ~10 copies/RBC (Grygorczyk and Schwarz 1983), 55 copies/RBC (Grygorczyk et al. 1984) or, more recently, (100 – 200) copies/RBC (Lew et al. 1982; Alvarez and Garcia-Sancho 1987).

Although increased intracellular Ca^{2+} is necessary in Gardos channel mediated K^+ efflux, Romero and co-workers have suggested that the channel behaviour remains under complex metabolic control (Romero and Rojas 1992). This additional control presumably would involve cAMP-mediated and non-mediated mechanisms, and among them direct ATP–channel interactions and/or phosphorylation of the channel proteins. Also recent studies of Tharp and colleges, which are based on analysis of the KCa 3.1 sequence, pointed on phosphorylation of C-terminus of the channel's protein as an activator of K^+ movement across the membrane (Tharp and Bowles 2009). However, the results of Pellegrino and Pellegrini studies (Pellegrino and Pellegrini 1998) are in opposition to above mentioned statement. Using patch clamp technique in I-O configuration it has been demonstrated that in contrast to Romero's work, Gardos channel is up-regulated by endogenous PKA. The enhancement of channel activity by cAMP stimulation was also found. In spite of these discrepancies, both groups hypothesised the presence of two types of Ca^{2+}-dependent K^+ channels in human erythrocytes. According to Low and co-workers, peroxiredoxin 2 (Prx2), a part of intracellular erythrocyte's antioxidant system, modulates the Gardos channel activity (Low et al. 2008).

In addition to the Gardos channel a Ca^{2+}-insensitive, voltage-dependent non-selective cation (NSVDC) channel was reported by Christophersen and Bennekou

(Christophersen and Bennekou 1991). Its conductance and kinetics were very distinct from those of Gardos channel (experiments in I-O, 500 mM salts concentration). Further experiments revealed that this channel is activated by acetylcholine receptor agonists (acetylcholine, carbachol and nicotine). Thus it can be characterized as an acectylcholine receptor channel of nicotinic type (Bennekou 1993) activated at depolarized membrane potential. The group of Bernhard, on the other hand, has shown that NSC channel is activated by strong depolarisation when e.g. cells are suspended in low-chloride medium or by prostaglandine PGE2 (Kaestner et al. 1999; Kaestner and Bernhardt 2002; Kaestner et al. 2004). Rodrighiero and co-workers in whole-cell experiments has found that Cl^- ions can exert a modulatory effect on NSC channel (Rodighiero et al. 2004). Finally it was agreed that existing discrepancies in channel gating were due to different experimental conditions and could be explained by the channels' prehistory (hysteresis of open probability of the channel). All these results let to conclude that NSC channel is permeable to mono- and divalent cations. Its conductance is ~20 pS and can be inhibited by amiloride, gadolinium and EIPA (Huber et al. 2001; Duranton et al. 2002; Lang et al. 2003).

II. 5. 3. 2. ....anionic channels....

During the same period of time, there have been few electrophysiological reports detailing anionic channels in human RBCs. Several tracer flux studies reported biophysical and biochemical evidence that anionic channels, corresponding to a permeability rate of ~10^{-7} cm/s, are present in the red cell membrane and account for 10^{-4} to 10^{-6} of the total Cl^- exchange. The present day picture of the human red cell chloride transport started emerging 50 years ago, when Tosteson (1960) raised the possibility that the chloride translocation across the red cell membrane could be a mediated process contrary to free electrodiffusion (Tosteson and Hoffman 1960).

The experimental tools at hand at the time were isolated red cells in suspension with measurements of fluxes, either as net fluxes or radiotracer fluxes, whereas determination

of the red cell membrane potential was out of reach. However, it was generally agreed that the red cell membrane was relatively impermeable to cations compared to anions, and consequently the membrane potential was identical to the Nernst potential for chloride, about -10 to -12 mV. This assumption was subsequently confirmed by direct measurements on Amphiuma cells with microelectrodes and with the fluorescence technique (Hoffman and Laris 1974) on both Amphiuma and human red cells. With the availability of compounds such as gramicidin and valinomycin, which selectively increase the cation permeability of the red cell membrane, Harris and Presman (1967) and Scarpa and co-workers (1970) showed that the net salt efflux from the red cells could be anion restricted, which lead to the concept of the two-components of the anion transport: a large exchange component and a much smaller electrogenic component (Harris and Pressman 1967; Scarpa et al. 1970).

Furthermore, using radiolabelled covalent inhibitors, a 100 kDa membrane protein was identified as the pathway for anion transport (Cabantchik and Rothstein 1972) and it was inferred that both components were mediated by the same protein, called band 3 (or AE1, or nowadays SLC4A1), based on the concomitant inhibition of total and net flux. Hunter in 1971 estimated the net permeability to be 4 orders of magnitude less than the tracer permeability, strongly suggesting the exchange concept, and in 1976 came up with an estimate of the human red cell conductance of about 10 µS/cm² (Hunter 1971; Hunter 1977). With an independent technique, membrane potential dependent fluorescence to determine the membrane potential, and with the electrogenic fraction of the Na^+-K^+-pump flux, Hoffman and co-workers arrived at a similar value (Hoffman and Laris 1974).

In spite of the differences between exchange and conductance it is commonly assumed that band 3 mediates both exchange and conductance (Wolosin et al. 1977; Alper et al. 2008). Originally it was proposed that the net flux could arise as a slippage in the exchange mechanism (Lassen et al. 1974). An alternative was tunnelling as proposed by

Knauf and Law (1983) and Frölich (1983); a channel-like mechanism where the anion is translocated without significant conformational changes of the protein (Fröhlich et al. 1983; Knauf et al. 1983).

In spite of the knowledge of the genome, the mechanism of the assumed conductive pathway has not yet been identified. Band 3 has been cloned, and successfully expressed in oocytes with regard to exchange, but only in the case of trout band 3 has concomitant conductance been observed. This could however be due to insufficient expression (Alper 2009).

How important is the AE1-mediated conductance for the well being of the red cell? Probably it is not very important. In vivo experiments have shown that even a rather high degree of reduction in the capacity of anion transport has no apparent adverse effect on mice (Bennekou et al. 2001). But lack of band 3 gives rise to severe conditions (Southgate et al. 1996; Ribeiro et al. 2000), pointing to the importance of structural disorders, leading to profound changes in the homeostasis of red cell.

Assuming band 3 to be channel-like, the prospects of ever observing channel behaviour is probably not very good. If, as seems probable, the major red cell conductance is divided between 1.000.000 copies of band 3, the unit conductance must be very small, or if gated, the mean open time very short. This leads to the question of anion channels proper in the red cell membrane.

Although patch clamp have been around for a good many years, until 2000 the only report of red cell anion channels came in 1983 from Schwarz and Passow reporting a 10 pS anion channel in normal cells (Schwarz and Passow 1983). Another study by Schwarz and co-workers reported small electrophysiological events, which were almost certainly due to anion transport (Schwarz et al. 1989).

Then in 2000, Desai and co-workers reported an inward rectifying channel in malaria infected cells, with a conductance of less than 10 pS at physiological salt concentration and with rectification due to voltage dependent gating (Desai et al. 2000). Since channels were not observed in control cells, it was assumed that the channel originated from the parasite, and was termed plasmodial surface anion channel or PSAC.

From then on, a number of apparently different anion channels have been reported in the human red cell membrane, apart from the PSAC a ClC-2 channel which has been shown to be activable in normal cells by oxidation (Duranton et al. 2002; Huber et al. 2004), and a small conductance channel, the SCC (Bouyer et al. 2006). However, there are indications that the PSAC, ClC-2 and SCC seem to be different names for the same channel under varied conditions (Bouyer et al. 2007). Furthermore, a 15 pS inward rectifying channel (IRC), with linear single channel conductance and an 80 pS outward rectifying channel (ORC) was shown to be present in malaria infected cells (Bouyer et al. 2006) as well as in cystic fibrosis cells (Decherf et al. 2007). With regard to the 15 pS IRC malaria induced channel, it was observed that activation required the presence of the normal CFTR, but that the characteristics of the induced channel differed from the CFTR channel, and it was proposed that the CFTR might have a regulatory function only. All of these channels have been reported to be present in control cells too.

What does this entire means? It has been noted that in normal cells channel activity is negligible, which is in accord with the estimates of the whole-cell conductance in normal un-stimulated cells of about 70 pS, and the calculated (40 – 50) pS from the suspension experiments. Although not finally settled, it seems probable that the observed channels originate in the red cell membrane. These channels can be activated experimentally, and become so under pathological conditions, but under normal experimental conditions they are dormant. Furthermore it should be noted that varied activation schemes can give rise to varied gating patterns.

Figure II. 1.

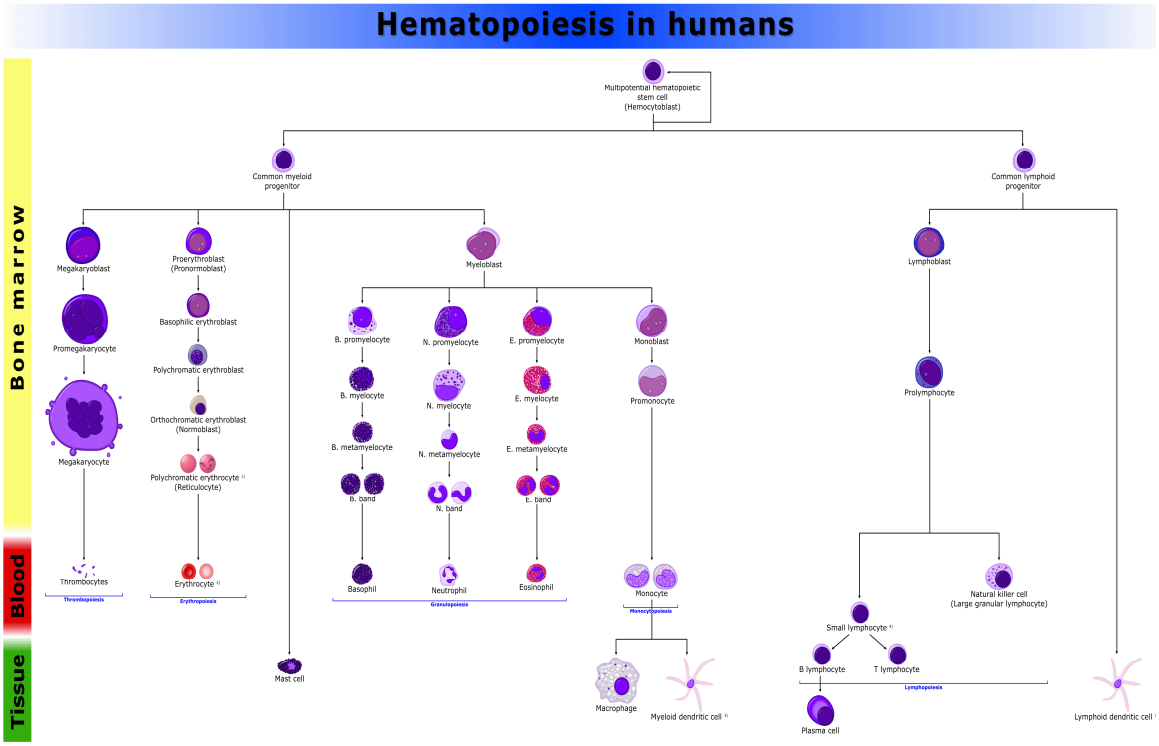

Figure II. 1. Haematopoiesis. "All blood cells are derivatives of haematopoietic stem cells. These cells differentiate and proliferate, forming different cell types that perform specialized functions. During this process, the pluripotent nature of stem cells is gradually restricted to a particular cell fate. Each blood cell lineage proliferates in a particular cytokine environment and different transcription factors regulate the lineage program." http://en.wikipedia.org/wiki/Erythropoiesis; (Kohn et al. 2006)

The enigma is then: Are patch clamp experiments on single cells or fragments of membrane representative for the red cell? The observed channels seem to be inactive in the 'resting cell', but can potentially give a very high single cell conductance, up to 50 to 100 times the normal conductance, when activated by phosphorylation, mechanical stress and so on. What is their molecular identity? What is their physiological role? One aim of this work was analyse in-depth recordings obtained using the cell-attached and excised inside-out configurations of the patch clamp technique in order to clarify and explain early confusing results and interpretations in the literature.

II. 5. 3. 3. ....physiological role of ionic channels....

When activated, Gardos channels mediated K^+ efflux decreases osmotic content of the cell and the cell shrink. This indicates that K^+ ions carry with them an equivalent amount of Cl^- and osmotically obligated water. The physiological role of Gardos channel is not defined yet. It has been suggested that Ca^{2+}-dependent K^+ efflux is one of the symptoms of eryptosis♣ (Romero and Rojas 1992; Lang et al. 2005) and/or can participate in blood clot formation (Kaestner and Bernhardt 2002) and/or plays a role in early erythroid♦ development (Maher and Kuchel 2003) (treatment of culture of human CD34-/CD28+ stem cells with clotrimazole inhibits proliferation and retards differentiation of the cells to maturity) and/or participates in plasma K^+ buffering concentration (RBCs at their normal Hct are large reservoir of K^+) (Hamill 1983).

♣ "To distinguish the death of erythrocytes from apoptosis of nucleated cells, we do suggest the term <**eryptosis**>". Lang, K., P. Lang, et al. (2005). "Mechanisms of suicidal erythrocyte death." Cell Physiol Biochem **15**(5): 195-202.

♦ "Hematopoiesis is the process by which the blood cells are generated. Hematopoiesis starts with hematopoietic stem cells (HSC), which are pluripotent, in that they are the common ancestor to every type of blood cell. There is massive cellular proliferation and division accompanied by differentiation as each HSC ultimately gives rise to billions of RBC, WBC and platelets.
HSC proliferate and undergo differentiation through a series of progenitor cells, which are progressively more limited in the types of cell they can form until the mature blood cell types are produced.
Cells of the first stage of differentiation from pluripotent HSC are multilineage progenitor cells that can give rise to a subset of different blood cell types. Multipotent progenitor cells have more restricted developmental potential than do HSC, in that they can give rise only to lymphoid cells (common lymphoid progenitors) or only to myeloid and **erythroid cells** and platelets (common myeloid progenitors)." Kohn, D., J. Nolta, et al. (2006). Hematopoietic stem cells. Encyclopedia of Life Science, John Wiley & Sons, Ltd: Chichester. See also Fig. II. 1.

Its presence is also manifested in haemoglobinopathies like sickle cells♥ diseases and hereditary spherocytosis♠. For the latter, it is hypothesised that Gardos effect plays an important protective role by compensating reduced A/V ratio and reduces haemolysis in erythrocytes with cytoskeletal impairments. On the other hand in whole-cell patch clamp configuration as well as in ghosts no Gardos channel activity could be registered (Hamill 1983; Schwarz and Passow 1983). Moreover no mutations with absent or reduced activity in KCa 3.1 channel have been reported in either human red cells or cells from other mammalian species which express Ca^{2+}-dependent potassium channel (Tiffert et al. 2001). In conclusion: to-date, there is no physiological role clearly demonstrated for the Gardos channel but its possible involvement in shear stress has been frequently assumed. Indeed, RBCs possess elastic properties allowing to bend and flow through the narrowest of capillaries where they are submitted to considerable shear stress and membrane deformation (Schmidt-Schonbein and Wells 1969; Larsen et al. 1981; Schmid-Schönbein and Gaehtgens 1981; Wiley and McCulloch 1982; Johnson and Gannon 1990; Johnson and Tang 1992; Johnson 1994). Whether physiological or experimental membrane deformation may trigger channel activity and particularly enhanced calcium permeability with subsequent Gardos channel activity with immediate consequences on blood viscosity was another aim of this work.

♥ "Conditions that change the primary globin chain structure constitute the chain 'variants'; depending on the amino acid that is changed, the chain variant may leave the haemoglobin function undisturbed or may produce manifestations and findings that occasionally acquire clinical importance.
Haemoglobin S: β6 (A3) glutamic acid!valine This is the most widespread haemoglobin variant; it occurs mostly in black people; but has also been frequently found around the Mediterranean Sea and in India. The mutation leads to prompt polymerization of the variant upon deoxygenation through the extensive formation of strong hydrophobic bonds, mainly between the newly inserted valine and the β chains of the adjacent haemoglobin molecules. The end result is marked deformation of the red cells, which acquire the **sickle cell** shape and hinder the microcirculation of the patient." Loukopoulos, D. (2002). Heamoglobinopathies. Encyclopedia of Life and Sciences, John Wiley & Sons, Ltd: Chichester.

♠ **Hereditary spherocytosis (HS)** is characterized by spherocytic red cells with increased osmotic and mechanical fragility and results in haemolytic anaemia. The spherocytic shape of these cells results from loss of membrane surface area relative to intracellular volume. HS has been associated with abnormalities in the red cell membrane proteins spectrin, ankyrin, band 3 and protein 4.2." Bruce, L. and M. Tanner (1999). "Erythroid band 3 variants and disease." Best Practice & Research Clinical Haematology **12**(4): 637-654.

The physiological role of the anionic channels remains also totally unclear. They set the membrane resting potential at the equilibrium potential for chloride so that there is no electrochemical gradient for anion movement, which optimize the role of the Cl^-/HCO_3^- exchanger. In steady-state conditions, H^+ and Cl^- distribution across the RBC membrane is purely passive and in accordance with a Donnan equilibrium, the intraerythrocytic proton concentration results from a physico-chemical equilibrium where Na^+ and K^+ movements across the RBC membrane are extremely slow and the Cl^- and HCO_3^- movements are approximately one million times faster. Chloride movements occur through a highly efficient, electrically silent Cl^-/HCO_3^- exchange mechanism that is fundamental to the CO_2 carrying capacity of the blood. Using the values for extra- and intracellular concentrations for Cl^- (145 mM and 95 mM, respectively), it is possible to calculate the reversal potential for Cl^- E_{Cl} = -10 mV which is similar to the membrane potential estimated from techniques like microelectrodes (Lassen and Sten-Knudsen 1968) or fluorescent dyes (Hoffman and Laris 1974). This is an indication that a chloride conductance normally determines the resting potential. Under these conditions the functional significance of a chloride conductance may be to set the RBC resting potential at E_{Cl} so that there is no electrochemical gradient for conductive anion movement (Hamill 1983). This voltage clamping of E_{Cl} may optimize the role of the Cl^-/HCO_3^-.

Another possibility is that they are involved in the transport of other anions such as ATP. Indeed, the membrane proteins involved in the release of ATP from RBCs appear to include ABC (ATP binding cassette) proteins and evidence was given that members of this family are present in the human red cell membrane: the multidrug transporter/P-glycoprotein (MDR), the multidrug resistance associated protein (MRP1) and, possibly, the CFTR protein (Al-Awqati 1995; Abraham et al. 2001; Abraham et al. 2001; Cantiello 2001). It was also shown in human RBCs that mechanical deformation activates the release of ATP from normal RBCs but not from cystic fibrosis patients RBCs. In this hypothesis the mechanosensitivity of the linear, small conductance Cl^- channel may

relate to the ATP transport pathway. These channels would then provide a pathway for ATP release and, thereby, play an important role in regulation of vascular resistance *in vivo* by the activation of purinergic receptors and synthesis of nitric oxide (Sprague et al. 1998; Bao et al. 2004; Locovei et al. 2006; Jiang et al. 2007).

Do the RBC channels play a role in volume regulation? Possibly! Indeed, keeping constant the volume of a bag with a high haemoglobin concentration, in a plasma environment that has a much lower protein concentration is not a trivial job; the formidable colloidosmotic pressure of ~7 mM of impermeable protein would tend to swell and lyse any water-permeable cell unless somehow balanced. The general strategy that RBCs evolved to live long (about 120 days in humans) and prevent bursting is to maintain very low membrane permeability to cations, particularly Na^+, the most abundant extracellular solute. The minor residual cation leaks can be balanced by the sodium and calcium pumps with only minute metabolic demands. Thus, cation-tight RBCs efficiently ferry O_2 and CO_2 during long life spans at minimal metabolic cost. However there are many conditions or treatments in which the RBC membrane becomes relatively permeable to cations, the best documented being those that raise intracellular calcium concentration by increasing the passive Ca^{2+} influx (Joiner 1993; Lew and Bookchin 2005; Ellory et al. 2007) and thereby cause a large selective increase in K^+ permeability with concomitant Cl^- efflux and water loss. Cell shrinkage must then be followed by return to initial volume and it has frequently been suggested that this process of volume recovery involves activation of a Na^+ conductance. Investigating this possibility was chronologically the first aim of this work.

III. MATERIALS AND METHODS.

"Per aspera ad astra."

Latin phrase

To address the different questions raised above we needed to carry out two types of techniques. First, we used lysis curves and osmotic fragility data in order to evaluate quantitatively the contribution of a putative cationic conductance (P_{cat}) in the process of dehydration-elicited rehydration; second we used the patch clamp technique of electrophysiology in order to describe at the molecular level the behaviour of ionic channels involved in the above mentioned processes.

III. 1. Contribution of ionic channels in dehydration-elicited rehydration: lysis curves and osmotic fragility data acquisition.

Osmotic fragility curves (OFCs) are extensively used to characterize the hydration state of RBCs in normal, pathological and experimental conditions (Lew et al. 1995; Raftos et al. 1996; Lew et al. 2003; Lew et al. 2005; Tiffert et al. 2005; Baunbaek and Bennekou 2008). With the advent of microwell plates and microplate readers new methodologies were developed (Lew et al. 1995; Raftos et al. 1996) to increase the throughput of OFC data, enabling OFCs to become an important tool for measuring dynamic changes in RBC hydration states, with important applications in research on the condition of intact RBCs in health and disease.

III. 1. 1. Experimental design.

To help follow the specific issues addressed here and the reasons for the chosen experimental protocol we need to review briefly the methodology and current understanding of osmotic fragility data. OFCs are obtained by rapidly diluting RBC samples into relatively large volumes of media with progressively reduced osmolalities.

The osmolalities are varied from plasma-like values (~290 mOsm/kg in humans) to distilled water, the unlysed cells are spun down, and the fraction of cells lysed in each of the hypotonic conditions is estimated from the fraction of Hb released to the supernatant by measuring light absorbance at 415 nm (Soret band; a plate reader Tecan, Switzerland working on Safire2 software). The water permeability of the RBC membrane is orders of magnitude larger than that of any of the transported solutes, so that osmotic equilibrium or lysis is attained within a few seconds of the cells mixing with the hypotonic media thus minimizing any contributions from net solute transfers. A key point to bear in mind is that the unlysed cells in each hypotonic condition retain their low solute permeability (Garcia-Sancho and Lew 1988); there is therefore no further lysis from cells that did not lyse immediately. OFCs are usually reported in plots of percent cells lysed as a function of relative tonicity (RT) (Fig. III. 1), the osmolality of each hypotonic medium expressed relative to physiological plasma osmolalities.

Figure III. 1.

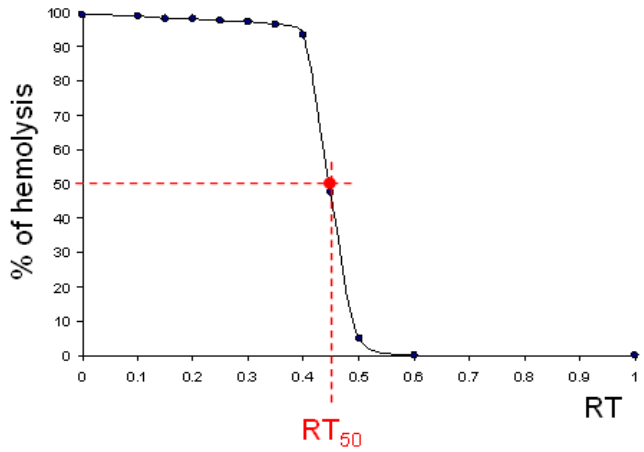

Figure III. 1. Osmotic fragility curve (OFC) is the graphical representation of fraction of haemolysed RBCs (in percentage) as a function of relative tononicity (RT). The abscissa represents the experimental setup – for chosen points hypoosmotic solutions were prepared (1 is the value of isosmotic solution, ~290 mOsm and 0 expresses the osmolality of water; the points between have reduced osmolality in relation to physiological value). Haemolysis of the cell in the pure water is the reference level for haemolysis in the other hypotonic and isotonic solutions. The RT_{50} coefficient gives the value of solution tonicity in which 50% of cells lysed.

The OFCs represent a cumulative measure because the fraction of lysed cells increases to 100% as RT goes from 1 to 0. The derivative of the OFCs is interpreted as a population distribution of the volume of fluid each cell needs to gain in order to attain its maximal spherical volume, usually described as the critical haemolytic volume (CHV) (Ponder 1948). The mean CHV for normal human RBCs is about 1.7 times the normal mean RBC volume (Ponder 1948).

The following equation (Eq. III. 1) describes the relation between the relative tonicity (RT) that causes maximal pre-lytic swelling in each cell (RTL) as a function of its membrane area (A) and of its osmotically active solute content (ΣQ), the two main factors assumed to determine the CHV of each cell (Svetina 1982; Cassady et al. 1989):

$$RTL = \frac{\frac{\sum Q}{C_{iso}}}{\frac{A^{1.5}}{6\sqrt{\pi}} - V_H} \qquad \text{(III. 1)}$$

where:

C_{iso} is a constant that defines isotonicity with plasma and is ~290 mOsm/kg (RT = 1); π = 3.14; V_H is the volume normally occupied by haemoglobin (Hb) molecules in one litre of originally packed cells (l_{oc}).

At water equilibrium across the RBC membrane:

$$\frac{\sum Q}{C_{iso}} = V_w \qquad \text{(III. 2)}$$

where:

V_W is the water content of the cell (in kg or litres cell water per litre of originally packed cells);

With a specific volume of 0.735 ml/g and a mean Hb content of 340 g/l_{oc}, the mean V_H is about 0.25 litre/l_{oc} (Bureau and Banerjee 1976; Lew et al. 1991) and a mean Hb content of 340 g/l_{oc}, the mean V_H is about 0.25 litre/l_{oc}. It can be seen that at constant *A* and V_H

there is a linear relation between RTL and ΣQ so that net losses or gains of solutes by the cells would cause left or right shifts of the OFCs along the RT axis, respectively, reflecting the need for the cells to gain more or less fluid than at their original ΣQ to attain pre-lytic sphericity. The term $\frac{A^{1.5}}{6\sqrt{\pi}}$ represents the spherical volume of a cell with area *A*, and it is therefore equal to its CHV in the traditional interpretation of this parameter

$$CHV = \frac{A^{1.5}}{6\sqrt{\pi}} \qquad \text{(III. 3)}$$

III. 1. 2. Solutions.

The compositions of the main solutions used in OFC experiments are defined in Tab. III. 1 and in Tab. III. 3.

Table III. 1. The composition of the solutions used in OFC experiments. All solutions were prepared in MiliQ water from stock solutions (in mol/l): NaCl (1), KCl (0.5), $MgCl_2$ (1), NaSCN (1.5). The osmolarities were (300 ± 5) mOsm/kg and pH were adjusted (NaOH or KOH – for high potassium solutions) to 7.4. Na-HEPES, pH 7.5 at 37℃.

Compound [mM] / Solution	NaCl	KCl	$MgCl_2$	Na-HEPES	EGTA	NaSCN
A	145.0	3.0	0.15	10.0	-	-
AK	48.0	100.0	0.15	10.0	-	-
B	145.0	3.0	0.15	10.0	0.1	-
C	135.0	3.0	10.0	10.0	-	10.0
D	35.0	100.0	0.15	10.0	-	10.0

SCN^- was used to bypass any rate-limiting effects of the anion permeability on the rate of dehydration or hydration of K^+-permeabilized RBCs (Parker 1983; Tiffert et al. 2001). In medium D the mean volume of K^+-permeabilized RBCs remains largely unchanged (Lew et al. 2007).

Unless specified otherwise in the legends of figures, the final concentrations of the most frequently added solutes were (in mM): $CaCl_2$, 0.05; ionophore A23187 (from 2 mM stock in ethanol) 0.01.

III. 1. 3. Preparation of red blood cells.

On day one, about 50 ml of blood from healthy volunteers was drawn into heparinized vacutainers after obtaining informed written consent. The blood was spun at 1800 g for 10 min at 10^{o}C, the plasma removed, and the RBCs washed twice by centrifugation and resuspension in solution B and twice more in solution A, with removal of the buffy coat after each spin. The cells were then suspended in RPMI medium (Annex #5) at 50% Hct and stored at 4^{o}C for use in experiments on days 2 and 4.

III. 1. 4. The biphasic OFC protocol.

RBCs contained in about 7 ml of the suspension in RPMI were washed twice in solution A and twice more in solution C before final suspension at 10% Hct in solution C, 12 ml. This suspension was divided in two 6 ml aliquots, one control and one test condition in each experiment, both suspensions kept at 37^{o}C. The test condition for each experiment is detailed in Results and in the legends of the figures. The protocol for the biphasic OFC control was as follows. After about 10 min for temperature equilibration, $CaCl_2$ was added from concentrated stock (200 mM) to a final concentration of 50 µM in the suspension. A 0.5 ml sample was taken for duplicate initial OFCs. At t = 0 min, the ionophore A23187 was added to a final concentration of 10 µM in the suspension. Further 0.5 ml samples for OFCs were taken at t = 10, 30, 60, 120, 180 and 240 min post-ionophore addition. To investigate the extent to which the biphasic OFC pattern of Ca^{2+}-loaded RBCs could be attributed to salt and water shifts as previously assumed (Lew et al. 2007), the cell water content was measured in parallel aliquots of the same samples used for OFCs during the biphasic OFC protocol in all control and test conditions. Osmotic fragility was measured by the profile migration method, as previously

described (Lew et al. 1995; Raftos et al. 1996). For water content determinations 0.5 ml aliquots of the cell suspension were distributed in polyethylene micro test tubes and centrifuged at 20 000 g for 10 min at 5°C. After centrifugation the packed cells were separated from the supernatant by slicing the tube with a razor blade above and below the top of the red cell column. After weighing, the packed cells were dried to constant weight for 24 h at 90°C and re-weighed. The measured water content in gram per gram of cell solids was then divided by 0.34 to express cell water content in units of litre cell water per 340 g of Hb, or its equivalent, litre cell water per litre original packed RBCs (l_{cw}/l_{oc}, as reported in the ordinate of the corresponding figures).

III. 1. 5. Measurement of the volume-fraction of RBC cytosol lost by Ca^{2+}-induced exovesiculation*.

The method followed guidelines derived from early work by Allan and Thomas (Allan et al. 1980). Washed RBCs were suspended at 10 % Hct in solution A or AK supplemented with $CaCl_2$, 0.15 mM, and incubated at 37°C. Samples of this suspension were taken before and 4h after addition of the ionophore A23187, placed in 15 ml centrifuge tubes and gently spun at 500g for 10 min to separate the intact RBCs from the supernatant which contained lysed cells and vesicles. The supernatant was then distributed in 0.5 ml aliquots in microfuge tubes and spun at 16000g for 30 min at 20°C to pellet the vesicles and ghosts. Pellets were recovered from the 4h samples. Microscopic observation of unfixed pellet material showed a dense grainy background and white ghosts. Pellets were pooled together as required for measuring the Hb content of the vesicles, and in preparation for transmission and scanning electronmicroscopy. Hb was measured by resuspending the vesicle pellet in distilled water with 0.01% Triton X-100.

* The paragraph III. 1. 5. 1 was realized by the collaborators in: Physiological Laboratory, Department of Physiology, Development and Neuroscience, University of Cambridge, UK as well as Laser Analytics Group, Department of Chemical Engineering and Biotechnology, University of Cambridge, UK, under Dr V. L. Lew supervision.

The haemoglobin released from the vesicles was measured by absorbance at 415 nm (the Soret band). After correcting for dilution, the Hb content of the vesicles was divided by the Hb content in the original volume of cells from which the vesicles had been sampled to calculate the volume-fraction of RBC cytosol released by exovesiculation.

III. 1. 5. 1. Processing of vesicle samples for transmission and scanning electronmicroscopy.

Pellets of vesicles destined for ultrastructural observation were initially fixed by 500-fold dilution in 4% formaldehyde in 0.1M phosphate buffer for 24 h at 20^{o}C. They were then rinsed in 0.1M PIPES buffer at pH 7.4 and post fixed in 2% glutaraldehyde in 0.1M PIPES buffer for a further 2 h. They were again rinsed in PIPES buffer and treated with 1% osmium tetroxide for one hour, rinsed in deionized water (DIW) and stained with 2% uranyl acetate in 0.05 M Maleate buffer. The pellets were then split into two samples one for TEM and one for SEM. **TEM :** The pellet was dehydrated in an ascending series of ethanol solutions from 70% to 100%, rinsed twice in acetonitrile and infiltrated with Quetol epoxy resin. The resin was cured at 60℃ for 48 hours. Thin sections were cut using a Leica ultracut UCT mounted on 300 mesh copper grids and stained with uranyl acetate and lead citrate. The sections were viewed in an FEI CM100 operated at 80 kV and images were recorded with a Deben AMT 16000 digital camera. **SEM :** The pellet was re-suspended in 250 µl of DIW and allowed to settle on a 12 mm diameter coverslip coated with poly-L-lysine for 5 min in a humid chamber. The coverslip was dehydrated to 100% ethanol and critical point dried in a Polaron B7010 critical point dryer. The coverslips were mounted on Cambridge SEM stubs, sputter coated with 5 nm of gold with a Quorum Emitech K575X sputter coater and viewed in a FEI XL30 FEGSEM operated at 5 kV.

III. 2. Electrophysiology.

III. 2. 1. Preparation of cells.

Venous blood was drawn into heparinized vacutainers from healthy volunteers. RBCs were washed thrice by centrifugation and resuspension in large volumes of culture RPMI medium (Invitrogen). The buffy coat containing platelets and white cells was removed by suction after each wash. After the last wash, the cells were suspended at 50% Hct in RPMI and kept at 4℃. They were suspended at 10% he matocrit in solution A and incubated at 37℃ for about 1 h prior to experiment s. Experiments were done at the room temperature.

III. 2. 2. Solutions.

The basic pipette and bathing solutions used in patch clamp experiments are listed in Tab. III. 2 and in Tab. III. 3.

Table III. 2. The composition of the solutions used in patch clamp experiments. All solutions were prepared in MiliQ water from stock solutions (in mol/l): NaCl (1), KCl (0.5), $MgCl_2$ (1). The osmolarities were (290 ± 5) mOsm/kg and pH were adjusted (NaOH or KOH – for high potassium solutions) to 7.4. Na-HEPES, pH 7.5 at 37℃.

Compound [mM] / Solution	NaCl	KCl	$MgCl_2$	HEPES	EGTA	glucose	NMDG	NaSCN
RnS	130.0	5.0	1.00	10.0	-	10.0	-	-
RnS-10SCN	135.0	3.0	0.20	5.0	-	10.0	-	10
RnS-NMDG	-	-	1.00	10.0	-	10.0	145	-
High-K	5.0	130.0	1.22	10.0	5.0	10.0	-	-

The calcium concentrations are adjusted to different pCa ($-\log[Ca^{2+}]$) in the pipette and bathing solutions (usually, pCa7 on the cytosolic side and pCa3 on the extracellular side). All solutions were filtered through 0.2 µm Millipore cellulose disks and equilibrated in air (oxygen partial pressure, pO_2 = 155 mmHg; carbon dioxide partial pressure, pCO_2 = 0.3 mmHg).

III. 2. 3. Current recordings.

Under a microscope, a small glass tube, the patch electrode, thinned to a cone-shaped end (usually ~1 μm^2 in area with ~10 MΩ tip resistance) and filled with an appropriate saline solution, is brought in contact with the surface of a cell with the purpose of generating a very high-resistance-electrical seal around the edge of the tip. Since the object is to detect and measure tiny electrical currents through channels in the cell membrane, the seal has to be highly resistant (> 10^9 Ohms) to prevent artefacts resulting from leaky seals. Patch pipettes (tip resistance (10 – 20) MOhm) were prepared from borosilicate glass capillaries (GC 150F Clark Electromedical), pulled and polished on a programmable puller (DMZ, Werner Zeitz, Augsburg, Germany). 4 to 20 GOhm seals were obtained by suctions of 10 mmHg applied for less than 10 s, using a syringe connected to the patch pipette. Once the seal is established, the membrane potential across the patch is fully under experimental control and may be held (holding potential, V_H) or varied at will. Currents are measured by applying voltage-steps across the membrane.

The patch clamp technique can be used in three distinct configurations (Fig. III. 2):

1: Cell-attached (C-A): for measuring the current through the approximately 1 μm^2 of membrane within the tip of the pipette. This configuration maintains the integrity of the cell and is therefore the most physiological; it does not, however, provide access to the cytosolic side of the membrane.

2: Excised inside-out (I-O): this configuration allows full control of the ionic composition of the cytosolic side of the membrane for selectivity and substitution experiments and for pharmacological assays. Both configurations enable measurements of unitary currents at the single channel level, thus allowing a biophysical characterization of all channel types present in the membrane under study. In these configurations, the success rate of experiments depends largely on the surface density of channels. Considering the small fraction of membrane under the patch, it takes hundreds of observations to build up a

reliable and comprehensive picture of the density and variety of channels present in the membrane.

3: Whole-cell configuration (W-C), obtained from the cell-attached configuration when the patch of membrane within the tip is ruptured by suction or by application of brief electric shocks, and the currents measured are those flowing through all the ionic channels present and active in the cell. In this configuration, the cell content changes dramatically as the cell cytosol equilibrates with the fluid within the patch pipette. The W-C configuration was not used in this work.

Figure. III. 2.

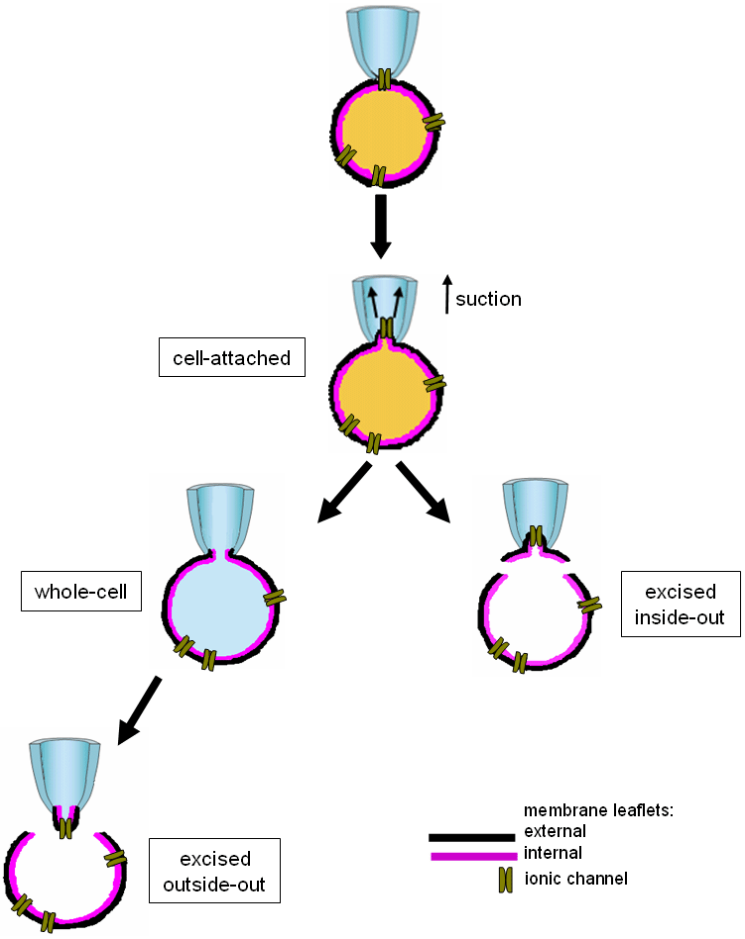

Figure III. 2. Modes of patch clamp configurations.

4. Outside-out (O-O) configuration is a complementary configuration to the I-O with the respect to the orientation of the membrane surface. The external side of the membrane is in contact with the bath solution whereas cytoplasmic face of the lipid bilayer contacts media in the pipette. This mode of patch clamp is particularly suitable for studying the action of transmitter substances and other types of chemicals or ions on the extracellular side of the membrane. Obtaining O-O mode is more laborious with a lower rate of success. Moreover this configuration appears to be a more delicate and less stabile structure. The O-O configuration was not used in this work.

In the C-A configuration the recordings of flickering currents provide important information on how single channel conductances and open-state probabilities vary with voltage. In W-C recordings, the conductance through the whole membrane area measures the number of active channels per cell if it can be assumed that the current is carried by one specific type of channel of known single channel conductance and open state probability distribution. The current-voltage (I/V) curves provide additional information on the collective kinetics of the channels. In general, I/V curves that deviate from the usual linear ohmic behaviour are described as rectified; conductances measured under patch clamp conditions are conventionally described as outward rectifiers if the current is reduced at negative membrane voltages (relative to the extracellular medium), and inward rectifiers if reduced at positive voltages. When applied to single channels, rectification properties reflect the kinetics of the molecular components controlling the aperture of the conductive path.

Single channel currents were recorded using a RK400 patch clamp amplifier (Biologic, Claix, France), filtered at 0.3 or 1 kHz, digitized (48 kHz) and stored on a hard disc of computer. The data have been analyzed in the WinEDR V2.8.0 computer program (Dempster, Strathclyde Electrophysiology Software).

The sign of the clamped voltage (V_P) refers to the pipette solution with respect to the bath and outward current (positive charges flowing across the patch membrane into the pipette) is shown as an upward deflection in the current traces. In the cell-attached configuration the imposed membrane potential (V_m) is referred to $-V_P$ according to Eq. III. 4:

$$V_m = E_m - V_P \qquad \text{(III. 4)}$$

where:

E_m is the resting membrane potential.

The I/V curves were constructed by plotting the mean current amplitude for each clamped potential. The P_o was determined as the fraction of digitized points above a threshold set midway between the closed and open peaks of current-amplitude histograms. P_o was determined from 60 seconds stable recordings. In these conditions, P_o was defined as the ratio of the total time spent in the open state to the total time of the complete record. Analyses were confined to patches containing one channel event histogram. Data are given as mean values ± SEM.

III. 3. Chemicals.

All chemicals were analytical reagent quality. RPMI was from GIBCO BRL, (France). NaSCN, EGTA (ethylene glycol tetraacetic acid), HEPES (4-(2-hydroxyethyl)-1-piperazineethanesulfonic acid), DMSO (dimethyl sulfoxide) and N-methyl-D-glucamine chloride (NMDG) were from Sigma-Aldrich (Saint Quentin Fallavier, France). $CaCl_2$, $MgCl_2$, NaCl, KCl were from FSA Laboratory Supplies (Loughborough, UK) or from Sigma-Aldrich (Saint Quentin Fallavier, France).

Table III. 3. The list of chemical compounds used in OFCs and patch clamp experiments.

Chemical	Concentration used	Supplier	Solvent
A23187	10 μM	Calbiochem-Novabiochem (UK) Ltd.	ethanol
Albumax	0.1 %	Sigma-Aldrich	H_2O
Ba^{2+}	10 mM	Sigma-Aldrich	H_2O
CLT	10 μM	Sigma-Aldrich	H_2O
Co^{2+}	400 μM	Sigma-Aldrich	H_2O
Choline chloride	145 mM	Sigma-Aldrich	H_2O
DIDS	10 μM	Sigma-Aldrich	DMSO
DIOA	100 μM	Sigma-Aldrich	DMSO
EIPA	100 μM	Sigma-Aldrich	DMSO
NPPB	1 μM, 10 μM, 100 μM	RBI	DMSO
NS309	10μM	Sigma-Aldrich	DMSO
Ouabaine	100 μM	Sigma-Aldrich	DMSO
Plasma (human)	0.5 %	Sigma-Aldrich	H_2O
Serum (human)	0.5 %	Sigma-Aldrich	H_2O
Valinomycin	1 μM	Calbiochem-Novabiochem (UK) Ltd.	DMSO
Vanadate	1 mM	Sigma-Aldrich	H_2O

III. 4. Red blood cell model.

The Lew-Bookchin mathematical-computational model of the homeostasis of human RBC is available as free-standing executable file from http://www.physiol.cam.ac.uk/staff/lew/index.htm.

IV. RESULTS.

"Only one who does nothing ever makes a mistake."

French proverb

IV. 1. First question: Are RBC's membrane channels involved in rehydration elicited by isosmotic dehydration?

IV. 1. 1. Results.

RBCs suspended in isotonic low-K^+ media and loaded with Ca^{2+} for extended periods of time with the use of Ca^{2+} ionophore show a biphasic pattern in the excursion of OFCs: a rapid initial left shift reflecting dehydration caused by the activation of a Ca^{2+}-sensitive K^+ channel (IK1, Gardos channel (Gardos 1958; Lew and Ferreira 1978; Vandorpe et al. 1998; Hoffman et al. 2003)) leading to the net loss of KCl and water, followed by much slower right shifts (Lew et al. 2007). These unexpected right-shifts were only observed in the presence of external cations and were therefore interpreted as reflecting a progressive rehydration of the RBCs by the net gain of salts and water. Moreover, Gardos channel inhibitors, or high external K^+ concentrations, prevented the initial left shift but not the slow right shifts in the OFCs from Ca^{2+}-loaded RBCs, suggesting that the hydration response was strictly Ca^{2+} -dependent and not dehydration-induced (Lew et al. 2007). The right shifts were therefore interpreted as supporting the existence of a Ca^{2+}-activated non-selective cation permeability channel, P_{cat}, considered a possible candidate in the mediation of the increased Na^+/K^+ concentration ratio detected in aging RBCs (Bookchin et al. 2000; Lew et al. 2007). However, the basic mechanism behind this interpretation, that OFC right shifts equal RBC hydration had never been directly

investigated. We test here the hydration hypothesis of the right shifts by directly measuring the water gains associated with dynamic shifts in osmotic fragility curves under a variety of experimental conditions.

Figure. IV. 1.

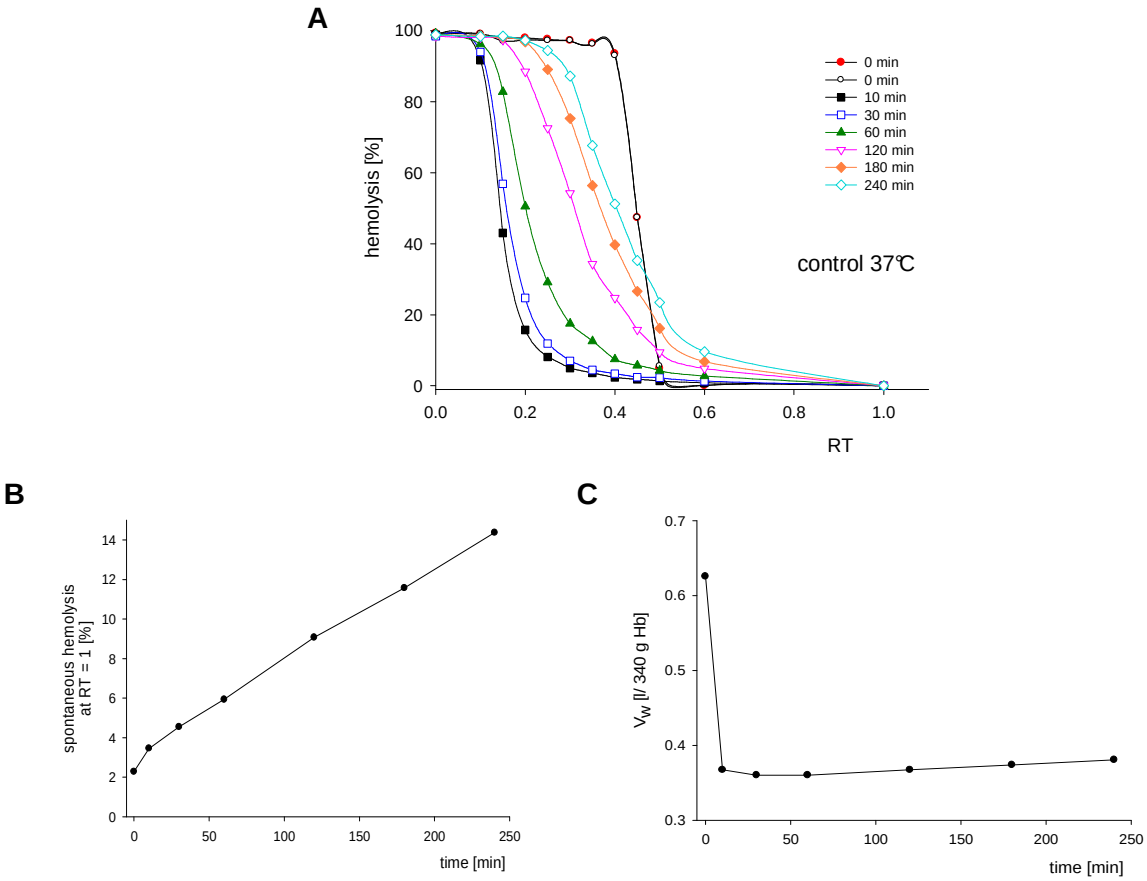

Figure IV. 1. Changes in osmotic fragility, spontaneous haemolysis and water content of RBCs during Ca^{2+}-induced biphasic dehydration-hydration protocol. The figure depicts the mean of 32 identical experiments used as control for each of the different conditions investigated (shown further in this section). The water content of the cells was measured in liter per g dry weight and converted to liter per 340 g dry weight; 340 g represents a standardized mean dry weight of haemoglobin in one liter of fresh packed red blood cells, presumed to remain invariant in unlysed RBCs of any volume. **(A)** Osmotic fragility curves over the 4 h duration of the experiments; duplicate controls were taken just before addition of the ionophore A23187. The spontaneous lysis level reported in (B) was subtracted as baseline for these curves. **(B)** Cumulative spontaneous cell lysis over 4 h; the percent haemolysis was recorded at a relative tonicity of 1 (RT = 1). **(C)** Changes in cell water contents (V_W) during the biphasic OFC protocol.

Figure IV. 1A-C shows the results of the biphasic OFC protocol, representing the means of 32 experiments used as paired controls for the different test conditions reported below. Figure IV. 1A shows the excursion of the OFCs over time. For the chosen sampling times, the maximal left-shift of the OFCs was observed at 10 min. Samples obtained over the next four hours show a slow and progressive right shift of the OFCs with gradually decreasing slopes. This agrees with previously reported patterns, in which the rapid initial dehydration mediated by Ca^{2+}-induced Gardos channel activation was followed by sustained right-shifts in the OFCs, interpreted as reflecting the progressive rehydration of the cells (Lew et al. 2007). Figure IV. 1B shows the time-course of spontaneous haemolysis in the original cell suspension (RT = 1). This may represent a cumulative fraction of right-shifting cells exceeding their CHV over the 4 h period of observation, a lytic membrane instability unrelated to cell volume affecting progressive cell fractions, or both. Figure IV. 1C shows the change in mean water content of the cells. The sharp initial drop accompanying the net KCl loss was followed by a slow, minute gain, linear with time, to a level marginally above that of the maximally dehydrated cells. This unexpected result revealed quite clearly that the contribution of rehydration to the right shift in the OFCs was minimal, amounting to no more that 8% in the different individual experiments of this series.

Right shifts in the OFCs following Ca^{2+} loads were previously observed also in conditions which prevented the initial dehydration, such as Gardos channel inhibition or high external K^+ (Lew et al. 2007). In the experiment of Fig. VI. 2A dehydration was fully prevented by clotrimazole, a Gardos channel inhibitor (Alvarez et al. 1992; Brugnara et al. 1996; Coupry et al. 1996) but the right-shifts in the OFCs were preserved. The mean content of cell water (Fig. IV. 2B) showed no sign of gain during the right shifts in the OFCs thus excluding hydration as their cause.

Figure. IV. 2.

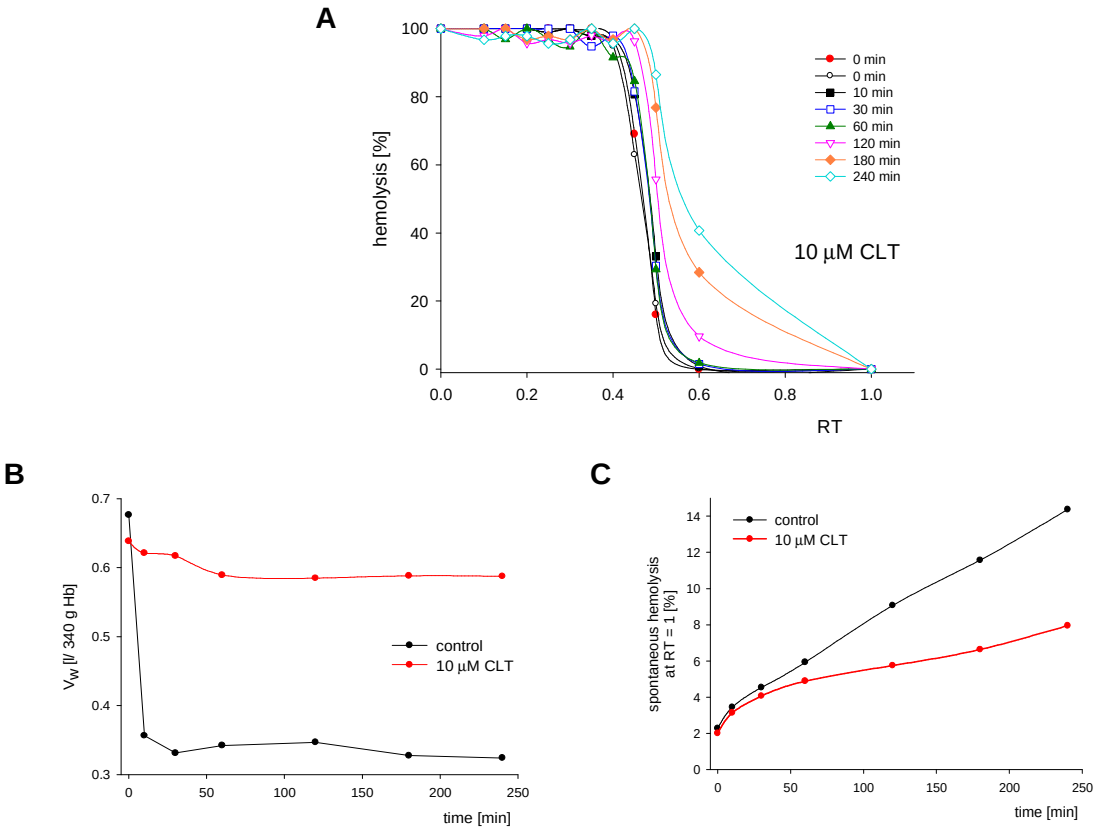

Figure IV. 2. Effects of a sustained Ca^{2+} load on the time-dependent changes in osmotic fragility and water content of RBCs in conditions that prevent Ca^{2+}-induced dehydration. RBCs were exposed to the biphasic OFC protocol in the presence of 10 µM clotrimazole (CLT) in the cell suspension. At this CLT concentration Gardos channel-mediated K^+ fluxes are fully inhibited and dehydration largely prevented, but the increase in osmotic fragility with time is still clearly apparent **(A)** without any parallel water gain **(B)**. Changes in cell water contents (V_W) during the biphasic OFC protocol. **(C)** Cumulative spontaneous cell lysis over 4 h; the percent haemolysis was recorded at a relative tonicity of 1 (RT = 1).

Ca^{2+} extraction from dehydrated, ionophore-treated RBCs by the addition of excess EGTA over Ca^{2+} in the medium was previously shown to markedly reduce subsequent right-shifts in the OFCs (Lew et al. 2007). Here we allowed the plasma membrane Ca^{2+} pump (PMCA) to extrude the ionophore-induced Ca^{2+} load by adding Co^{2+} in excess of Ca^{2+} in the medium one minute after ionophore addition (Dagher and Lew 1988). Co^{2+} instantly blocks Ca^{2+} transport by the ionophore allowing rapid Ca^{2+} extrusion by the PMCA thus reducing $[Ca^{2+}]_i$ to levels below Gardos channel activation within about 4 min

of Co^{2+} addition (Lew et al. 2003). The results are shown in Fig. IV. 3A-C. Co^{2+} addition one minute after ionophore reduced the extent of maximal dehydration by 67% relative to the paired control because of early Gardos channel deactivation. The subsequent right-

Figure. IV. 3.

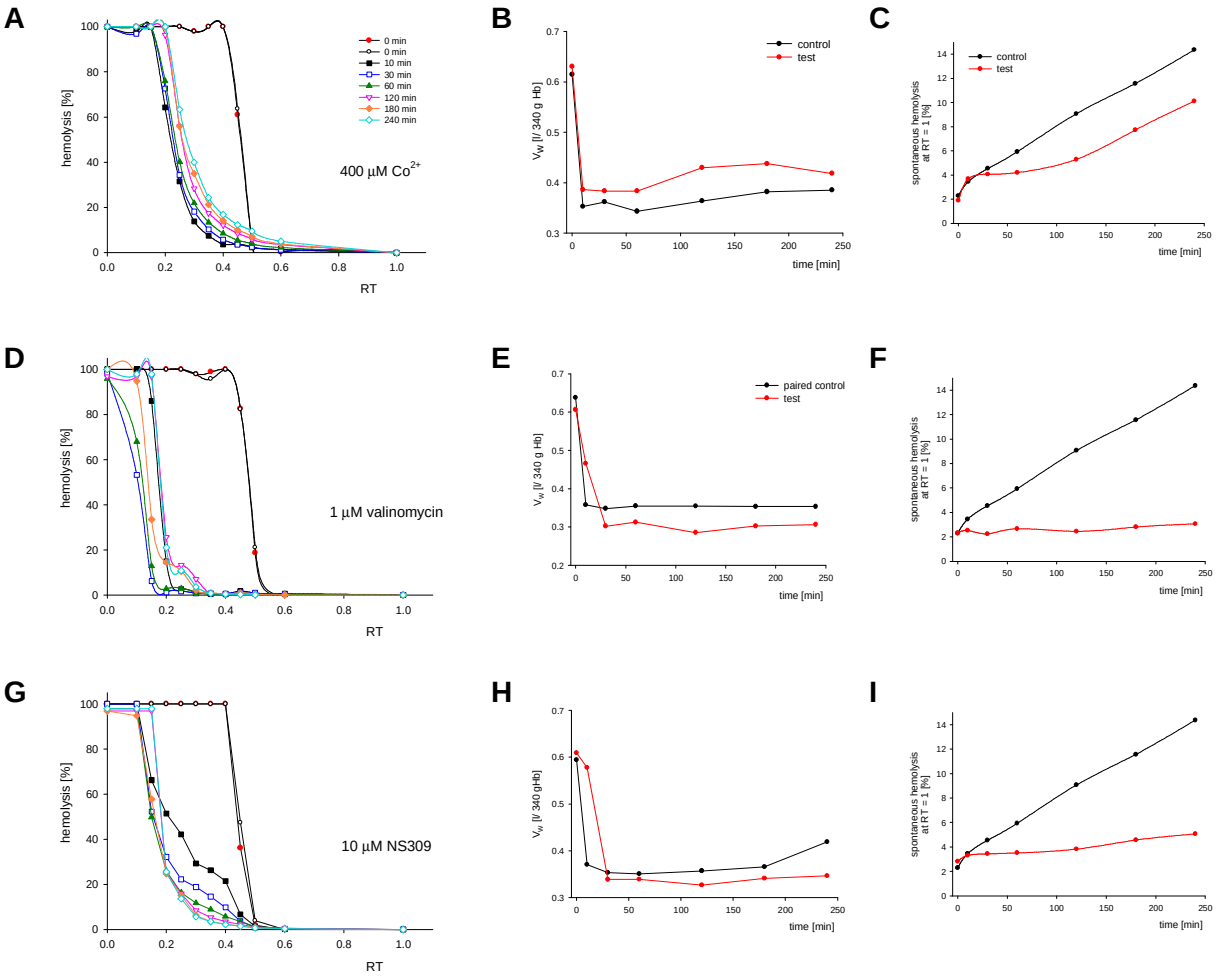

Figure IV. 3. Effects of RBC dehydration without elevated $[Ca^{2+}]_i$ on the osmotic fragility of the cells. (A – C). Co^{2+} (400 µM) was added to the cell suspension one min after ionophore A23187 to block further ionophore-mediated Ca^{2+} transport and allow rapid Ca^{2+} extrusion by the plasma membrane calcium pump. **(D – F)**. Valinomycin (1 µM) was added to the cell suspension at t = 0 instead of ionophore A23187. **(G – I)**. NS309 (10 µM), a positive modulator of Gardos channels was added at t = 0 instead of A23187. **A**, **D** and **G**: osmotic fragility curves. **B**, **E** and **H**: water content of the cells. The controls in B, E and H represent the water content measured in cells from the same batch exposed to the biphasic OFC protocol (paired control). All conditions caused initial dehydration but the subsequent increase in the osmotic fragility of the cells was absent (D and G) or much reduced (A), and water gains were comparable to those in the controls (B, E and H).

shifts in OFCs were reduced by about 80% relative to the paired control. The minor water gain after dehydration was similar to that in controls (Fig. IV. 3B), but here its magnitude may be sufficient for rehydration to account for the observed right shifts.

The effects of RBC dehydration on OFC shifts were investigated without Ca^{2+} loading of the cells. We used valinomycin or NS309 to dehydrate the cells. NS309 is a recently developed positive modulator of the Gardos channel which acts by increasing its Ca^{2+} sensitivity (Strobaek et al. 2004; Baunbaek and Bennekou 2008). With both these agents $[Ca^{2+}]_i$ remained at physiological or sub-physiological levels. Valinomycin-treated RBCs dehydrated to a similar extent and with a similar time-course as Ca^{2+}-loaded RBCs but the subsequent right shifts in OFCs were minimal (Fig. IV. 3D). Water gain post-dehydration was negligible (Fig. IV. 3E). Figure IV. 3G shows the effect of 10 μM NS309 on the OFCs in the presence of 50 μM $[Ca^{2+}]_o$. Dehydration was substantially slowed down relative to controls, and there was no significant right shift over the 4 h period following NS309 addition. Haemolysis remained below 2% by 4 h and there was no detectable water gain (Fig. IV. 3H). The results showed in Fig. IV. 3, together with the results depicted in Fig. IV. 1 and Fig. IV. 2 indicate that it is the sustained presence of elevated intracellular calcium, not dehydration per se, that is responsible for the large increases in osmotic fragility that cannot be explained by cell hydration. The effect of the magnitude of the Ca^{2+} load on the extent of right-shift in the OFCs, on water gain and on spontaneous haemolysis is shown in Fig. IV. 4. It can be seen that increasing Ca^{2+} loads induce progressive increases in the extent of right-shifts (Fig. IV. 4A), spontaneous haemolysis (Fig. IV. 4B), and water gains (Fig. IV. 4C). However, the actual magnitude of the water gains was minimal at all calcium loads (Fig. IV. 4C), stressing further the notion that the contribution of hydration to the right-shifts in OFCs is marginal.

Figure. IV. 4.

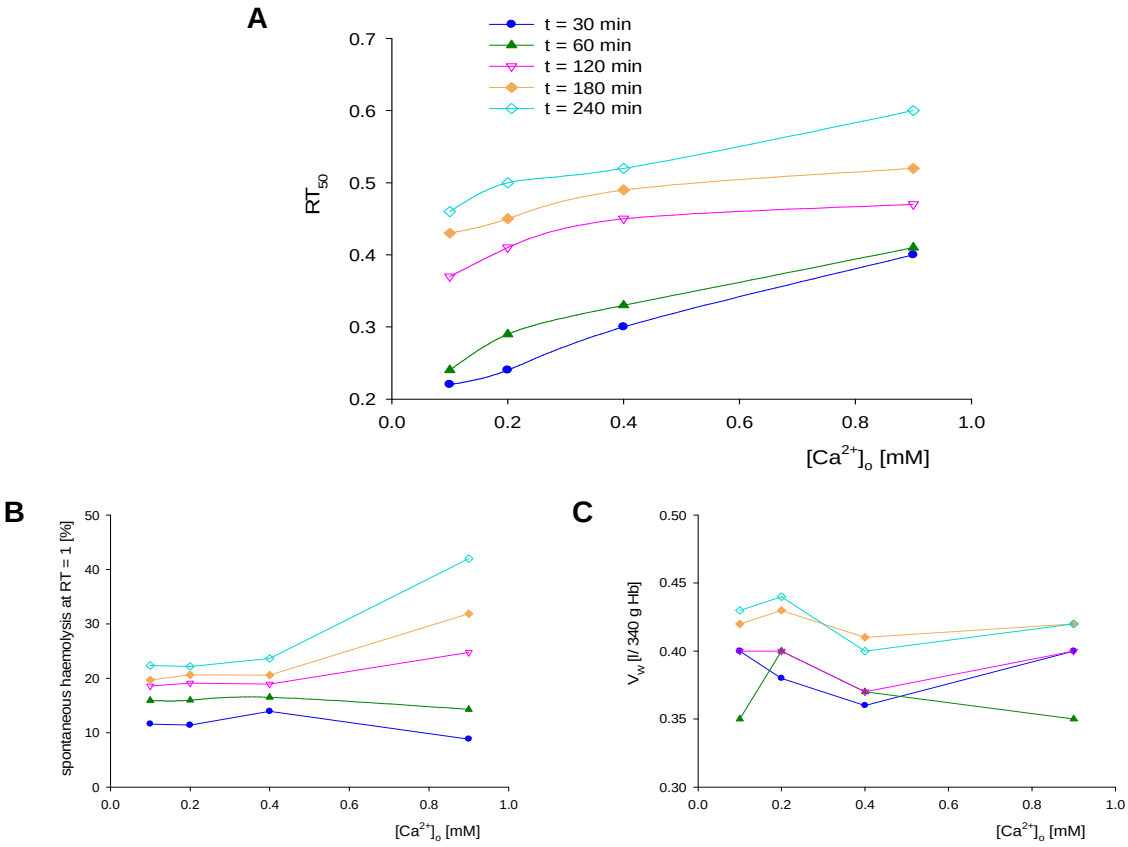

Figure IV. 4. Effect of the magnitude of the A23187-mediated Ca^{2+} load on osmotic fragility, spontaneous lysis and water content of the cells as a function of time. The abscissa reports the initial external Ca^{2+} concentration in the suspending medium $[Ca^{2+}]_o$, before addition of the ionophore A23187. **(A)** Relative tonicity for 50% haemolysis (RT_{50}) is used here to describe the time-dependent shifts in the osmotic fragility curves; **(B)** spontaneous haemolysis; **(C)** water content of the cells.

The participation of different ion transport systems of the RBC membrane on the osmotic fragility effects elicited by elevated $[Ca^{2+}]_i$ was investigated with the use of transport inhibitors and ion replacements. Ba^{2+}, DIOA, EIPA and NPPB tested at their highest effective doses, showed no significant differences with controls (Fig. IV. 5). Vanadate slightly enhanced the right-shifts post-dehydration (Fig. IV. 6) whereas sodium replacement by choline slightly reduced them (Fig. IV. 7), confirming earlier results (Lew et al. 2007).

Figure. IV. 5.

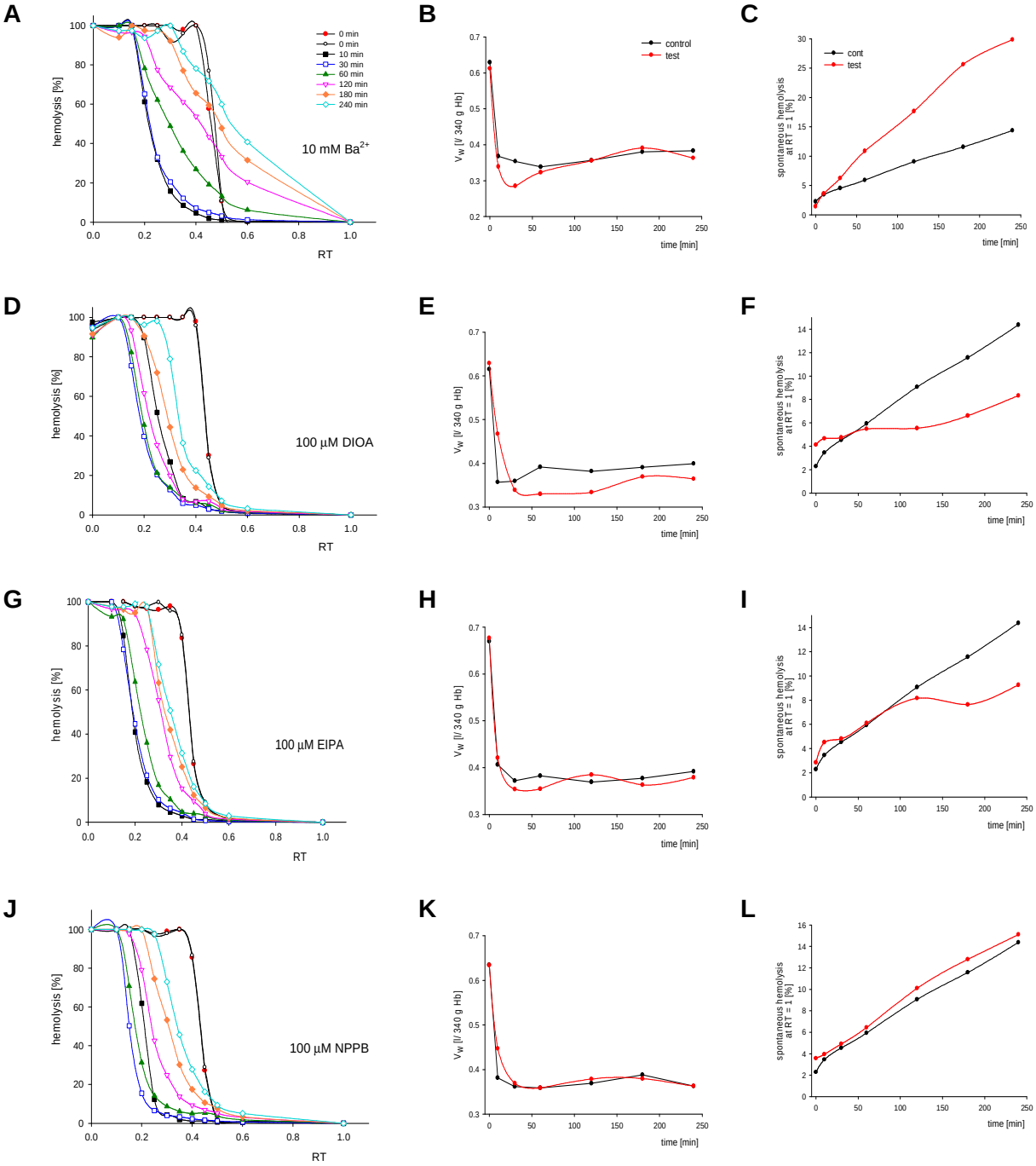

Figure IV. 5. The participation of different ion transport systems of the RBC membrane on the osmotic fragility effects elicited by elevated $[Ca^{2+}]_i$. The OFCs **(A, D, G, J)**, the water content **(B, E, H, K)** and spontaneous heamolysis at RT = 1. **(C, F, I, L)** are depicted for Ba^{2+} (10 mM) **(A, B, C)**, DIOA (100 µM) **(D, E, F)**, EIPA (100 µM) **(G, H, I)** and NPPB (100 µM) **(J, K, L)**.

Figure. IV. 6.

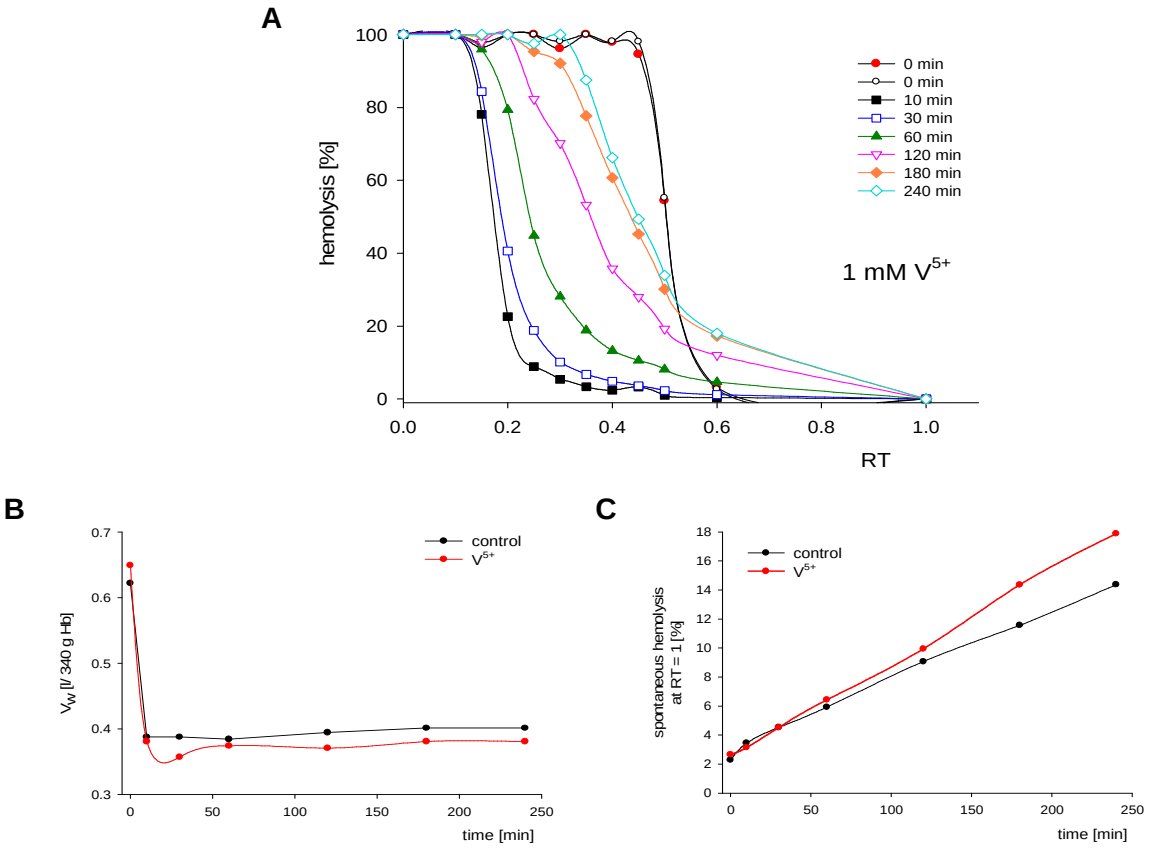

Figure IV. 6. Effects of vanadate (1 mM) on the time-dependent changes in osmotic fragility, water content and spontaneous haemolysis of RBCs. (A) Osmotic fragility curves over the 4 h duration of the experiments; duplicate controls were taken just before addition of the ionophore A23187. The spontaneous lysis level reported in (C) was subtracted as baseline for these curves. **(B)** Changes in cell water contents (V_W) during the biphasic OFC protocol. **(C)** Cumulative spontaneous cell lysis over 4 h; the percent haemolysis was recorded at a relative tonicity of 1 (RT = 1).

The results so far show that hydration is a minor contributor to the slow right shifts in the OFCs of Ca^{2+}-loaded RBCs. It can be seen from equation III. 1 that an increase in RTL, equivalent to an increase in osmotic fragility, could also be elicited by a reduction in membrane area. This poses the question of whether the Ca^{2+}-induced right shifts in OFCs could be explained by Ca^{2+}-induced membrane area loss. Elevated $[Ca^{2+}]_i$ has been shown to cause the release of Hb-containing spherical vesicles with diameters in the (80 – 100) nm range, free of the main cytoskeletal proteins: spectrin and actin

(Lutz et al. 1977).

Figure. IV. 7.

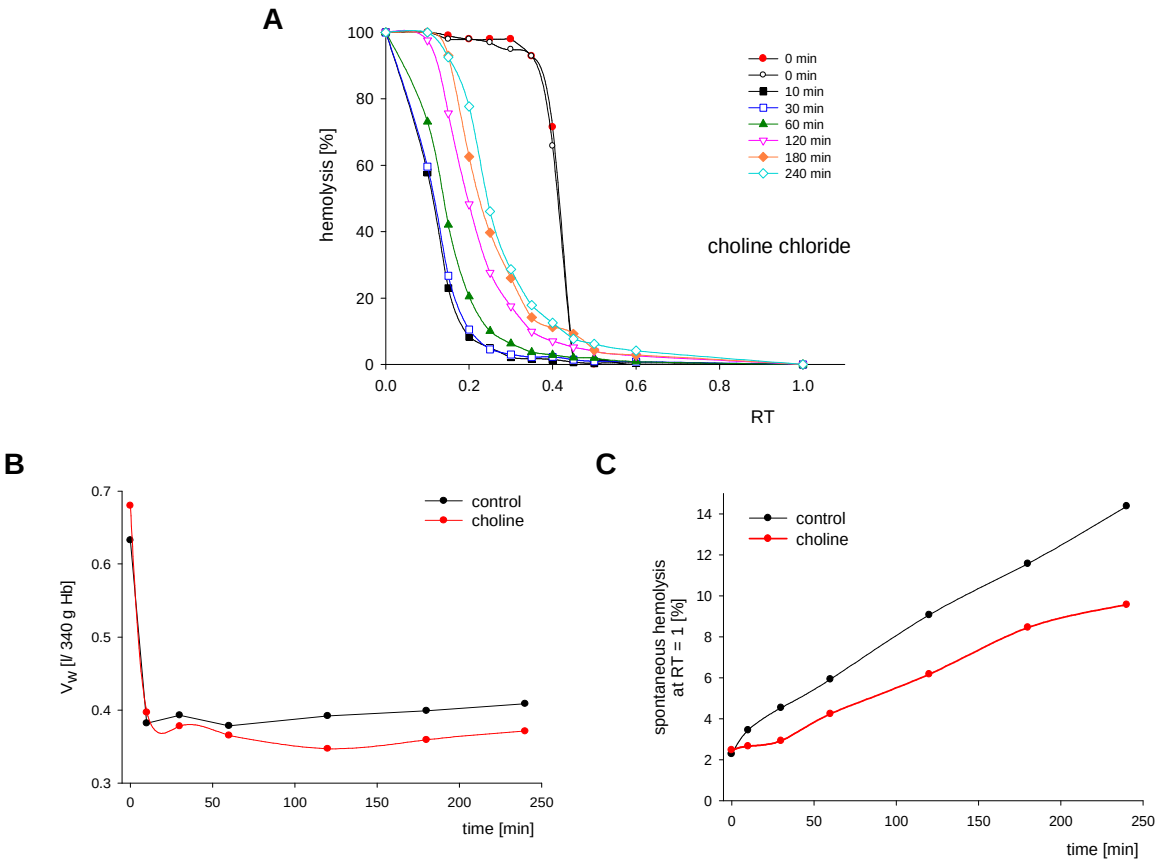

Figure IV. 7. Effects of Na^+ substitution by choline chloride (145 mM) on the time-dependent changes in osmotic fragility, water content and spontaneous haemolysis of RBCs. (A) Osmotic fragility curves over the 4 h duration of the experiments; duplicate controls were taken just before addition of the ionophore A23187. The spontaneous lysis level reported in (C) was subtracted as baseline for these curves. **(B)** Changes in cell water contents (V_W) during the biphasic OFC protocol. **(C)** Cumulative spontaneous cell lysis over 4 h; the percent haemolysis was recorded at a relative tonicity of 1 (RT = 1).

Although the experimental conditions in which such observations were made were very different from those applied here, loss of membrane area by exovesiculation offers a plausible alternative to hydration as the explanation of the right shifts in the OFCs.

Figure IV. 8.

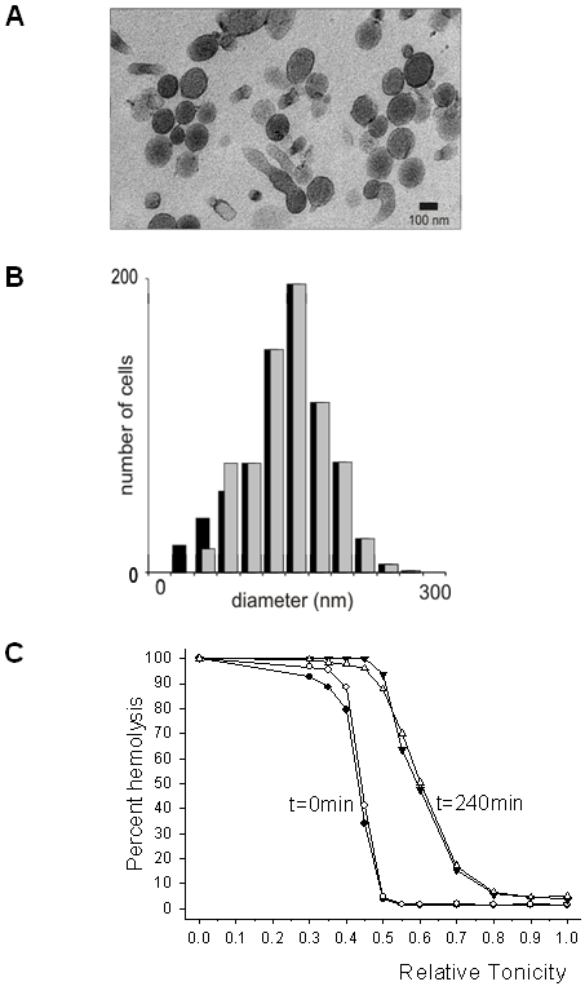

Figure IV. 8. Ca^{2+}-induced exovesiculation. RBCs were Ca^{2+}-loaded as for the standard biphasic protocol except that the suspending medium was either A or AK and the Ca^{2+} concentration in the suspension was 150 µM. The vesicles were harvested after 4 h incubation at 37°C as described in paragraph III. 3. 2. **(A)**. Transmission electronmicrograph showing representative sample of vesicles and membrane fragments from spontaneously lysed ghosts. **(B)** Distribution of vesicle diameters in a population of 732 vesicles (gray bars). The distribution was extrapolated to zero (black bars) for analysis by the method of Giger and Riedwyl*. This analysis rendered a mean and standard deviation of (160 ± 40) nm for vesicle diameters. **(C)** RBCs suspended at 5% Hct in a 100 mM $[K^+]$ medium (AK solution) with 0.15 mM initial $[Ca^{2+}]_o$ and incubated at 37°C with continuous magnetic stirring. The ionophore A23187 was added at t = 0 to a final concentration of 10 µM in the cell suspension. Cells were sampled in duplicate for osmotic fragility and vesiculation just before ionophore addition and at t = 4h.

* Giger H, Riedwyl H. Bestimmung der Größenverteilung von Kugeln aus Schnittkreisradien. Biometrische Zeitschrift. 1970;12:156-162.

To investigate the contribution membrane area loss makes to the right-shifts in OFCs, if any, we measured the loss of cell volume and membrane area from Ca^{2+}-loaded RBCs exposed to the biphasic OFC protocol and also from RBCs suspended in a 100 mM $[K^+]_o$ medium (AK) whose 4 h OFC shift is shown in Fig. IV. 8C. The loss of cell volume was estimated from the total content of Hb recovered in the vesicle pellets and from the mean Hb concentration in the cells from which the vesicles were formed, estimated at 34 g/dl in the initially normal-volume cells suspended in the 100 mM $[K^+]_o$ medium. In the dehydrated cells, whose measured water content was reduced from 0.62 to a mean of 0.38 l/(340 g Hb) over the 4 h period of vesicle pellet collection (Fig. IV. 1C), the mean Hb concentration was calculated to 55 g/dl. The volume of RBC cytosol within vesicles released by 4 h after the initiation of the Ca^{2+} load amounted to 0.44% of the total cytosolic volume contained within the dehydrated RBCs, and 0.41% for the cells incubated in the 100 mM $[K^+]_o$ medium. The electron microscopical appearance of the Hb-containing vesicles is shown in Fig. IV. 8A. The material released from the Ca^{2+}-loaded cells shows abundant round vesicles containing dense material, and also a variety of irregularly shaped membrane-bound structures derived from the spontaneously lysed RBCs during the processing stages for EM. There were no detectable differences in the appearance of the vesicles derived from dehydrated and non-dehydrated cells. The strong membrane staining helped distinguish equatorial sections of vesicles displaying a sharply defined edge from those obtained at a slanted angle away from the equatorial plane showing a more diffuse membrane edge. The distribution of diameters in all circular, well defined vesicles was analyzed by the method of Giger and Riedwyl[*], and the results are shown in Fig. IV. 8B. Analysis of 732 vesicles rendered a mean and standard deviation of (160 ± 40) nm for the vesicle diameters. The contribution membrane area loss makes to the right shift in the OFCs according to these results

[*] Giger H, Riedwyl H. Bestimmung der Größenverteilung von Kugeln aus Schnittkreisradien. Biometrische Zeitschrift. 1970;12:156-162

is considered in detail in the section IV. 1. 2. Discussion.

IV. 1. 2. Discussion.

The present results show that the increase in the osmotic fragility of human RBCs induced by prolonged exposure to elevated $[Ca^{2+}]_i$ is associated with barely detectable water gains (Fig. IV. 1C and Fig. IV. 4C) contrary to the conventional wisdom that shifts in OFCs represent changes in the hydration state of RBCs in all conditions. We analyse next the significance of these observations and consider the possible mechanisms responsible.

There are three general mechanisms that can elicit increased osmotic fragility in RBCs: i) cell hydration following net solute gains, ii) membrane area loss, and iii), altered membrane properties generating a propensity for pre-spherical membrane rupture during rapid volume expansion, as induced in the course of osmotic fragility measurements. The present results show that the contribution of cell hydration to the observed right shifts is minimal, not exceeding 8% over 4 h. Therefore, over 90% of the shifts must result from membrane area loss, altered membrane properties, or both. The contribution of membrane area loss from Ca^{2+}-loaded RBCs is analysed next.

To estimate the contribution of exovesiculation to the right shifts we need to calculate first the fraction of membrane area lost (f_A) from RBCs as a function of mean vesicle diameter ($\overline{d}$) and then the expected right shift in RTL (Eq. III. 1) as a function of f_A. For a vesicle volume-fraction f_v, mean RBC volume and area, $\overline{V_C}$ and $\overline{A_C}$ respectively, f_A can be estimated from:

$$f_A = \frac{6 f_v \overline{V}_C}{\overline{A}_C \overline{d}} \qquad \text{(IV. 1)}$$

This function is plotted in Fig. IV. 9A and shows the hyperbolic dependence of f_A on $\overline{d}$.

Figure IV. 9.

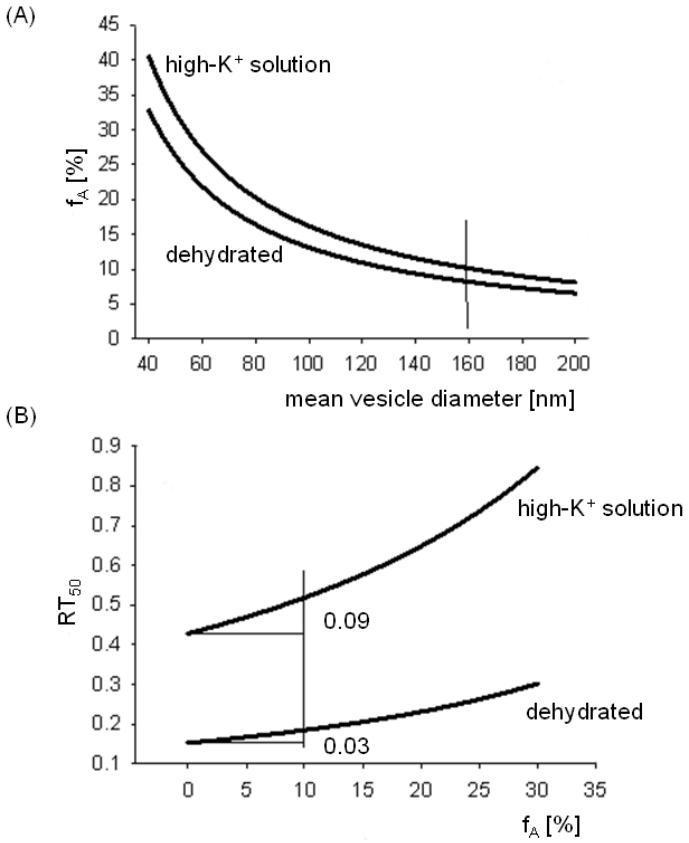

Figure IV. 9. Effects of membrane area loss by exovesiculation on the osmotic fragility of Ca^{2+}-loaded RBCs. (A) The fractional membrane area loss (f_A) as a function of mean vesicle diameter was estimated for dehydrated (lower curve) and normal-volume (upper curve) RBCs (such as those incubated in 100 mM K^+, Fig. IV. 8C), as detailed in Discussion (paragraph IV. 1. 3). The thin vertical line indicates the mean vesicle diameter obtained from the results shown in Fig IV. 8. **(B)** Osmotic fragility shifts, estimated as RT_{50} displacements, as a function of fractional membrane area loss (f_A) for dehydrated (lower curve) and normal-volume RBCs (upper curve). The value of the RT_{50} displacements predicted for a 10% membrane area loss for dehydrated and non-dehydrated RBCs are shown next to the vertical line at f_A = 10%.

Bottom and top curves were estimated from $f_v\overline{V_C}$ values corresponding to dehydrated (0.0044x57 μ^3) and normal-volume (0.0041x90 μ^3) RBCs, respectively, and a mean initial membrane area of 140 μ^2. The estimated membrane area loss by the release of vesicles with a mean diameter of 160 nm is about 10% (Fig. IV. 9A). To estimate the magnitude of the expected shifts in osmotic fragility we rewrite Eq. III. 1 expressing the right shift in the OFCs at the 50% lysis level, as an arbitrary displacement index. Thus, RTL becomes

RT_{50}, as follows:

$$RT_{50} = \frac{V_w}{\frac{(A_C(1-f_A))^{1.5}}{6\sqrt{\pi}} - V_H} \quad \text{(IV. 2)}$$

and plot RT_{50} as a function of f_A (Fig. IV. 9B). It can be seen that the right shift in RT_{50} for an estimated membrane area loss of about 10% is about 0.03 RT units for the dehydrated RBCs (Fig. IV. 9B, dehydrated) and about 0.09 RT units for the RBCs incubated in the 100K media (Fig. IV. 9B, 100 K^+). These values fall short of the observed 0.22 and 0.16 RT units shift after 4h in the OFCs of dehydrated and normal-volume RBCs, respectively, estimated at their 50% lysis level in Fig. IV. 1A and Fig. IV. 8C. The measured shifts correspond to exovesiculation contributions of 14% and 56% in dehydrated and normal-volume RBCs, respectively. Two important caveats to bear in mind, however, concern the large coefficient of variation in vesicle size distribution, of about 25% (Fig. IV. 8B), and the fact that the contribution of smaller vesicles to membrane area loss is much more substantial than that of larger ones (Fig. IV. 9A). The calculations above, based only on the measured means of Hb concentration and vesicle diameter, underestimate the true contribution of exovesiculation to membrane area loss. A detailed mathematical analysis of this asymmetry is currently being undertaken, but it is outside the scope of the present work.

IV. 2. Second question: Does membrane deformation induce channel activity?

IV. 2. 1. Results.

In recent electrophysiological investigations performed in the lab on human RBC membrane, the C-A configuration was used for measuring on intact cells the current through the membrane patch trapped within the tip of the microelectrode (Bouyer et al. 2006; Bouyer et al. 2007; Decherf et al. 2007; Lapaix et al. 2008). This configuration has been seldom used due to the extreme fragility of the human RBC membrane and very

few related papers are available in the literature. However, in spite of inherent technical difficulties, patch clamping intact cells, because it respects the integrity of the intracellular machinery, is the most suitable technique for describing the channels contribution to the maintenance of cell homeostasis or to adaptative processes in experimental situations close to physiological environment.

In the RBC patch clamp technique, the glass microelectrode (~1 μm^2 in area) filled with an appropriate solution, is brought in contact with the surface of a cell and GOhm seals are obtained by slight depression of 10 mmHg applied in the microelectrode pipette for less than 5 s. Comparable good seals can be obtained without depression but this manoeuvre increases considerably the success rate of this critical phase. Once the seal is established, the membrane deformation induced by the glass pipette, regardless of the intensity of depression, is not under experimental control and may vary from one cell to another.

In the previous studies carried out in this group, it was constantly observed that spontaneous channel activity was not frequently recorded when cells were bathing in physiological saline solution. However, it was sometimes possible to detect transient activity immediately following seal formation when contact was facilitated by depression. These observations prompted this work aimed at determining to what extent membrane deformation accompanying seal formation could induce channel activity.

Because this activity was visible only in cells suspended in Ca^{2+}-containing media, we made the hypothesis that local deformation of the human RBC could activate a calcium conductive pathway resulting in increased intracellular calcium level and subsequent Ca^{2+}-sensitive K^+ channel (Gardos channels, IK1, hSK4) activity. This assumption was supported by previous observations of enhanced Ca^{2+} permeability induced by physio-

logical shear stress (Johnson and Gannon 1990; Johnson and Tang 1992; Johnson 1994) and by reports of mechanosensitive calcium influx into RBCs (Cordero and Romero 2002; Egee et al. 2002; Bao et al. 2004; Brain et al. 2004). In addition, the well documented instance of P_{sickle}, indicates that a poorly selective Ca^{2+} permeability pathway is present in human RBC and may become active in deoxygenated RBCs from sickle cell anaemia patients (Ney et al. 1990; McGoron et al. 2000; Lew et al. 2002; Lew and Bookchin 2005; Lew et al. 2005; Oyewole et al. 2008).

In this series of experiments more than 500 GOhm seals were obtained by imposition of a slight depression in the pipette. The mean duration of a C-A seal was (25 – 35) min. The noiselevel remained always in the ± 0.08 pA range which constitutes excellent conditions for detection and measurement of tiny electrical currents through channels in the cell membrane at the spontaneous membrane potential.

IV. 2. 1. 1. Evidence for spontaneous channel activity following seal formation.

Using the C-A configuration with solution RnS (150 mM NaCl, pCa3) in the pipette and bath, RBC membrane displayed no single channel activity when recordings were performed more than 10 min after seal formation at the spontaneous membrane potential, i.e. in absence of pipette potential ($-V_P$= 0 mV), whatever the degree of membrane deformation induced by depression. However, recordings made during the first 10 min following seal formation frequently displayed inward current at the spontaneous membrane potential corresponding to long channel openings followed by long silent intervals (Fig. IV. 10A). The presence of channel activity at hyperpolarizing or depolarizing voltages in this specific configuration was not the initial purpose of this study and for the sake of clarity will be addressed further in this work.

In contrast, when NaCl was replaced by KCl (solution High-K, pCa3) in pipette solution, channel activity was always observed immediately following seal formation as bursts of

Figure IV. 10. Evidence for spontaneous channel activity following seal formation. Patch-clamp single-channel recordings of red blood cell membrane electrical activity obtained during the first 10 min following seal formation at the spontaneous membrane potential, *i.e.* in absence of pipette potential (-Vp= 0 mV). Panel **A** shows two typical recordings obtained with solution A (containing, in mM/l, 150 NaCl, 5 KCl, 1 MgCl2, 10 Hepes, 10 glucose, adjusted to pH 7.4 and pCa3) in the pipette and bathing solutions. (**B**) shows four different recordings, obtained with solution B (containing, in mMl/l, 150 KCl, 5 NaCl, 1 MgCl2 10 Hepes, adjusted to pH 7.4 and pCa3) in the pipette and solution A in the bath. Dashed lines indicate the baseline corresponding to the closed state, dotted lines correspond to full open states. Panel **C** presents an example of I/V plot obtained when 1 min ramps of depolarizng or hyperpolarizing voltages were imposed in the pipette in the following order: (in mV) 0, -10, +10, -20, +20, -30, +30, -40, +40, immediately following seal formation.

Figure IV. 10.

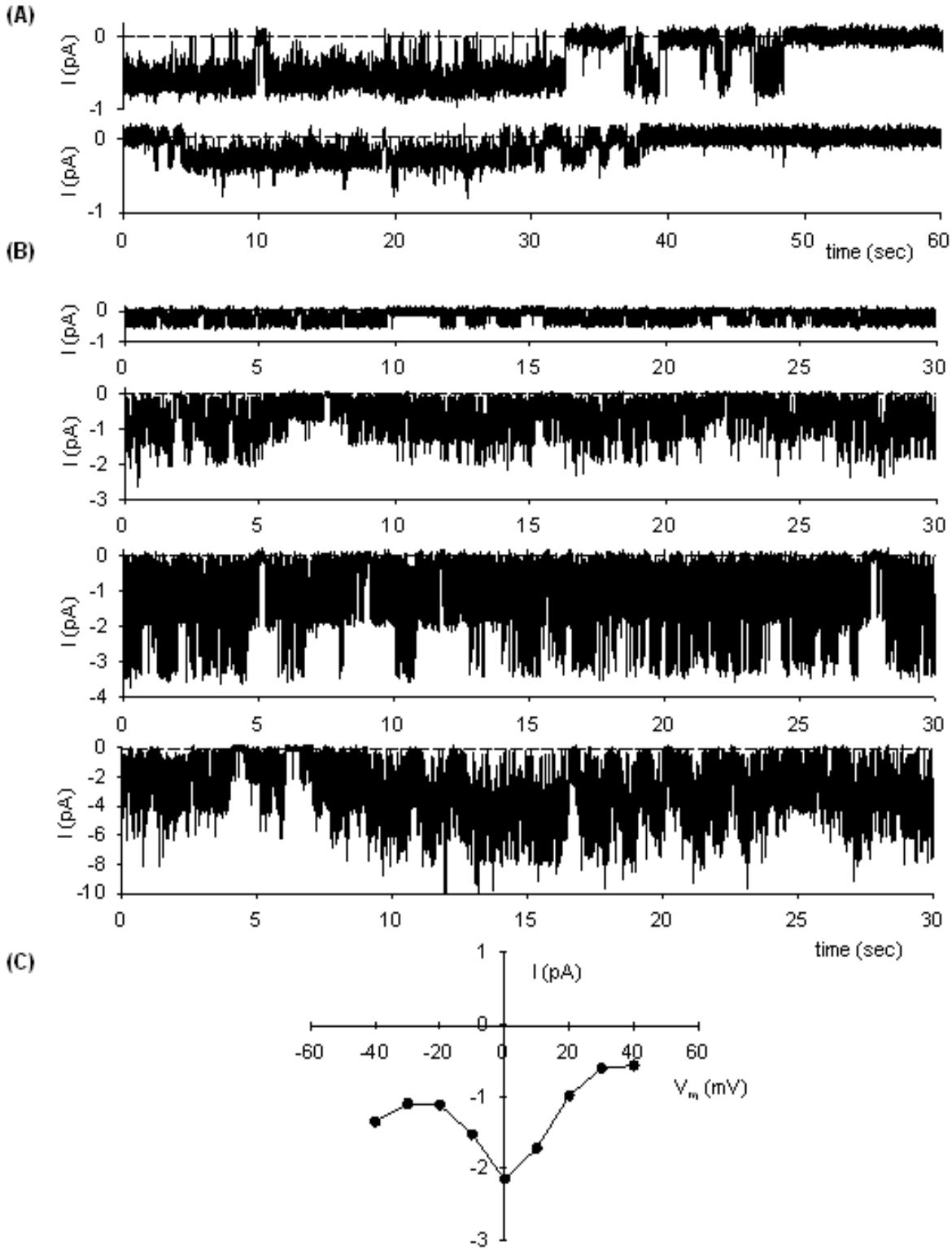
(A)
I (pA)
0
-1
0
-1
0
10
20
30
40
50
60
time (sec)
(B)
I (pA)
0
-1
0
5
10
15
20
25
30
I (pA)
0
-1
-2
-3
I (pA)
0
-1
-2
-3
-4
I (pA)
0
-2
-4
-6
-8
-10
time (sec)
(C)
I (pA)
1
0
-1
-2
-3
-60
-40
-20
0
20
40
60
V_m (mV)

channel openings separated by brief closures and all patches contained one or more active channels (Fig. IV. 10B). The intensity of the current recorded at V_m= 0 mV varied from one cell to another in the range -0.30 pA to -2.5 pA indicating an inwardly directed movement of cations or an opposite movement of anions. It is important to note at this point that the intensity of the recorded current was not correlated with the intensity of the depression imposed.

IV. 2. 1. 2. Transient nature of recorded currents.

In first attempts to characterize this channel activity we started a protocol of hyperpolarizing and depolarizing ramps aimed at establishing I/V curves and kinetics calculations. To help follow the issues addressed here we need to describe a typical sequence of voltage changes. 60-second-long current recordings were usually obtained for each imposed voltage in the following order: (in mV) 0, ±10, ±20,..., ±100. Using this protocol we constantly obtained unusual V-shaped I/V curves (Fig. IV. 10C) which could be explained by assuming continuous decline with time of the channel activity whatever the value of potential imposed to the patch membrane.

Figure IV. 11 validates this assumption since most of the currents recorded during the first minutes at 0 mV (panel A) displayed rapid reduction. Panel B depicts minute by minute the evolution with time of currents recorded at 0 mV in 35 different patches. It appears clearly during the first 5 min all patches exhibited a large variety of current amplitudes in the range (-0.3 – -2.5) pA but none of them were silent. After the first 5 min an increasing number of patches displayed extinction of electrical activity whilst the others continued their progressive decline which was always completed within ~17 min after seal formation. The patterns of P_O evolution also varied from one cell patch to another and it was remarkable that the rapid evolution of large current amplitudes were not associated to rapid reduction of P_o. Hence, P_o values (panel C) corresponding to the

Figure IV. 11. Transient nature of recorded currents. (A) provides an example of progressive decline of a large channel activity recorded at different times after seal formation with High-K solution in the pipette solution and RnS solution in the bath at 0 mV pipette potential. **(B)** summarizes the evolution of currents recorded from 35 separate patches during the first 16 min and **(C)** displays the corresponding evolution of the open probability (P_o). Once the current was stable in the range (-0.3 – -0.5) pA, the currents obtained by evoking a series of test potentials from -100 to +100 mV for 15 s from a holding potential of 0 mV were recorded as shown in the example of panel **D** and the corresponding I/V pairs were collected in the I/V plot displayed in **(E)** (127 points from 14 experiments).

Figure IV. 11.

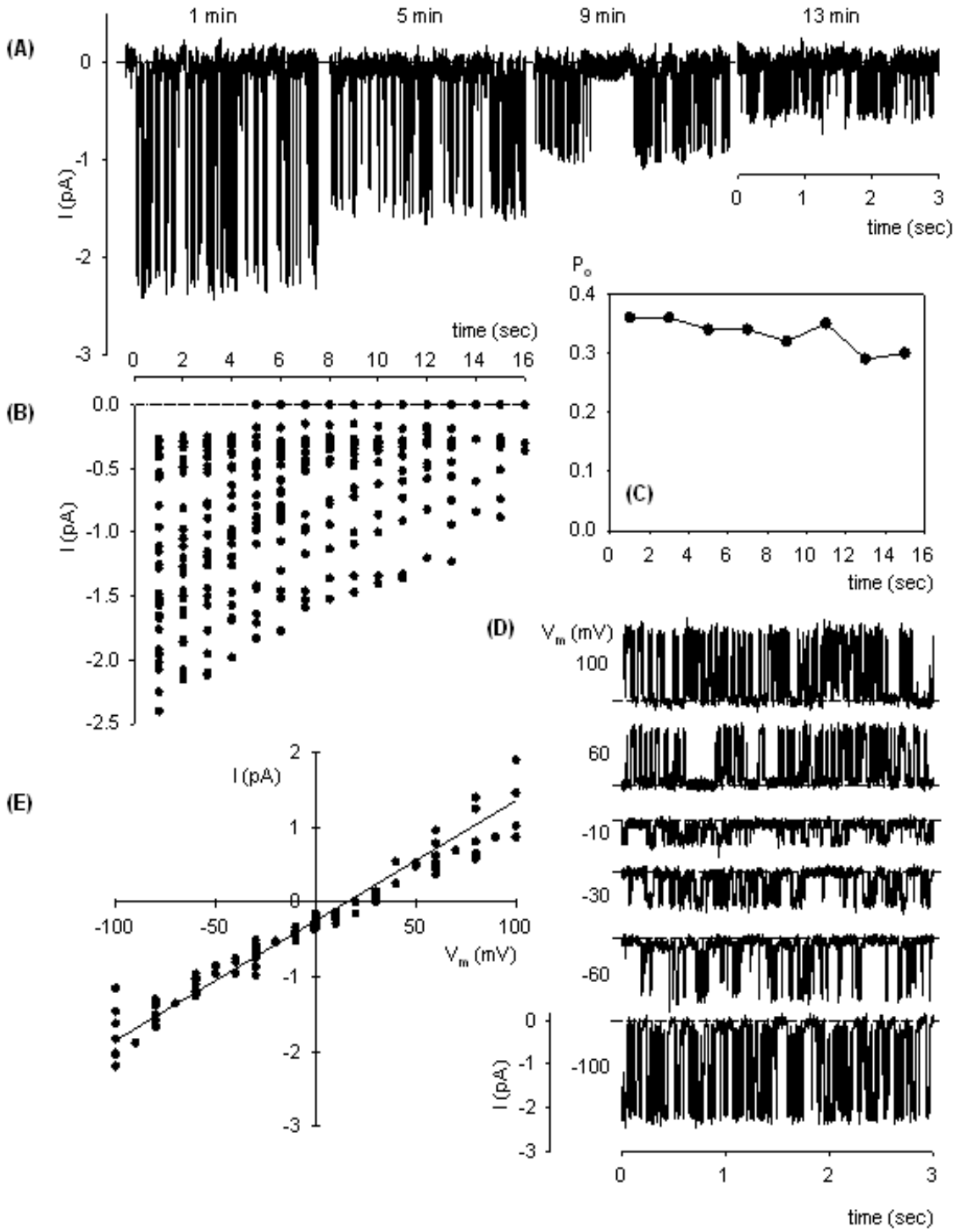
(A)
1 min
5 min
9 min
13 min
I (pA)
time (sec)
(B)
I (pA)
time (sec)
(C)
P_o
time (sec)
(D)
V_m (mV)
100
60
-10
-30
-60
-100
I (pA)
time (sec)
(E)
I (pA)
V_m (mV)

current amplitudes depicted on panel A showed no significant decline whilst the amplitude fell by more than 1.5 pA. We constantly observed that most currents recorded after reaching the (-0.3 – -0.5) pA range remained constant at this level for a few minutes before total extinction of channel activity, and that this final extinction occurred at constant current amplitude by progressive decline of P_o. We took advantage of this time of relative stability to record the currents obtained at different imposed potentials (Fig. IV. 11D). The mean I/V curve presented in Fig. IV. 11E was established in the voltage range -100 mV to +100 mV by steps of 10 mV. It shows no significant deviation from linearity and the ohmic channel conductance calculated between -100 mV and +100 mV is 14.5 pS (127 points from 14 experiments).

We must now complete this description by saying that in many case we could record very fast transitions (Fig. IV. 12). These current changes could happen in either of three ways: as fast (3 s) but progressive transition from large current to (-0.3 – -0.5) pA level (Fig. IV. 12A), as an instantaneous transition from large to (-0.3 – -0.5) pA (Fig. IV. 12B-C), as an instantaneous transition from a large to an intermediary current (Fig. VI. 12D) which thereafter followed its progressive decline to total extinction. The addition of these different patterns on a multi-channel patch could thus lead to confusing situations where large and small currents were superimposed, some channels being in the process of decline whilst other channels had already reached the (-0.3 – -0.5) pA level.

IV. 2. 1. 3. Identification of Gardos channels.

In another series of investigations we changed the initial pipette and bathing solutions and first tested the effect of having 150 mM KCl (pCa3) in the extracellular compartment. Patch clamping RBCs in high extracellular potassium conditions with 150 mM KCl in the pipette resulted in symmetrical channel activity with reversal potential at 0 mV as shown in Fig. IV. 13A. When pipettes were filled with RnS solution whilst the bathing solution

Figure IV. 12. Fast transitions. In margin of the typical progressive decline of electrical activity, three types of fast transition could be recorded: **(A)**, fast (3 s) but progressive transition from a large current (-1.4 pA in the present case) to a stable (-0.3 – -0.5) pA current. **(B)** and **(C)**, instantaneous transition from large (-1.8 pA in the present case) to a stable (-0.3 – -0.5) pA current. **(D)**, instantaneous transition from a large (-1.7 pA in the present case) to an intermediary current (-0.9 pA in the present case) which thereafter followed progressive decline to a stable (-0.3 – -0.5) pA current level.

Figure IV. 12.

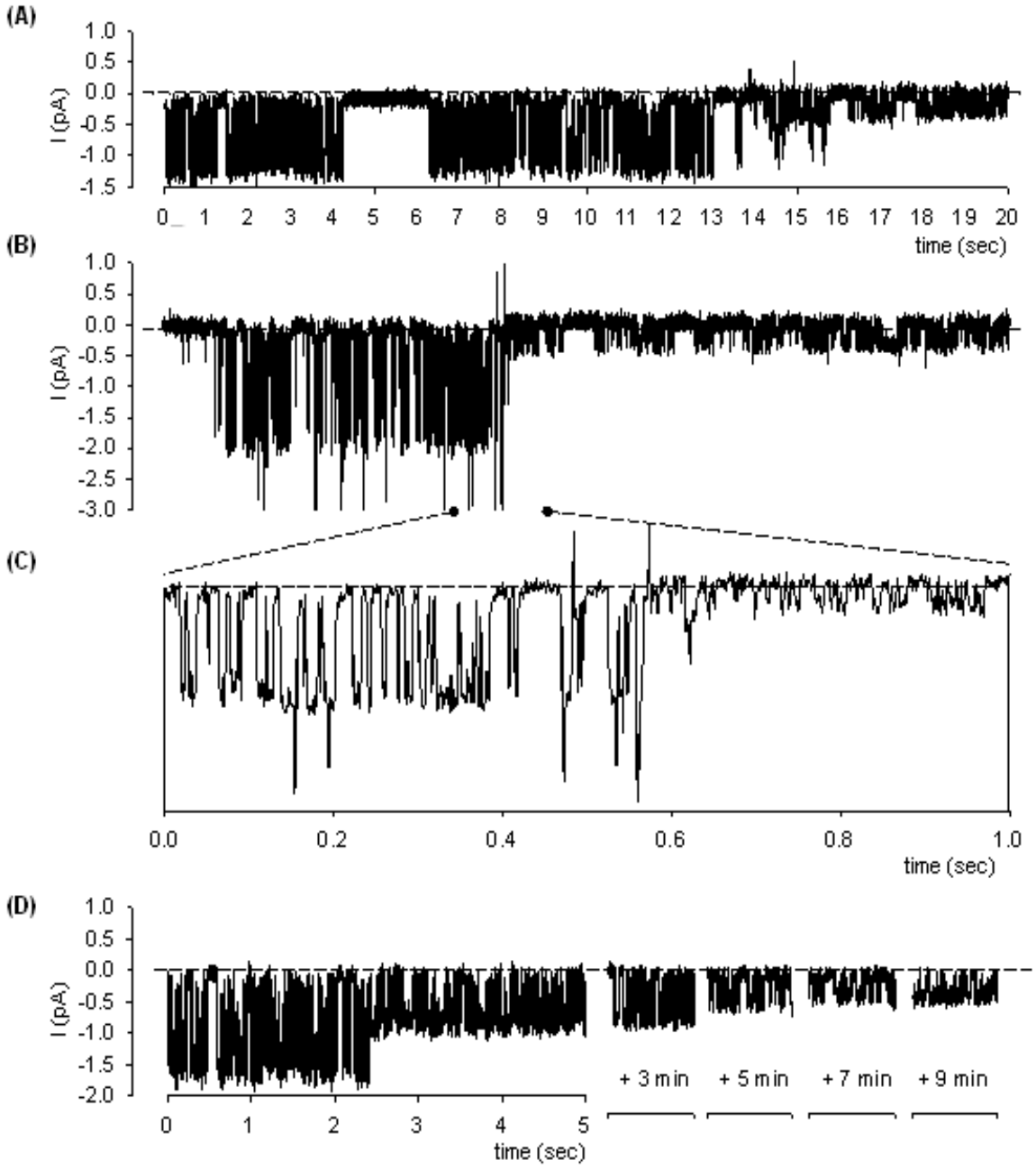
(A)
I (pA)
time (sec)
(B)
I (pA)
(C)
time (sec)
(D)
I (pA)
+ 3 min
+ 5 min
+ 7 min
+ 9 min
time (sec)

Figure IV. 13. Identification of Gardos channels. (A) and **(B)** Patch clamp single-channel recordings and corresponding I/V relationships of red blood cell membrane electrical activity obtained **(A)** with High-K solution in the pipette and High-K solution in bath, and **(B)** with High-K solution in bath and RnS solution in the pipette. The inset displays the corresponding evolution of the P_o (closed symbols: (A); open symbols: (B)). **(C)** and **(D)** show, at 0 mV and -40 mV pipette potentials, inhibition of channel activity by clotrimazole (C: control; D: clotrimazole added in the bathing solution at the concentration of 10 µM). Requirement of extracellular calcium for activation of Gardos channels is demonstrated in **(E)** by almost total absence of channel activity whatever the imposed pipette potential (0 mV and -40 mV in the presented recordings) when the bathing solution was RnS solution adjusted to pCa7 and pipettes contained High-K solution adjusted to pCa7.

Figure IV. 13.

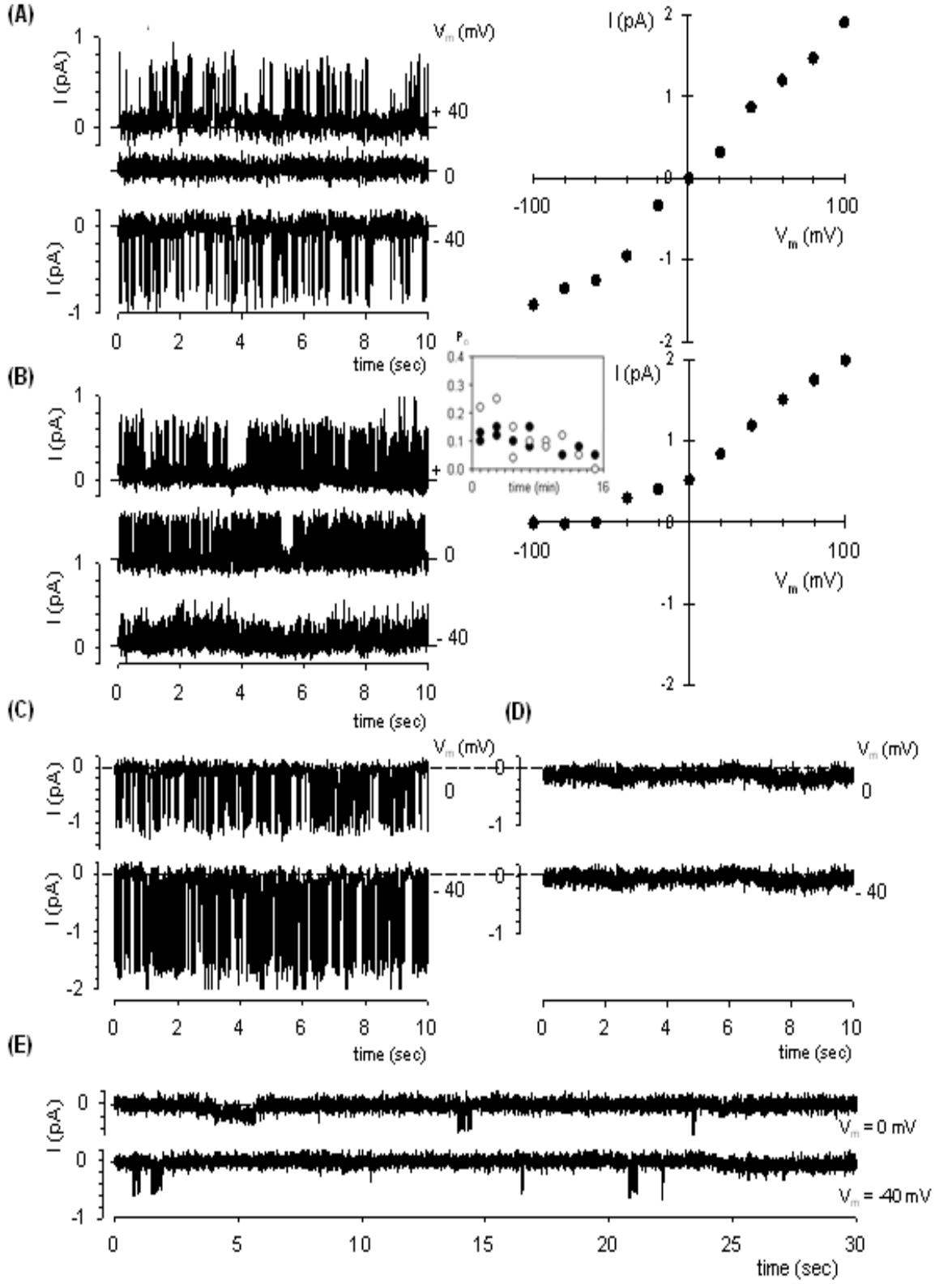
(A)
(B)
(C)
(D)
(E)
I (pA)
V_m (mV)
+ 40
0
- 40
time (sec)
P_o
time (min)
-100
100
V_m = 0 mV
V_m = -40 mV

still contained high potassium, only outward currents could be observed at all imposed potentials (Fig. IV. 13B). These changes in current direction, in agreement with changes in potassium gradients (whilst chloride gradients remained constant), denoted a cationic channel activity which could be clearly identified as a Gardos channel activity after inhibition by CLT (Fig. IV. 13C-D) added in the bathing solution at the concentration of 10 µM and by typical conductance and kinetic properties.

This conclusion was comforted by the observation that strictly no channel activity was detected, whatever the voltage imposed, when pipette and bathing solution contained low level of calcium (pCa7) (Fig. IV. 13E). This absence of activity was also reported for the configuration pCa7 in bath/pCa3 in pipette, whereas activity was still visible in the configuration pCa3 in bath/pCa7 in pipette. It is important to note that conditions of low calcium concentrations in the bathing solution reduced considerably the success rate of getting GOhm seals (less than 25% instead of 50%).

The above data demonstrate that activation of a calcium permeability pathway leading to sudden increase in intracellular free calcium concentration was responsible for the observed activation of IK1 channel immediately following seal formation.
In absence of $[Ca^{2+}]_i$ measurement, the only way to determine if this activation was constant or transient was to compare with the activity recorded in the presence of vanadate which, at the concentration of 1 mM, inhibits 80% of calcium extrusion by PMCA and thereby maintain relatively constant the intracellular free calcium level.

Added in the bathing solution (2 – 3) min before seal formation, vanadate did not modify the initial diversity of current amplitudes which also underwent progressive decline (Fig. IV. 14A), but considerably delayed this evolution. Following seal formation, none of the 25 patches of this series of experiments ceased electrical activity. Fig. IV. 14B shows

that during the first 5 min the mean P_O value remained constant indicating that during this interval all amplitude variations occurred at constant P_O, whereas without vanadate the constant decline of the mean P_O value indicates that only a limited number of patches displayed this pattern.

Figure IV. 14.

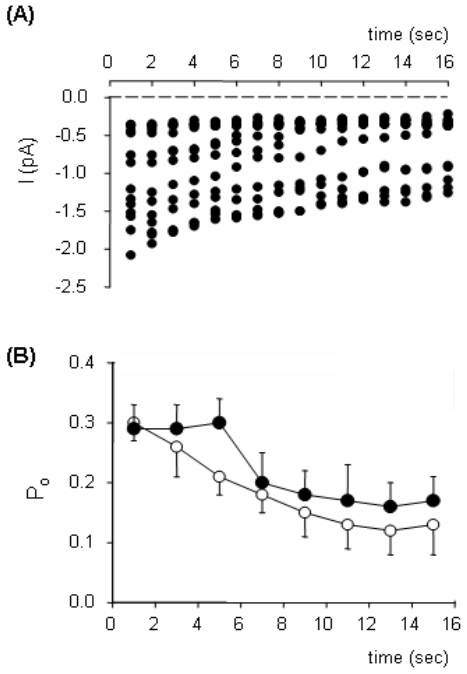

Figure IV. 14. Inhibition of calcium extrusion by plasma membrane calcium pump (PMCA). (A) shows that vanadate (1 mM) delayed the progressive decline of current amplitude depicted in Fig. IV. 11. Following seal formation, none of the 25 patches of this series of experiments ceased electrical activity during the first 16 min. **(B)** shows similar evolution of P_o values in control (open symbols) and in the presence of vanadate (closed symbols).

IV. 2. 1. 4. Simulation by mathematical RBC model.

Although the induction of a large K^+ movement from the KCl containing pipette to the intracellular compartment could intuitively be understood as resulting from the massive extrusion of K^+ ions from the cell interior to the NaCl containing extracellular medium, the reasons for the rapid decline of the current intensity and the nature of other associated electrolytic and acid-base changes deserved further calculations and experiments.

At this point, the rapid increase and subsequent decline of the recorded K^+ currents could be erroneously interpreted as resulting exclusively from a massive entry of calcium followed by its rapid extrusion by PMCA. Indeed, a reduction of current amplitude without variation in open probability is not a characteristic feature of Gardos channel extinction (Grygorczyk 1987; Leinders et al. 1992; Dunn 1998) , which suggests an explanation rather related to rapid variations in the electrochemical driving force for K^+ movement through the channel. To address this possibility we used the integrated model originally developed by Lew and Bookchin (Lew and Bookchin 1986) for normal human red cell, with the initial aim to follow the evolution of membrane potential and intracellular K^+ concentration ($[K^+]_i$) when the permeability constant of K^+ through electrodiffusional pathway is suddenly increased. The model is designed as a two compartment closed system (the cells and their surrounding medium) which simulates a red cell suspension in a test tube. After computing the initial reference steady-state representing our experimental conditions (first 2 min) the model described the evolution of the system after sudden activation of an electrodiffusional permeability for K^+ ions (P_K^G).

Figure IV. 15A shows that increasing P_K^G to a value of 10 h^{-1} (which represents a 10^4-fold increase in the ground K^+ permeability of the red cell membrane (Lew and Bookchin 1986) and is within the observed range of valinomycin-induced effects) induces immediate hyperpolarization of the red cell membrane from -12 mV to -60 mV and that the E_m remains quite constant thereafter. In these conditions the drop in the difference $E_m - E_K$ is in keeping with the observed initial K^+ channel activity but the stability of this difference with time and the very limited change in $[K^+]_i$ (Fig. IV. 15B) cannot account for the subsequent decline of measured K^+ currents. The initial simulation had therefore to be re-evaluated by simulating the effect of parallel on-setting of channel-mediated anion permeability which could be reasonably hypothesized according to theoretical and experimental data on K^+-permeabilized red cell (Lew and Bookchin 2005).

Figure IV. 15. Simulation by mathematical RBC model. The predicted effects of sudden and maximal Gardos channel activation on the membrane potential E_m and intracellular K^+ concentration ($[K^+]$) are presented in **(A)** and **(B)**. Electrodiffusional permeability for K^+ ions (P_K^G) was increased to a value of 10 h^{-1} at time t = 2 min. The parameter values chosen for this simulation were 5 mM KCl and 150 mM NaCl in external bathing solution. The initial P_K^G value was 0.001651 h^{-1}; for other steady state default parameters refer to (Lew and Bookchin 1986). **(C)** and **(D)** present the simulated effects on E_m, E_K (equilibrium potential for K^+ ions) and E_A (equilibrium potential for anions) of sudden and maximal Gardos activation (as above) followed by sudden activation of anionic electrodiffusional permeability (P_A^G). At time t = 7 min, P_A^G was changed from 1.2 h^{-1} to 10 h^{-1} (C) or 50 h^{-1} (D) corresponding to moderate and large activations. When the model was run to simulate the effects on the same variables of progressive increase in anionic electrodiffusional permeability **(E)**, P_A^G was changed from 1.2 h^{-1} to 5 h^{-1} at t = 3 min and incremented by 5 h^{-1} each min to reach P_A^G = 35 h^{-1} at t = 18 min). **(F)** displays the corresponding calculated evolution of intracellular K^+ and A^- concentrations.

Figure IV. 15.

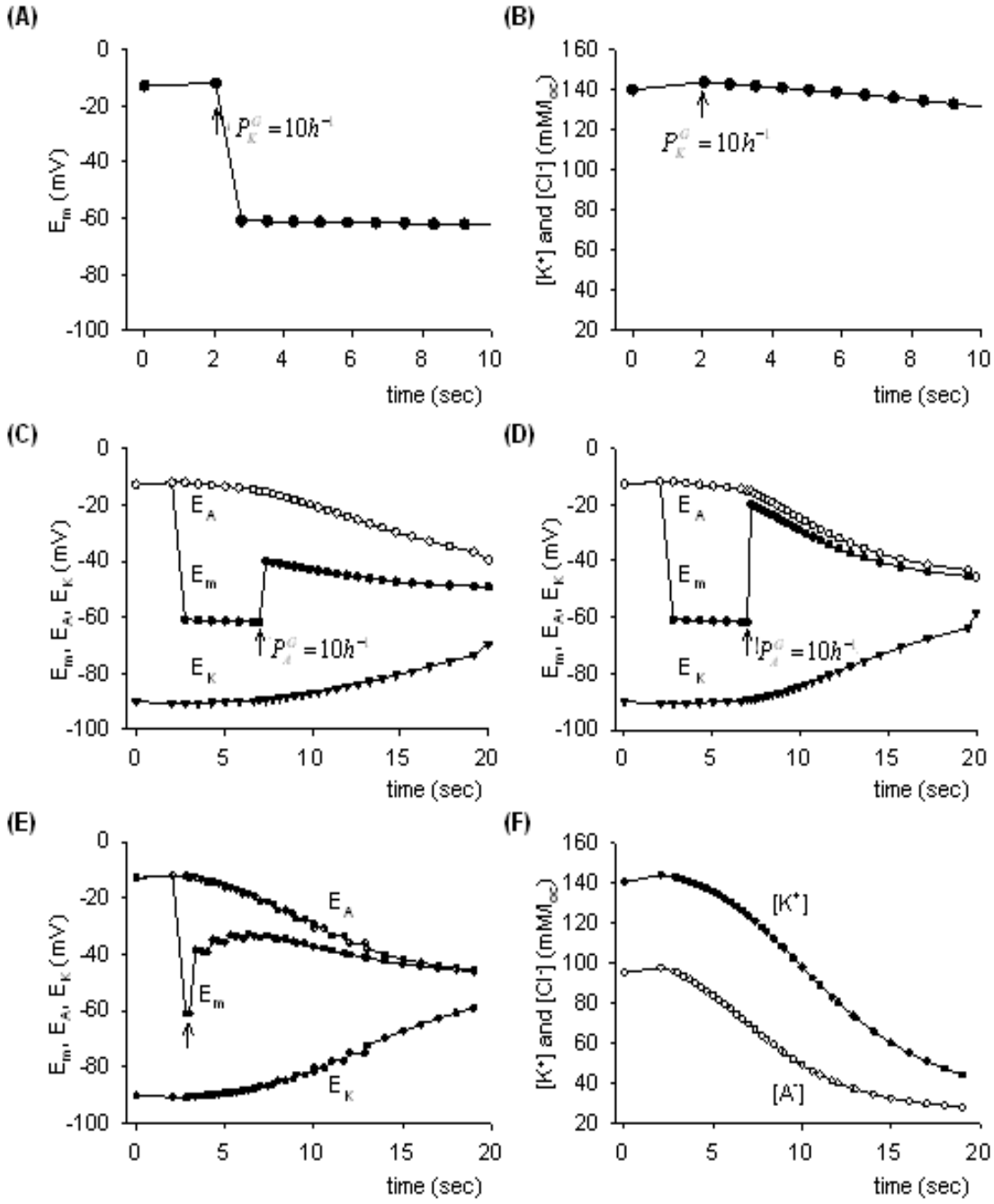
(A)
(B)
(C)
(D)
(E)
(F)
$P_K^G = 10h^{-1}$
$P_A^G = 10h^{-1}$
E_m (mV)
[K+] and [Cl-] (mM$_\infty$)
E_m, E_A, E_K (mV)
time (sec)
E_A
E_m
E_K
[K+]
[A-]

Figure IV. 15C and Fig. IV. 15D show the results of typical simulations with activation of electrodiffusional permeabilities for anions (P_A^G). P_A^G of 10 h^{-1} and P_A^G of 50 h^{-1} can be considered as moderate and large, respectively (Lew and Bookchin 1986). In both cases, when P_A^G activation was simulated 5 min after the onset of P_K^G, the model predicted a large reduction of the hyperpolarization with a shift of E_m towards E_A (equilibrium potential for anions). If we ran the simulation of the effect of sudden and large Gardos channel activation (P_K^G = 10 h^{-1} at t = 2 min) and progressive anionic channel activation (P_A^G = 5 h^{-1} at t = 3 min to P_A^G = 35 h^{-1} at t = 18 min), we observed, as depicted in Fig. IV. 15E, that the initial hyperpolarization declines slowly towards E_A. In this case the observed decline in the recorded K^+ current may reflect the fact that the increase in K^+ permeability hyperpolarizes the cell which generates a driving force for net anion efflux through diffusional pathways. It is important to note that the model also predicts an accompanying water loss which rises concentration of impermeant solutes leading to intracellular dilution of K^+ and diffusible anions, as shown in Fig. IV. 15F.

IV. 2. 1. 5. Evidence for anionic channel activation.

Where, then, are the experimental evidences for anionic channels? In fact they are omni-present on our single channel recordings. Indeed, all recordings presented in the previous figures were selected, for the sake of clarity, because they displayed exclusively Gardos channel activity but it is a matter of fact that, most of the time, this activity was intermingled with another type of channel activity mainly characterized by long openings followed by long closure intervals. Figure IV. 16A presents four characteristic examples of activity commonly recorded where the baseline underlying the K^+ channel current was suddenly shifted due to additional current resulting from the onset of another type of channel activity. These C-A recordings were obtained at the spontaneous membrane potential in absence of imposed pipette potential. The intensity of this current varied slightly from one patch to another and declined with time in a similar manner as the K^+

Figure IV. 16. Evidence for anionic channel activation (a). Patch clamp single-channel recordings of red blood cell membrane electrical activity obtained during the first 10 min following seal formation in absence of pipette potential (-Vp= 0 mV). **(A)** shows four different recordings, obtained with High-K solution in the pipette and RnS solution in bath. The sudden shifts of the baseline underlying the K^+ channel current reflects the onset of an additional type of channel activity. **(B)** presents a sample of recording where the Gardos channel and an anionic channel are present simultaneously and the recording displayed in **(C)** shows, on the same patch, that after total inhibition of channel activity by clotrimazole, added in the bathing solution at the concentration of 10 µM, the remaining activity was characterized by long openings followed by long closure intervals.

Figure IV. 16.

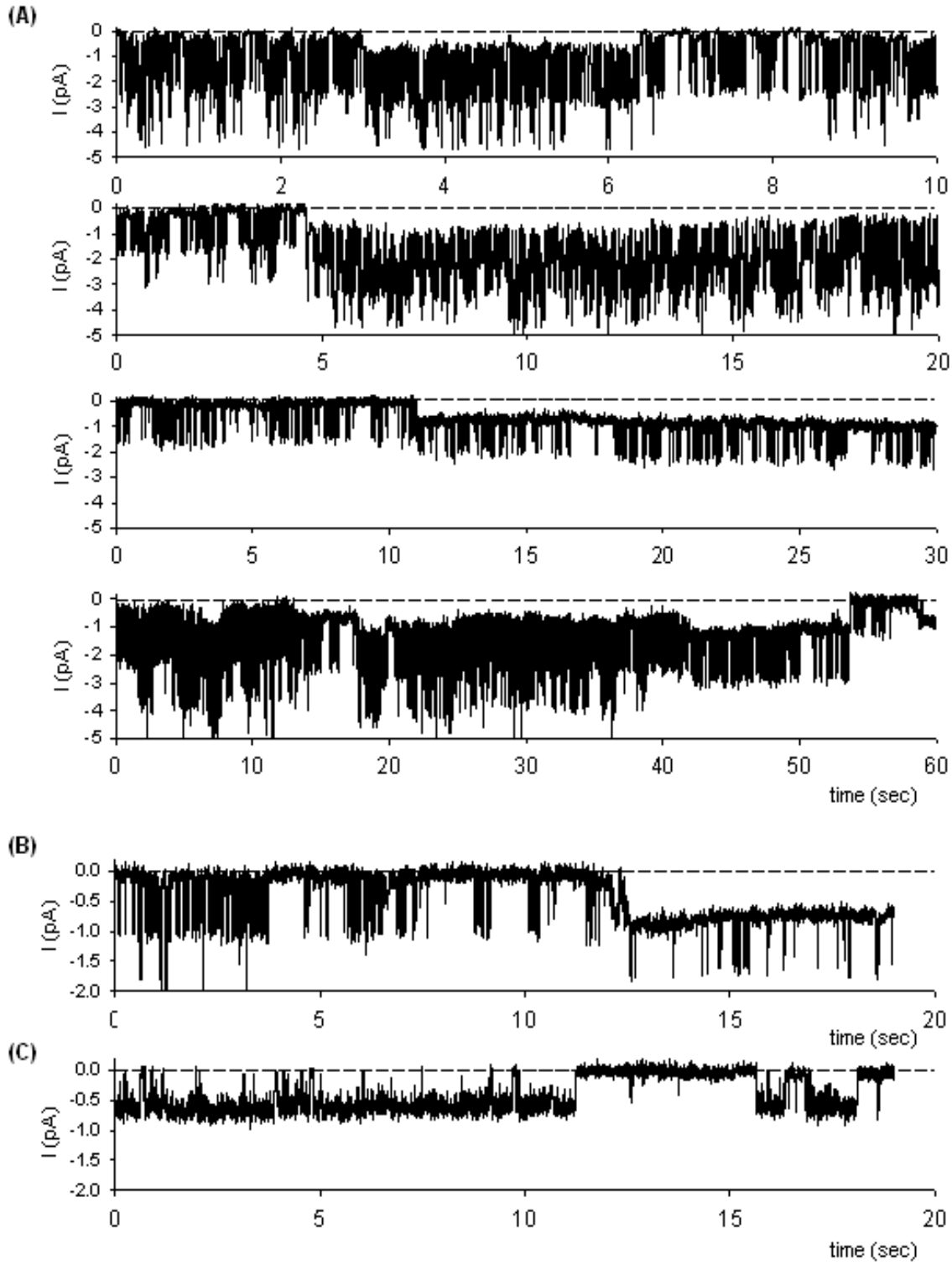

channel activity but the range of these variation remained much smaller (-0.5 mV to -1 pA). Figure IV. 16B-C show that after extinction of the Gardos channel, by adding CLT in the bathing solution at the concentration of 10 µM, the remaining activity displayed long intervals of open state separated by long intervals of closed state. The anionic nature of this activity was evidenced by NPPB and DIDS inhibition and by excision in the excised I-O configuration. In another series of experiments, illustrated in Fig. IV. 17, the small cations Na^+ and K^+ were replaced in pipette and bathing solutions by the large impermeant cation NMDG. Figure IV. 17A shows typical C-A channel activity recorded within the 5 min following seal formation at different imposed potentials. The corresponding I/V curve (Fig. IV. 17B) confirms an inwardly directed current at the spontaneous membrane potential with a reversal potential close to +30 mV. In this NMDG-Cl configuration the Gardos channels activated by seal formation at the whole cell level remained invisible for the C-A recording since le pipette did not contain K^+ ions. This allowed neat recordings of anionic channel activity which, again, could be confirmed by pharmacology and excision. These experiments bring us back to Fig. IV. 10 where recordings made with NaCl in pipette and bathing solutions during the first 10 min following seal formation frequently displayed inward current at the spontaneous membrane potential corresponding to long channel openings followed by long closure intervals which simply reflected the visible anionic activity induced by Gardos activity which remained undetectable by the NaCl-containing pipette.

IV. 2. 2. Discussion.

IV. 2. 2. 1. Activation of Gardos channels.

This work provide the first direct electrophysiological evidence of a Gardos channel activity obtained in absence of ionophore-induced divalent cation permeability (e.g. A23187) or selective activators of IK/SK channels (e.g. compound NS309), by the sole effect of membrane deformation of intact cell. Since the presence of calcium in the

Figure IV. 17. Evidence for anionic channel activation (b). An example of patch clamp single-channel recordings obtained during the first 10 min following seal formation at different membrane potentials, with RnS-NMDG (pCa3) in the pipette and bathing solutions and corresponding I/V relationship.

Figure IV. 17.

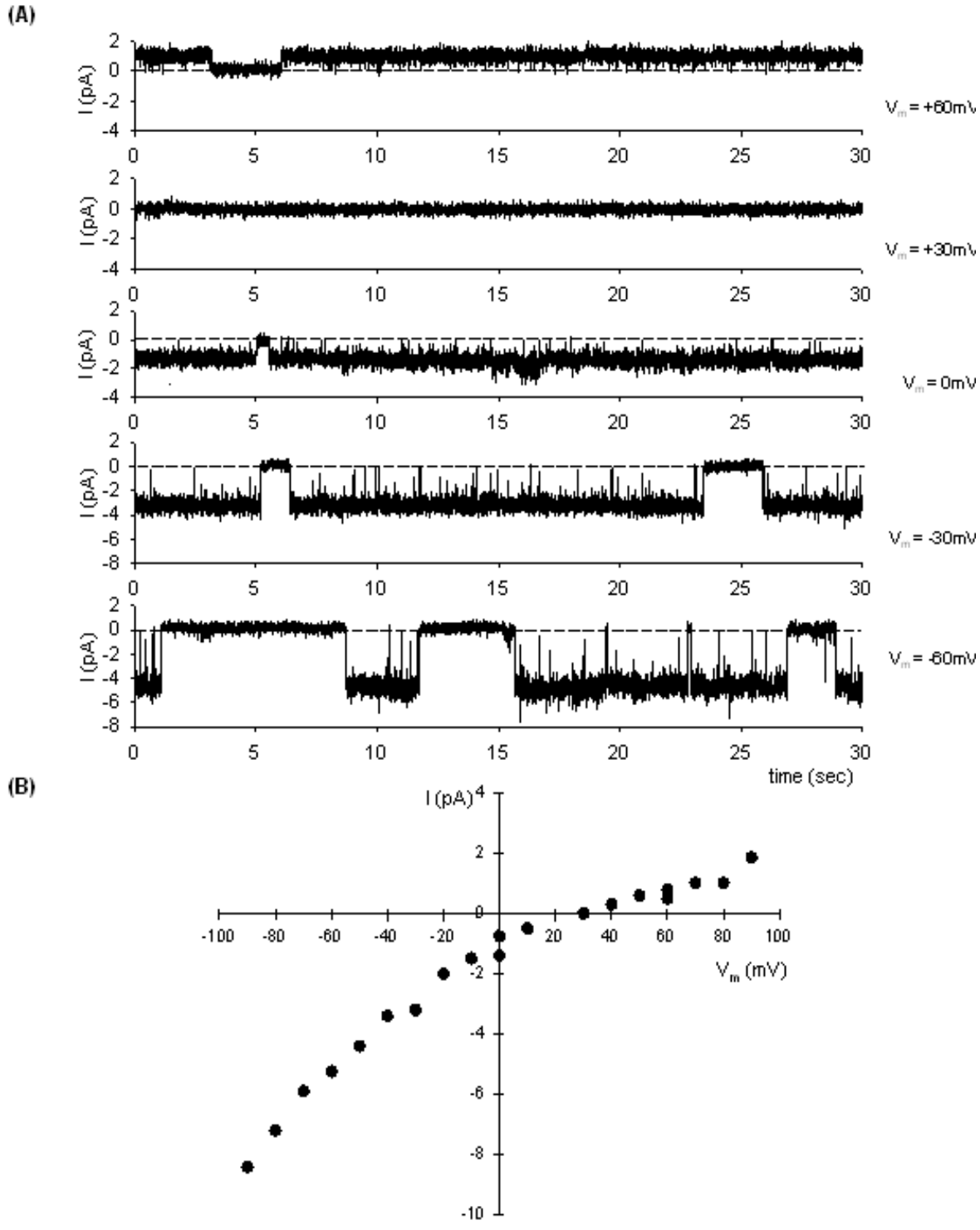

Figure IV. 18.

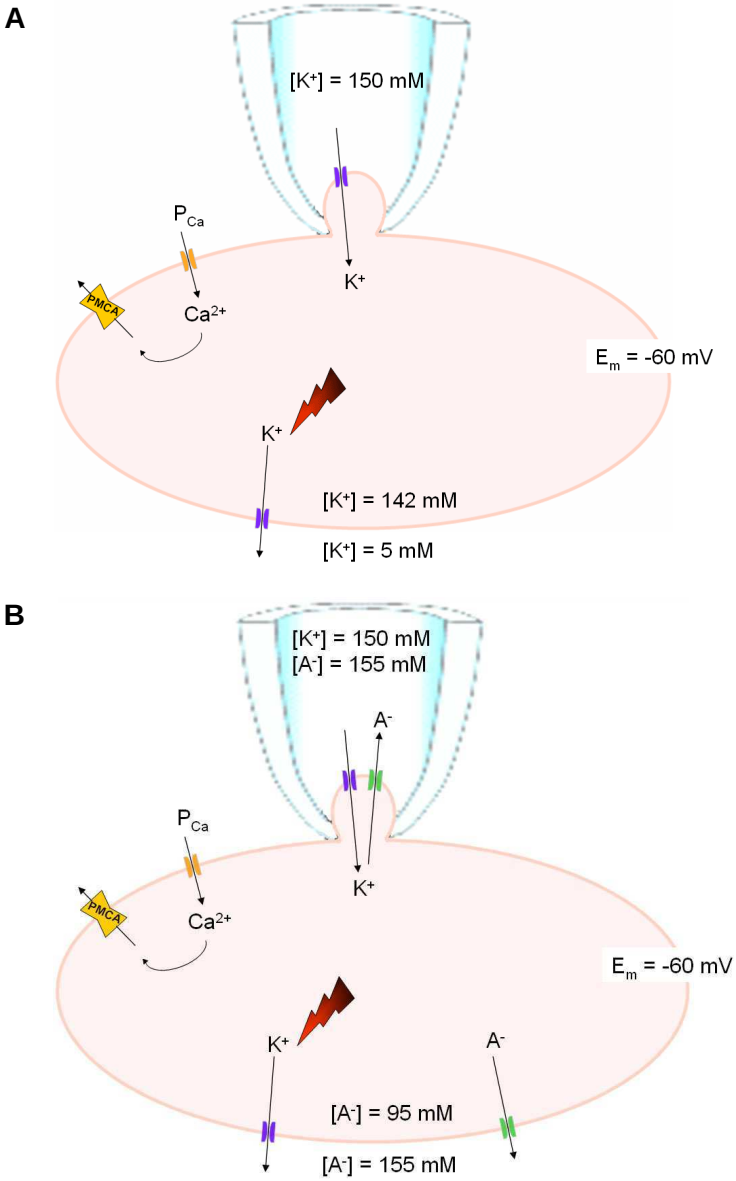

Figure IV. 18. Membrane transporters that participate in the observed events. (A) Upon membrane deformation, calcium enters the cell driven by a steep inward gradient and elevated $[Ca2+]_i$ activates Ca^{2+}-sensitive K^+ channels. K^+ channels activity mediates membrane hyperpolarization which increases the driving force for inward movement of K^+ ions from the high-K^+ pipette solution to the cell interior. In physiological extracellular low-K^+ condition the three compartments (extracellular medium, cell interior, patch pipette) are then in series and the K^+ fluxes are oriented from the pipette to the cell and from the cell to the extracellular compartment. Elevated $[Ca^{2+}]_i$ at the inner membrane surface stimulates uphill Ca^{2+} extrusion through PMCA. **(B)** Hyperpolarization also sets the driving force for net anions loss through A^- electrodiffusional pathways. The slight chemical gradient existing between the bath/pipette (155 mM) and the cell interior (95 mM) was largely overcome by the electrical gradient created by the Gardos channel activation resulting in outward movement of anions both at pipette and whole cell levels.

extracellular medium was crucial in this process, we conclude that it results from activation of a Ca^{2+} permeability pathway. As summarised in Fig. IV. 18, this implies that upon membrane deformation, calcium entered the cell driven by a steep inward gradient and elevated $[Ca^{2+}]_i$ activated Ca^{2+}-sensitive K^+ channels (Gardos channels, IK1, hSK4) via constitutively bound CaM (Fig. IV. 18A). It remains to be elucidated whether the Ca^{2+} entry occurs via an electrodiffusional conductive pathway with a finite Ca^{2+} conductance (P_{Ca}) or via a mechanosensitive stretch-activated NSC channel or via other permeability pathways.

In the present experimental configuration, Gardos channel activity mediated membrane hyperpolarization which increased the driving force for inward movement of K^+ ions from the high-K^+ pipette solution to the cell interior. In physiological extracellular low-K^+ condition, the three compartments (extracellular medium, cell interior, patch pipette) are in series and the K^+ fluxes are oriented from the pipette to the cell and from the cell to the extracellular compartment. Extracellular high-K^+ prevented hyperpolarization following Gardos channel activation and, although the three compartments remained in series, there was no significant K^+ flux between extracellular medium and cell interior, and the electrical activities recorded through the membrane patch obeyed solely to electrochemical driving forces resulting from pipette composition and/or from imposed voltage.

A minimum of one copy of the Gardos channel was present under the pipette tip and it was not unusual to count as much as 4 copies simultaneously open, which suggests that saturating calcium loads and maximal activation were frequently obtained, at least in the vicinity of the local domain of membrane deformation. If we assume that the Gardos channels are uniformly spread and that their number varies between 100 and 200 copies per RBC (Alvarez and Garcia-Sancho 1987; Lew and Bookchin 2005), we can estimate

that up to (2 – 4)% of membrane area might penetrate into the patch pipette upon seal formation.

Red cells are endowed with the powerful, ATP-fueled PMCA maintaining a physiological intracellular Ca^{2+} concentration of (20 – 50) nM (Maher and Kuchel 2003; Lew and Bookchin 2005; Baunbaek and Bennekou 2008). At this level Gardos channels are quiescent but they become active when a threshold of ~150 nM is reached (presented as level **a** in Fig. IV. 19) (Lew and Bookchin 2005). Activation is then proportional to $[Ca^{2+}]_i$ until a second threshold is reached (level **b**) corresponding to maximal activation.

Figure IV. 19.

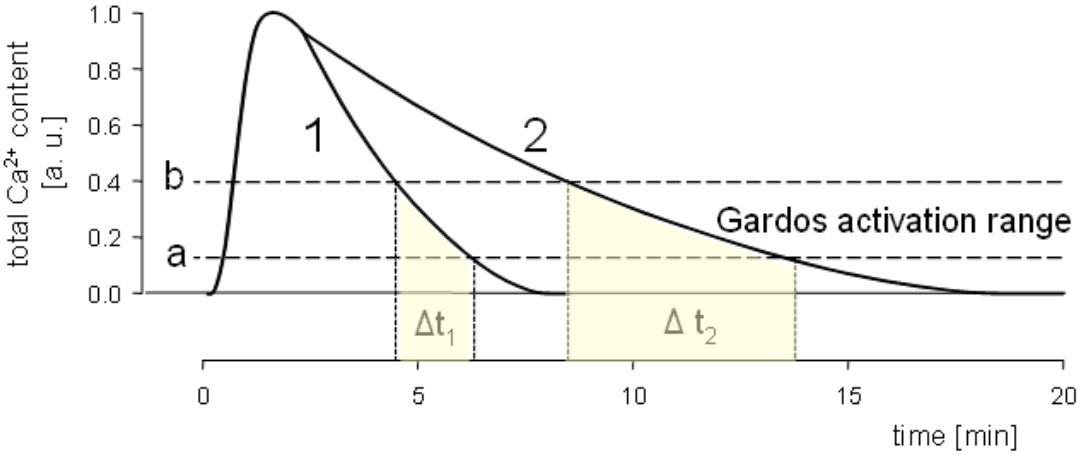

Figure IV.19. Schematic representation of the expected time course of changes in $[Ca^{2+}]_i$. Upon membrane deformation, calcium enters the cell driven by a steep inward gradient, inducing a rapid cell Ca^{2+} load toward a maximal level of total calcium content (1.0 arbitrary unit). The elevated $[Ca^{2+}]_i$ stimulates uphill Ca^{2+} extrusion through PMCA and the initial total calcium content (0.0 arbitrary unit) is eventually resumed. The ability of PMCA to remove all the excess intracellular calcium declines monotonically with RBC age as illustrated here by two hypothetical time courses corresponding to young cells (1) or old cells (2). The dashed line (a) figures the threshold of Gardos channel activation. The dashed line (b) figures the level of total calcium content where the Gardos channel reaches its maximal activity. During the process of Ca^{2+} extrusion through PMCA, the time spent between level (b) and level (a) varies with cell age from a short time (Δt_1) to a long time (Δt_2). During these intervals of time Gardos channel activity displays declining open probability before total extinction.

In absence of $[Ca^{2+}]_i$ measurement, the diversity of K^+ current amplitudes recorded following seal formation may be attributed to different degrees of Ca^{2+} permeability resulting in a large variety of $[Ca^{2+}]_i$ levels. These initial differences may then be amplified by the Gardos channel mediated membrane hyperpolarization which creates a driving force for additional calcium influx via voltage-independent Ca^{2+} channels in a positive feedback loop. On top of this we cannot exclude that this driving force induces calcium release from calcium pools retained in membrane vesicules and susceptible of rapid mobilization (Borgers et al. 1983; Lew and Bookchin 2005). It is therefore possible that the sum of these contributions balances the powerful Ca^{2+} extrusion capacity of the PMCA during the initial peak response.

IV. 2. 2. 2. Activation of anionic channels.

Hyperpolarization also sets the driving force for net anions loss through A^- electrodiffusional pathways and this work provides the first electrophysiological evidence of their parallel activation consutive to massive Gardos channels activity. It might seem paradoxical that the inward current recorded through the membrane patch, corresponding to anionic electrical activity, reflected an exit of anions from the cell to the pipette, whilst at the same time the flux of anions followed the flux of K^+ ions through the rest of the red cell membrane (Fig. IV. 18B). This can easily be understood by the fact that the pipette and bathing solutions had the same high Cl^- concentration (155 mM) and, more importantly, by the fact that the membrane potential under the C-A pipette always follows very closely the W-C membrane potential (Mason et al. 2005). Hence, in absence of additional electrical stimulation in the pipette, the slight chemical gradient existing between the bath/pipette (155 mM) and the cell interior (95 mM) was largely overcome by the electrical gradient created by the Gardos channel activation resulting in outward movement of anions both at pipette and whole cell levels.

IV. 2. 2. 3. Transient nature of Gardos channel activity.

The presence of two distinct phases was a characteristic feature constantly observed in the progressive reduction of Gardos channel activity following initial peak response. The first phase displayed reduction of current amplitude without variation of P_O whilst the second phase, starting when current amplitude reached (-0.3 – -0.5) pA, corresponded to extinction by reduction of P_O.

There are few possible hypothesis to explain a progressive decline at constant P_O. The most likely is a progressive decline of the electrical driving force for K^+ extrusion which could result from progressive rather than instantaneous on setting of membrane anionic conductance as simulated in Fig. IV. 15E-F. In this case, the initial hyperpolarization, activating a slowly increasing number of anionic channels yields progressive return of the membrane potential toward E_A. The specific design of our experimental conditions did not permit to validate or to infirm this hypothesis. It is known that the anion permeability in human red blood cells is low (2×10^{-8} cm/s) if compared to Gardos (2×10^{-7} cm/s) at saturating $[Ca^{2+}]_i$ levels and constitutes a rate limiting factor for K^+, Cl^- and water efflux (Hamill 1983; Lew and Bookchin 2005), but that this low anionic permeability could influence the time course of E_m variations remains to be demonstrated.

Upon membrane deformation, calcium enters the cell driven by a steep inward gradient, inducing a rapid cell Ca^{2+} load toward a maximal level of total calcium content which may vary between cells. When the level of total calcium content reaches the threshold of Gardos channel activation (level **a** in Fig. IV. 19) the channel activity is characterized by increasing P_O until reaching a level of maximum activity above which P_O does not increase anymore (level **b** in Fig. IV. 19). Upon seal formation the level of total calcium content may or may not reach this level. Following the initial peak response, the elevated $[Ca^{2+}]_i$ at the inner membrane surface stimulates uphill Ca^{2+} extrusion through PMCA and

initial physiological $[Ca^{2+}]_i$ is eventually resumed more or less rapidly. It is well documented that the ability of PMCA to remove all the excess intracellular calcium declines monotonically with RBC age (Lew et al. 2007). Therefore, during the process of Ca^{2+} extrusion through PMCA, the time spent between level (**b**) and level (**a**) may vary with cell age from a short time to a long or very long time explaining the great diversity of time courses shown in Fig. IV. 11B. During this interval of time Gardos channel activity displays declining P_O before total extinction.

Thus, calcium extrusion and E_m variations must contribute unevenly and not simultaneously to Gardos channel inactivation. The progressive reduction of E_m should contribute predominantly as long as $[Ca^{2+}]_i$ remains above the maximal activation level (**b**), whereas they probably both participate to final extinction characterized by declining P_O when total calcium content is comprised between levels (**b**) and (**a**).

IV. 2. 2. 4. Fast transitions.

A surprising finding was the recording of extremely fast transitions from large to reduced or minimal currents. It is difficult to attribute these fast transitions to a greater ability of young cell PMCA to remove the excess intracellular calcium because these fast transitions are usually followed by a long time of minimal channel activity indicating that $[Ca^{2+}]_i$ is still above the threshold of activation for a long while. A possible explanation is that large anionic currents are suddenly activated at the whole cell level (thus escaping to direct recording by our microelectrode) and fast transitions correspond to sudden reductions of the membrane potential as simulated in Fig. IV. 15D. The large variations preceding the sudden transitions might reflect these movements at the whole-cell level. Even though we have not had the opportunity to record such activity of a maxi channel under the patch pipette in these series (Mignen et al. 2000) of experiments we have growing evidences that anionic channel activities recorded in human erythrocytes corres-

pond to different kinetic modalities of a type of maxi anion channel with multiple conductance levels, gating properties and pharmacology, depending on conditions (unpublished data). The anionic current recorded under the patch pipette would thus correspond to the low conductance levels, (5 – 20) pS, near the closed state of the channel and sudden opening of high conductance levels outside the patch pipette could explain the fast transitions.

IV. 3. Third question: What is the molecular identity of anionic channels present in RBC membrane?

Using the C-A and excised configurations of the patch clamp technique our research group in Roscoff identified a medium (~15 pS) linear conductance channel activated by adenylate cyclase using forskolin in the C-A configuration, and by exposure to the catalytic subunit of cAMP-dependent protein-kinase in the excised I-O patches (Egee et al. 2002; Decherf et al. 2004; Decherf et al. 2007; Merckx et al. 2008). Channel activity was often observed as simulta-neous gating of two channels (Decherf et al. 2007). Such pronounced cooperative gating appeared consistently at high (< -80 mV, > 80 mV) membrane potentials and this behaviour suggested that these channels function as dimers that favour pairs of channels being simultaneously open. This channel was visible in more than 80% of membrane patches whereas a large outwardly rectifying anion channel ((75 – 85) pS at positive membrane potentials) was only present in less than 5% of cell patches. In excised I-O configuration, the activity of this large conductance channel was not stable in time and run-down was always rapidly observed leading to disappearance of any stable channel opening within few minutes.

These studies have shown that the same halide selectivity ($I^- > Br^- > Cl^-$) was obtained in both channel types which also shared the same pharmacology. Total inhibition of channel activity was obtained by treatment with 100 µM NPPB, 100 µM niflumic acid,

100 µM 9-AC, 1 mM DPC and 10 µM tamoxifen. DIDS, at a concentration of 100 µM, induced a variable partial block in all cases.

The molecular nature of such anionic channels is, as yet, unknown.

The linear conductance Cl^- channel identified by single channel recording in human RBCs displays some of the functional characteristics (small conductance, pharmacology and mode of activation) of CFTR (cystic fibrosis transmembrane regulator) channel but differs by its selectivity sequence ($I^- > Br^- > Cl^-$ instead of $Cl^- > Br^- > I^-$) and mechanosensitivity (which is not found in CFTR channels). W-C observations carried by Verloo and co-workers in 2004 put forward that among the anionic channels present in the red cell membrane one is possibly a CFTR channel but it would only play a role of regulator of a second shrinkage-activated channel (Verloo et al. 2004). The presence of CFTR protein has never been clearly demonstrated electrophysiologically and, in spite of accumulating evidence that CFTR protein resides in human RBC's membrane (Abraham et al. 2001; Sprague et al. 2001; Verloo et al. 2004; Schillers 2008), transcripts for CFTR protein were not found in the cDNAs prepared from human erythroid progenitor cells and CFTR protein could not be detected by use of different specific antibodies in RBCs ghosts (Hoffman et al. 2004).

Outwardly rectifying anion channels have been described in a wide variety of epithelial cells and also in non-epithelial cell membranes. They are supposed to share the major role in chloride secretion with the CFTR playing a role of regulator (Schwiebert et al. 1999). However, the occurrence of the ORC channel is usually extremely low which makes its study rather difficult. Some studies, using the W-C configuration suggest that ORC channels could be activated in the RBC's membrane by oxidation (Duranton et al. 2002). NPPB-sensitive sorbitol-induced lysis of erythrocytes was observed after oxidation which links oxidation-induced conductances to the transport of uncharged solutes (Huber et al. 2002; Huber et al. 2004) as stated for Plasmodium falciparum-infected RBCs (Kirk and Horner 1995; Kirk 2001). On the basis of studies of the effects of organic solutes on W-C

currents, the group of Florian Lang has proposed that the outwardly rectifying channel is responsible for organic solute transport across the infected cell membrane (Huber et al. 2005; Huber et al. 2008). This group also found that conductances similar to each of those seen in infected cells can be activated in uninfected erythrocytes by oxidation, suggesting a single unifying mechanism of activation by the parasite and pointing towards modified endogenous channels as the basis of altered permeability.

In all cases, human plasma (0.5%) or serum (0.5%) or albumax (0.1%), added to patched cells prepared in salines, induced immediate increase in the outward current and, sometimes, slight reduction of inward current (Staines et al. 2003; Duranton et al. 2008; Huber et al. 2008). Furthermore, the current activated by serum is carried by a conductive pathway presenting a different sensitivity to NPPB since addition of NPPB at the concentration of 1 µM resumed the initial I/V curve which itself was suppressed at the concentration of 10 µM NPPB.

The above information obtained by different groups using totally different experimental procedures and patch clamp configurations are rather confusing; but, considering that the existence of multiple channel types in the red cell membrane is quite unlikely, we made the hypothesis that this diversity corresponds to different manifestations of a unique channel type displaying different kinetic modalities, gating properties and pharmacology, depending on conditions.

The third part of this thesis is an in-depth analysis of recordings obtained preferably in the C-A configuration which remains very seldom used because of technical difficulty in spite of its obvious advantages resulting from the respect of cell integrity.

We thus tested:

1/ the evolution with time of the anionic conductance activated following seal formation and Gardos channel-induced membrane transient hyperpolarization shown in the second part of this thesis work.

Figure IV. 20.

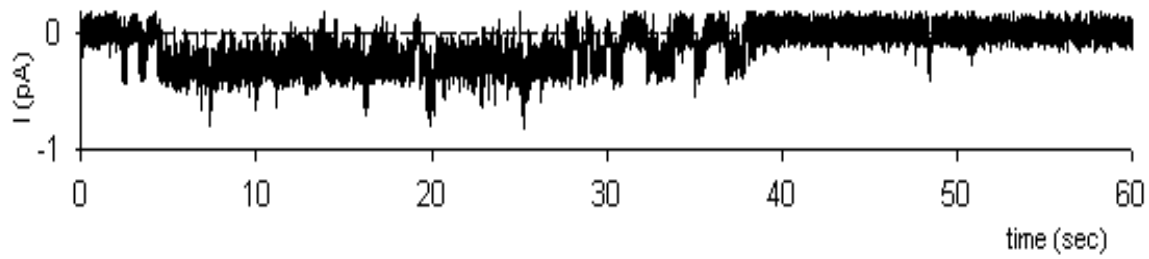

Figure IV. 20. Anionic channel activity following seal formation. Patch clamp single-channel recordings of red blood cell membrane electrical activity obtained during the first 10 min following seal formation at the spontaneous membrane potential, i.e. in absence of pipette potential (V_m = 0 mV) with solution A (containing, in mmol/l, 150 NaCl, 5 KCl, 1 $MgCl_2$, 10 Hepes, 10 glucose, adjusted to pH 7.4 and pCa3) in the pipette and bath.

possible preference of the anionic pathway(s) for SCN^- ions. Indeed, in dehydration-elicited rehydration experiments presented in first part of this work, SCN^- was used to bypass any rate-limiting effects of the anion permeability on the rate of dehydration or hydration of K^+-permeabilized RBCs as stated in many previous works without satisfactory explanation for this statement (Parker 1983; Tiffert et al. 2001).

3/ the effect of serum on single channel activity to help clarify the “serum effect” well documented in the W-C configuration (Staines et al. 2003), without any explanatory information at the molecular level.

Figure IV. 20 shows recordings made with RnS solution in pipette and bath the first 10 min following seal formation displaying inward current at the spontaneous membrane potential corresponding to long channel openings followed by long closure intervals which simply reflected the visible anionic activity induced by Gardos activity which remained undectable by the KCl-containing pipette. As already said above, the intensity of this current varied slightly from one patch to another and declined with time toward 0 pA in a similar manner as the K^+ channel activity but the range of these variation remained much smaller (-0.5 pA to -1 pA). Because of this transient instability following seal formation, we usually waited (10 – 15) min before further recording anionic channel activity.

Under these conditions, using NaCl in the pipette and bathing solution, channel activity remained relatively steady during the following (10 – 15) min and channel activity could be tested in a large range of voltages (-100 mV to +100mV) (Fig. IV. 21.). Short periods of activity (50 ms – 1 s) were separated by long periods of inactivity at hyperpolarizing voltages whilst long bursts of channel activity (1 s – 10 s) were separated by long periods of inactivity (1 s – 10 s) at positive voltages. The average P_o calculated in steady state for each voltage varied considerably from one cell to another but always remained very

Figure IV. 21.

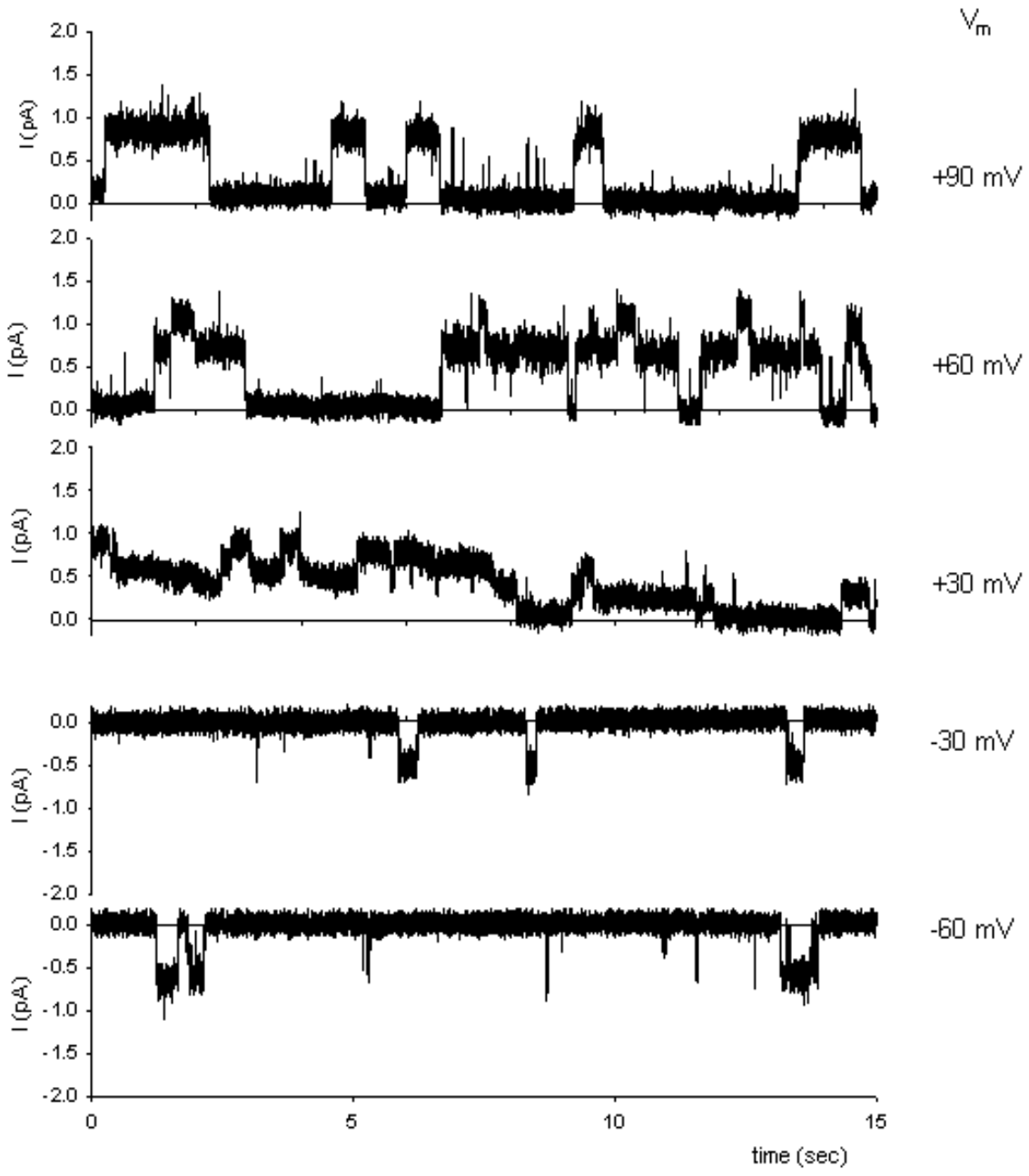

Figure IV. 21. Anionic channel activity in steady state. The currents obtained by evoking a series of test potentials from -100 to +100 mV for 15 s from a holding potential of 0 mV. The shown records were registered in condition with solution A (containing, in mmol/l, 150 NaCl, 5 KCl, 1 $MgCl_2$, 10 Hepes, 10 glucose, adjusted to pH 7.4 and pCa3) in the bath as well as in the pipette.

low. In six experiments, a calculation of P_o values for single channel activity recorded at +100 mV indicated (0.25 ± 0.05). The mean current–voltage relationships showed linear unitary currents and the unit conductances was (11.0 ± 1.1) pS (n = 12). The reversal potential was close to zero indicating that anions were in apparent equilibrium after initial activation by the Gardos activity. “Full channel openings” were obtained more frequently at high voltages (< −60 mV and > +60 mV) and amplitude distributions oscillated in general in a non-discrete manner between several substates (1/4 and 3/4).

All this is in keeping with previously published results and the progressive disappearance of channel activity explains why it was usually said that RBCs are devoid of channel activity in physiological saline solutions containing NaCl.

What follows is probably a major point of this work. Indeed, when we replaced 10 mM of Cl^- ions by SCN^- ions in pipette and bathing solutions (RnS-10SCN), or when we added 0.5% serum or human plasma to the bathing solutions, anionic channel activity increased dramatically as shown in Fig. IV. 22 and Fig. IV. 23. These examples are representative of tens of experiments and could be repeated over and over again. Channel behaviour is now characterized by maximal P_o at positive potential and albeit to a lower extent, at negative potential. This activity remained constant with time and was sometimes interrupted by periods of sudden and transient inactivity as shown in Fig. IV. 23. We initially thought that this sudden activity was due to the recruitment of new copies of the same channel type since two to five apparently similar currents were consistently superimposed on the same recording, whatever the voltage imposed. However, closer examination backed to an analysis of variance performed with the help of Poul Bennekou revealed that instead of recruitment of multiple new copies, this behaviour reflects the opening of new substates of larger amplitude. The current amplitudes of clearly visible substates (more than 1 s in duration) were then plotted against the corresponding voltage values. The example shown on Fig. IV. 24 displays a large variety of points symmetrically distributed. The corresponding P_o values are not quantified yet, but quali-

Figure IV. 22. Effect of SCN^- ions. Typical example of patch clamp single-channel recordings of red blood cell membrane electrical activity obtained at V_m = +70 mV after replacement of 10 mM of Cl^- ions by SCN^- ions with pipette and bathing solutions (RnS-10SCN, pCa3).

Figure IV. 23. Effect of 0.5% serum. Patch clamp single-channel recordings of RBC membrane electrical activity obtained at V_m = +70 mV after adding 0.5% serum in RnS solution (pCa3). This recording shows a rapid transition from multiple conductance levels to temporary inactivation.

Figure IV. 22.

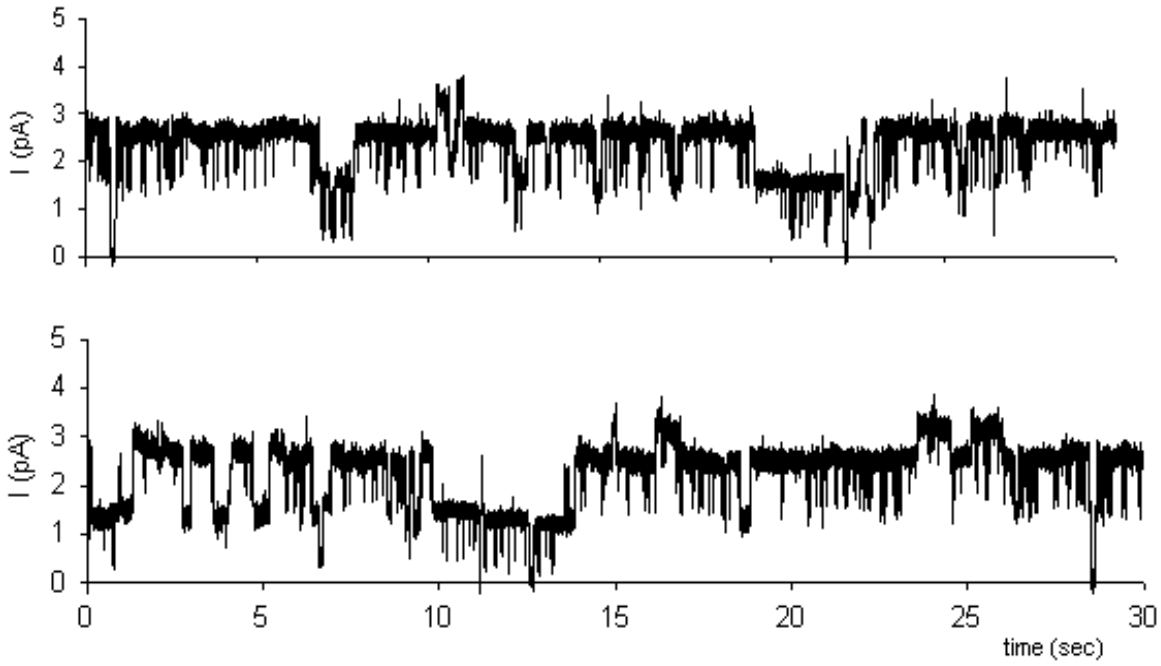

Figure IV. 23.

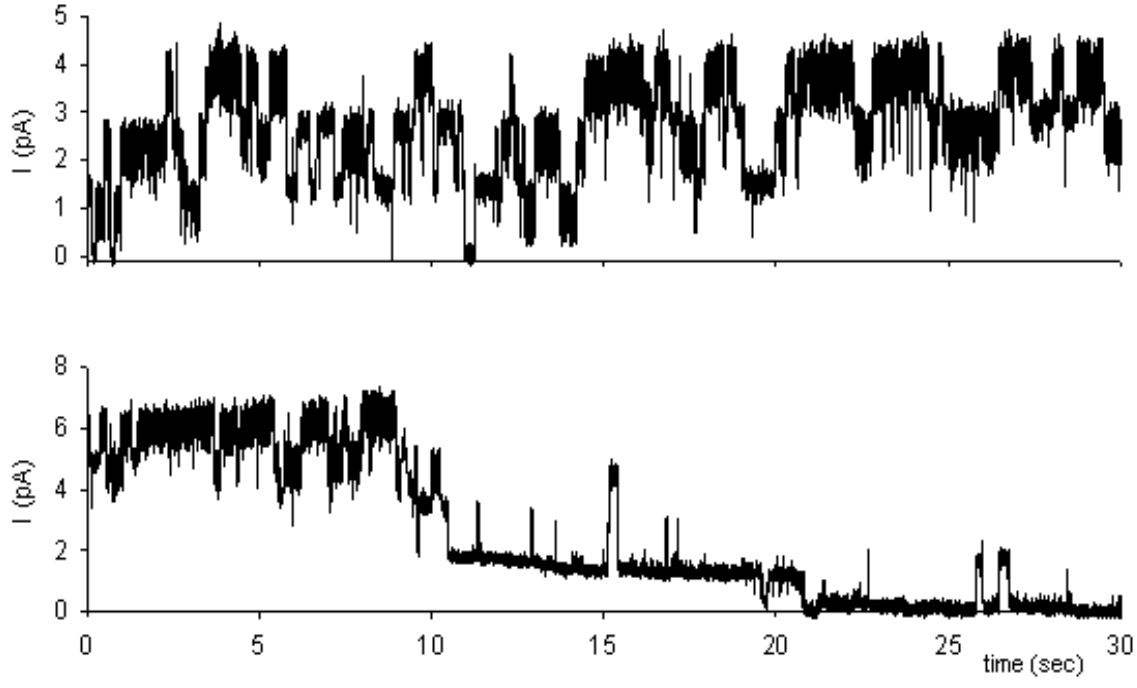

Figure IV. 24.

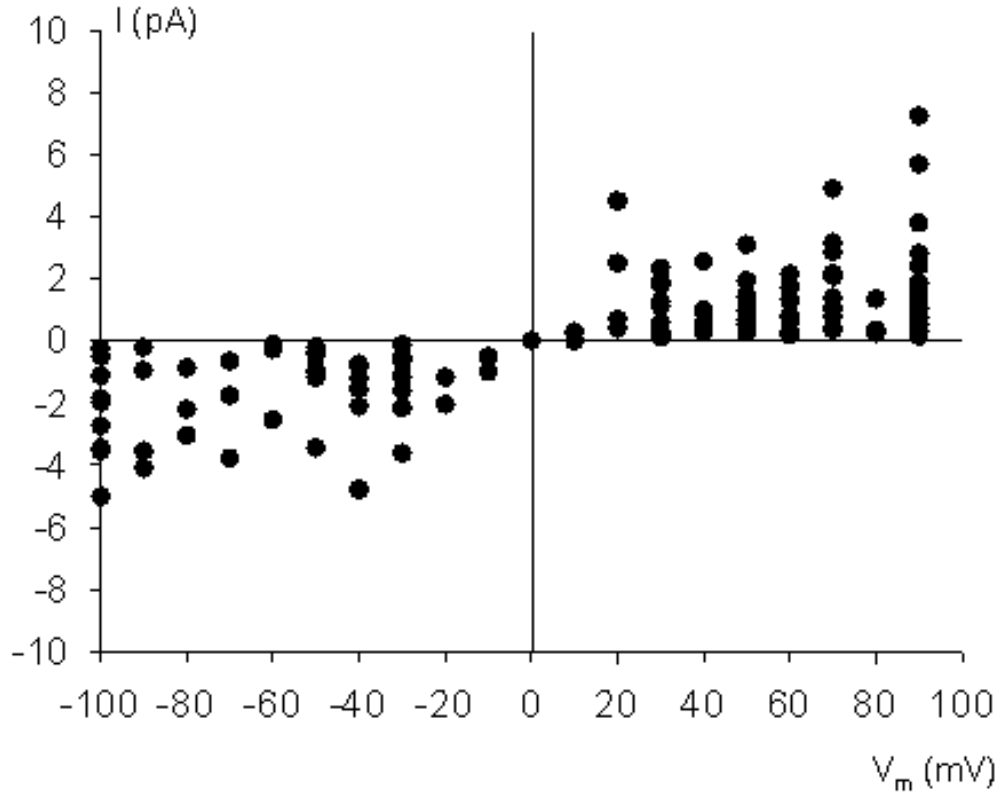

Figure IV. 24. I/V plots corresponding to Fig. IV. 22 and Fig. IV. 23 pooled together. The current amplitudes of clearly visible substates (more than 1 s in duration) were plotted against the corresponding voltage values.

tatively it must be kept in mind that the open probability was always much higher at positive membrane potentials and although the number of substates could reach 3 to 5, the corresponding number observed at negative potentials remained frequently limited to 1 to 3. More interestingly, in these experimental conditions, intervals of much higher conductances could be sometimes detected where, starting from a well established 1 pA, current amplitude could suddenly reach values as high as 10, 20 or 30 pA, depending on the imposed voltage as shown in Fig. IV. 25. Fig. IV. 26 and Fig. IV. 27. These episodes are characterized by abrupt step like channel openings and closures showing complex open-closed kinetics with fast flickering. Some substates seem more stable than others and the channel tends to stay open at these levels for long periods (even many seconds) with only brief flickering to another open state. Analysing such complex kinetics and gating is not straightforward and will deserve further studies. Figure IV. 28 shows that for one given channel the presence of SCN^- ions and serum may activate at positive membrane potential series of current values spread on multiple I/V curves corresponding to conductance values ranging between 40 and 400 pS and could be misattributed to separate outwardly rectifying anionic conductances. When possible, we tested the effect of NPPB on these high subconductance levels and could observe, as illustrated in Fig. IV. 29., that progressive inhibition could be obtained with this anionic channel blocker at the concentration 1 µM, which denotes higher sensitivity relative to the lower subconductance levels where total inhibition is usually obtained at the concentration 10 µM.

This finding could help clarify and explain early confusing results in the literature by demonstrating that the diversity of anionic channel activities recorded in human erythrocytes correspond to different kinetic modalities of a unique type of maxi anion channel with multiple conductance levels and probably multiple gating properties and pharmacology. Unfortunately, to date we still have no information on the key activators of

Figure IV. 25.

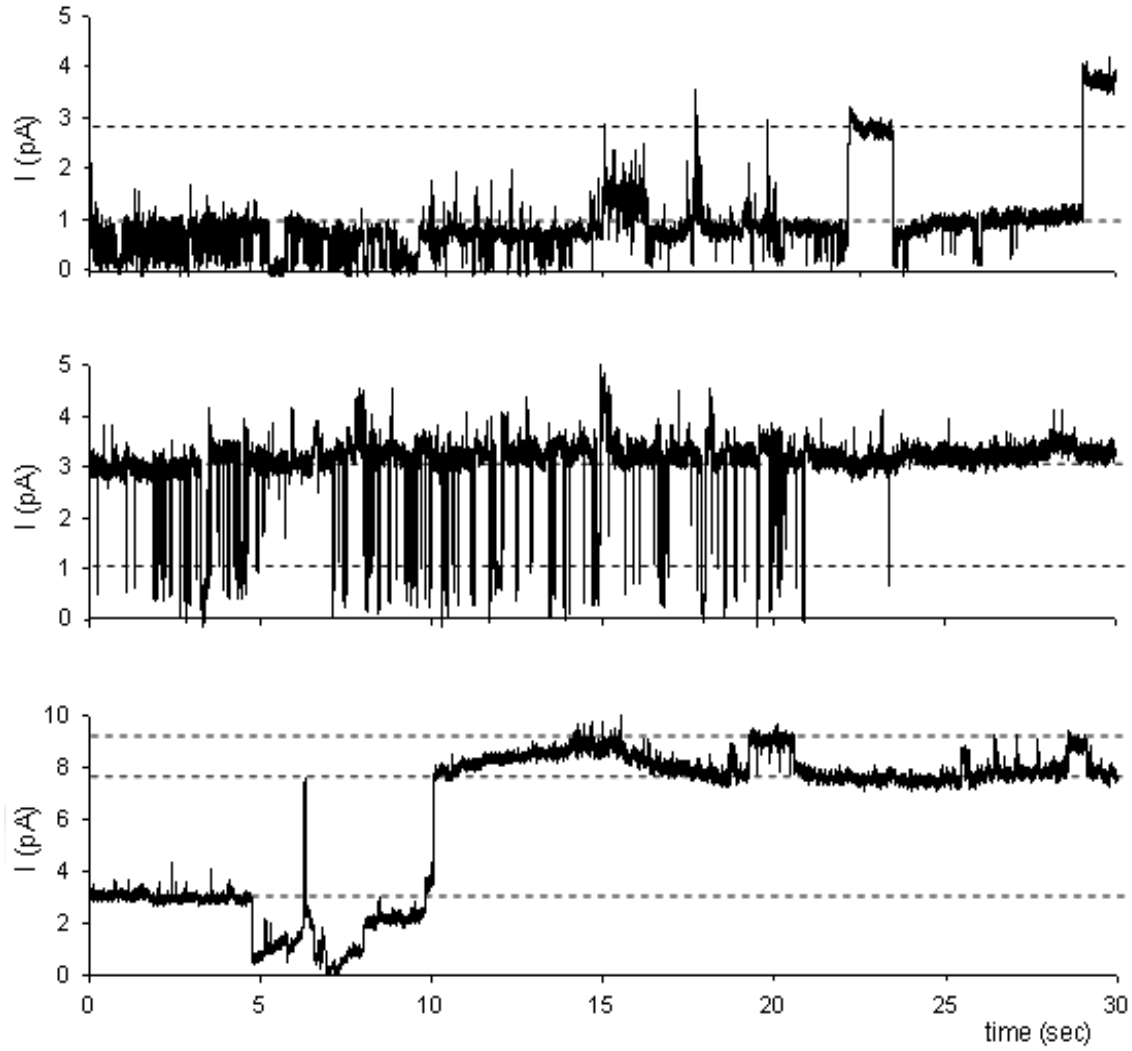

Figure IV. 25. Recording of higher conductance levels (1/3). Typical example of patch-clamp single-channel recordings of red blood cell membrane electrical activity obtained at V_m = +90 mV showing sudden activation of high and stable conductance levels.

Figure IV. 26. Recording of higher conductance levels (2/3). Another typical patch-clamp single-channel recording of red blood cell membrane electrical activity obtained at V_m = +50 mV showing complex cyclic open-closed kinetics with fast flickering.

Figure IV. 27. Recording of higher conductance levels (3/3). Another typical patch-clamp single-channel recording of red blood cell membrane electrical activity obtained at V_m = +80 mV showing complex cyclic open-closed kinetics with fast flickering and “full open state”.

Figure IV. 26.

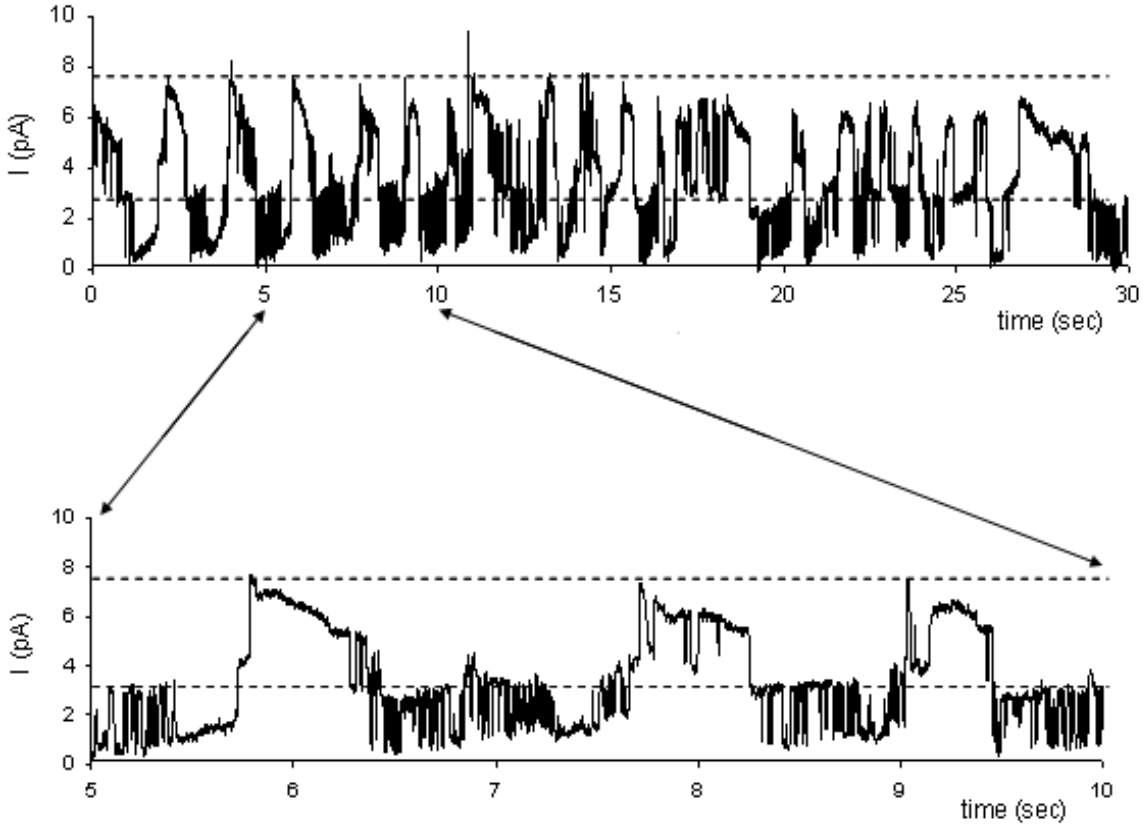

Figure IV. 27.

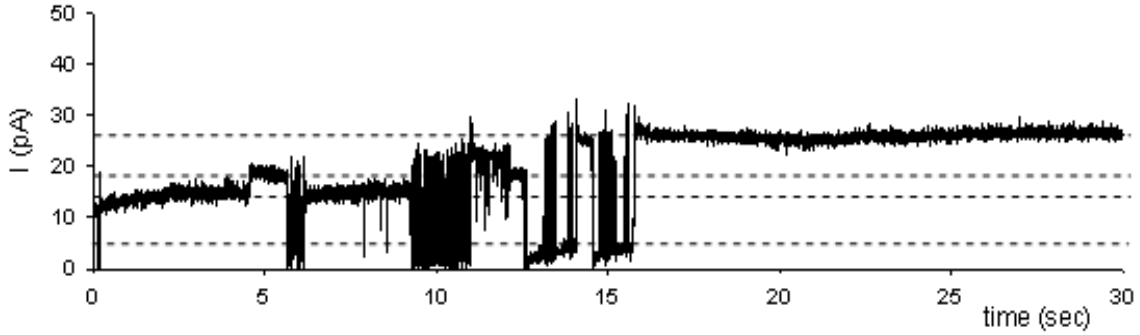

Figure IV. 28.

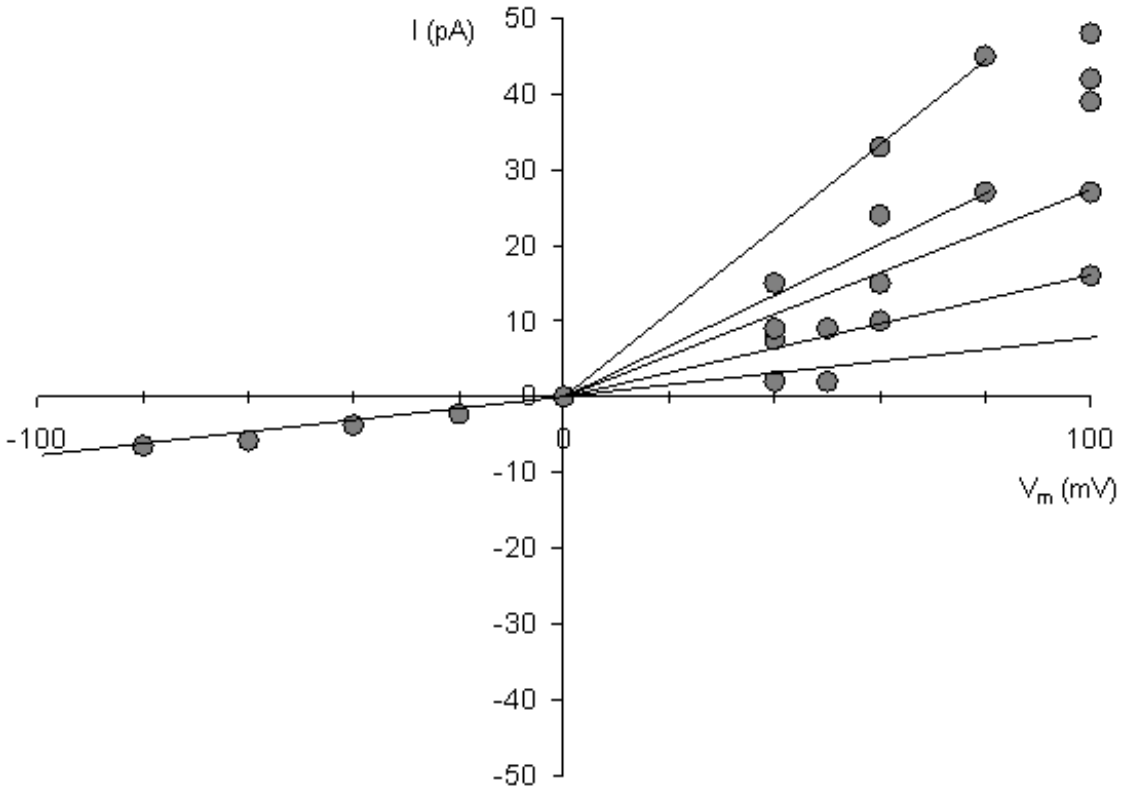

Figure IV. 28. I/V plot of high conductance levels. For one given channel the presence of SCN^- ions, serum and cholesterol may activate at positive membrane potential series of current values spread on multiple I/V curves corresponding to conductance values ranging between 40 and 400 pS as shown in this typical example.

Figure IV. 29.

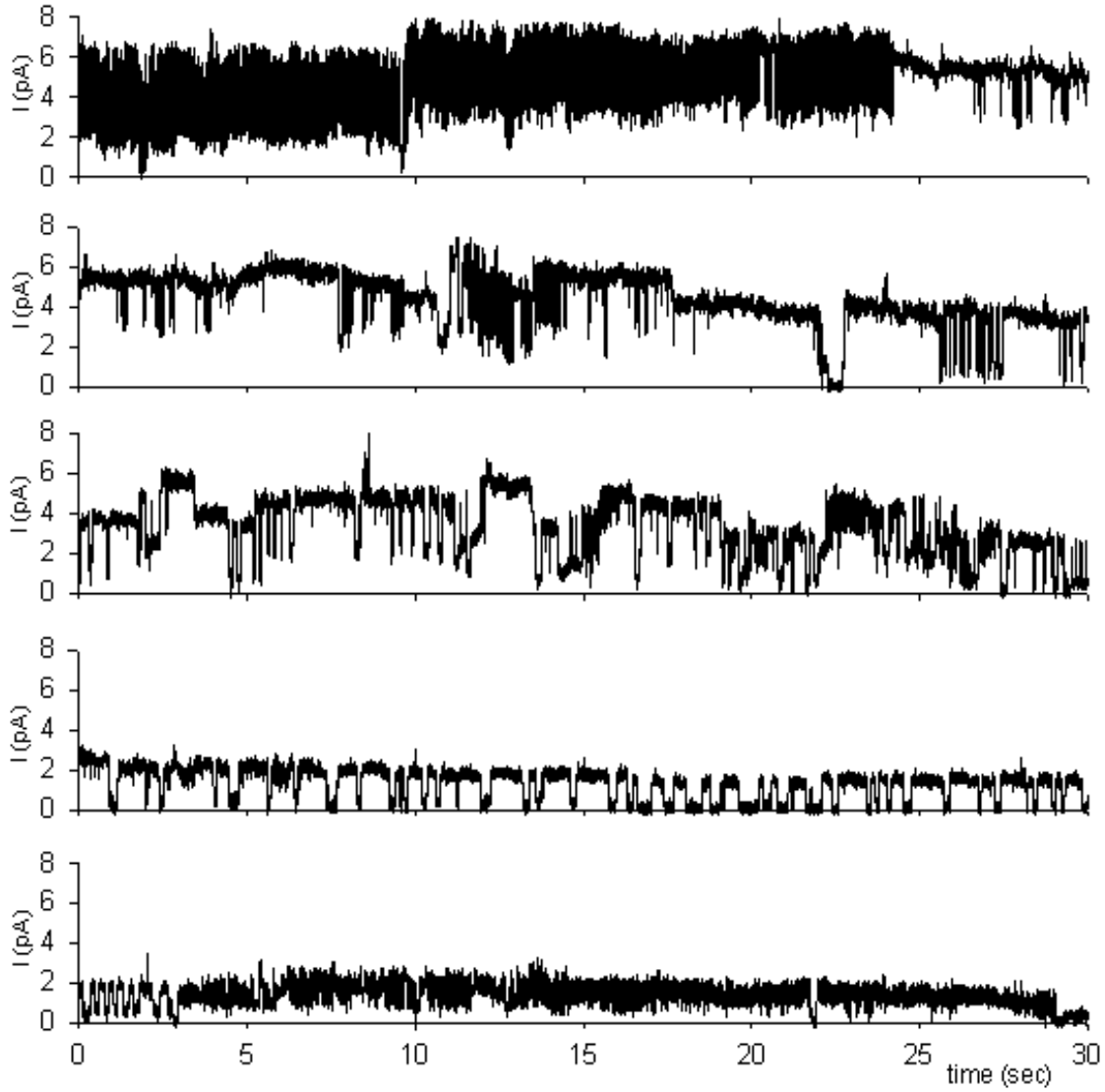

Figure IV. 29. Inhibition by 1 µM NPPB. Progressive inhibition could be obtained with the anionic channel blocker NPPB at the concentration 1 µM. This example was recorded at V_m = +90 mV.

the large conductance substates which prevents from comprehensive study of selectivity, gating and pharmacological properties of these subconductances.

V. GENERAL CONCLUSIONS AND PROSPECTS.

"In preparing for battle I have always found that plans are useless, but planning is indispensable."
Dwight D. Eisenhower

The present work was carried out with the intention to address:

1/ the physiological role played by cationic and anionic channels in cell volume regulation and more specifically the involvement of cationic conductance in cell volume recovery after experimental shrinkage induced by the ionophore A23187 and subsequent massive activation of Gardos channel;

2/ the probable activation of ionic channels by artificial membrane deformation with bearing in mind the possibility to infer from these data some clues on the physiological role played by these pathways in physiological situations like shear stress;

3/ the dynamical behavior, electrophysiological characterization and molecular identity of anionic channels for which too many dissonant and confusing data have been published recently.

First question:
Are RBC's membrane channels involved in rehydration elicited by isosmotic dehydration?

This question, as it is phrased here, will remain pending since the major information obtained in this part of work is that the observed rapid return to osmotic fragility described by many authors (Raftos et al. 1996; Tiffert et al. 2001; Lew et al. 2005; Lew et al. 2007) using the same experimental procedure is not in close correlation with cell volume recovery. The aim of this analysis was 1/ to relate direct measurements of water content of RBCs with the parameters of osmotic fragility curves and with predictions derived from the mathematical model of RBC homeostasis (RCM), all in isotonic condi-

tions. This relation was important to establish whether or not there is consistency across different methodologies presumed to measure the same parameters, and also to test the extent of the quantitative understanding encoded in the RCM. To illustrate the kind of questions this analysis could answer we considered RBCs dehydrated in isotonic conditions by the net loss of KCl and water, a condition elicited in vivo and in vitro either by the activation of Ca^{2+}-sensitive K^+ channels (Gardos channels) or by the action of valinomycin, a K^+-selective ionophore; 2/ to relate the evolution of water content of RBCs with the underlying transporters and more specifically with the activity of conductive pathways recorded using the patch clamp technique.

This study demonstrates that in Ca^{2+}-loaded RBCs dynamic changes in red cell osmotic fragility are caused rather by exovesiculation-induced membrane area loss than cell hydration per se. Further studies are required to establish whether or not exovesiculation can fully account for the observed OFC right shifts. If not, pre-spherical lysis on rapid volume expansion may have to be considered a possible contributing mechanism. Such a mechanism has been implicated in the increased osmotic fragility of Plasmodium falciparum-infected RBCs containing parasites in advanced maturational stages (Lew et al. 2003; Lew et al. 2004; Esposito et al. 2008; Mauritz et al. 2009). It is important to bear in mind the possibility of the variable participation of these processes in other physiological, pathological or experimental conditions. The correlation between shifts in osmotic fragility and hydration state can no longer be assumed to be valid in all conditions.

Second question:
Does membrane deformation induce channel activity?

In these experiments deformation was obtained by depression applied in glass microelectrode brought in contact with red cell membrane. We present here electrophysiological evidence that Ca^{2+}-sensitive K^+ channel are transiently activated

when seal formation induces membrane deformation and that this phenomenon can result only from activation of a permeability pathway with a finite Ca^{2+} conductance. This transient activity generates secondary transient anionic channel activity.

This is an important finding if we consider that any attempt to establish a seal on a red cell membrane for electrophysiological studies induces automatically this phenomenon whatever the purpose of the electrophysiological investigation. This means that all data published previously on electrophysiology of the red cell membrane have to be revisited with this question in mind: did this transient activation of channel activity interfere with the reported data? Very little was published in the C-A configuration on cationic channel activity where interference could have a major impact, but one important question will be to determine whether or not this phenomenon could impact on the W-C data, where, for instance, it has never been possible to record Gardos channel activity. Concerning the anionic channel data reported by our group in the past, the slight right shift of the reversal potential frequently observed might well find an explanation in the temporary driving force for outward movement of anions induced by Gardos activity.

This is also an important finding if we consider the physiological role of the Gardos channel. Indeed, no physiological role has been attributed to the Gardos channel up to now and its experimental activity was always induced by use of ionophore or ATP-depletion. This work validates the hypothesis frequently suggested that shear stress could induce transient calcium permeability (Larsen et al. 1981; Johnson and Gannon 1990; Ney et al. 1990; Johnson and Tang 1992; Johnson 1994; Brakemeier et al. 2003; van Bavel 2003; Brain et al. 2004) with subsequent activation of Gardos channel activity and loss of water. This might help the red cells to bend and flow through the narrowest of capillaries or in the spleen where they are submitted to considerable shear stress and

membrane deformation (Schmidt-Schonbein and Wells 1969; Skalak and Branemark 1969; Chien 1987). Future experiments using calcium fluorescent probes should be planned to give evidence that calcium enters the cell, and to what extent, in the present experimental conditions as well as in situations where erythrocytes enter a glass capillary hardly larger than a patch clamp pipette.

Third question:

What is the molecular identity of anionic channels present in RBC membrane?

As said above, the enigma is: Are patch clamp experiments on single cells or fragments of membrane representative for the red cell? The observed channels are inactive in the "resting cell", but can potentially give a very high single cell conductance when activated by phosphorylation, mechanical stress and so on. What is their molecular identity? What is their physiological role?

To these questions the present work provides some important elements of answer. The most important finding is that the diversity of anionic channel activities recorded in normal human erythrocytes corresponds to different kinetic modalities of a unique type of maxi anion channel with multiple conductance levels, gating properties and pharmacology, depending on conditions. This being said, the identity of this maxi-anion channel is not defined yet. In an analysis of the human red cell proteome 91 unique membrane protein sequences was found, of which 10 to 15 were unknown, and considering how little protein a few hundred channels represent, it is anybody's guess how many there could be below the detection limit. Investigations are in progress in our group to clarify this point and an obvious candidate displaying similar selectivity, complex gating and pharmacological properties is the voltage-dependent anionic channel (VDAC). Whole-cell experiments showed a membrane conductance less than 100 pS, which is in fair agreement with the value calculated from experiments on cell suspensions from normal donors, which is in the range 40 to 50 pS range. Since channels activity was

negligible in cells suspended in physiological saline solution, 10 to 20 min following seal formation, although not finally settled, it seems probable that the observed channels can be activated experimentally, and become so under pathological conditions, but under normal experimental conditions they are dormant. The observed channels seem to be inactive in the “resting cell”, but can potentially give a very high single cell conductance, up to 50 to 100 times the normal conductance. Could there be conditions where the red cells needed to loose volume fast? As noted in the beginning, the normal cell has only a limited ability to loose salt or volume. At maximum Gardos channel activation, the cell can loose only about 0.3 mM/s of KCl, corresponding to a volume loss of only 0.2 %/s. However, the sudden parallel opening of large anionic conductance could help the cell to loose volume fast. A major task for the future is to understand the dynamical aspects of red cell electrophysiology for cells in circulation. A possible picture could be that most of the time the “resting cell” is the valid regime, but transiently the need could arise for a very high, but transient anion conductance, caused for example by full activation of the Gardos channel, the NSC channel, or channels yet to be found, for example normally dormant sodium channels.

ANNEX #1.

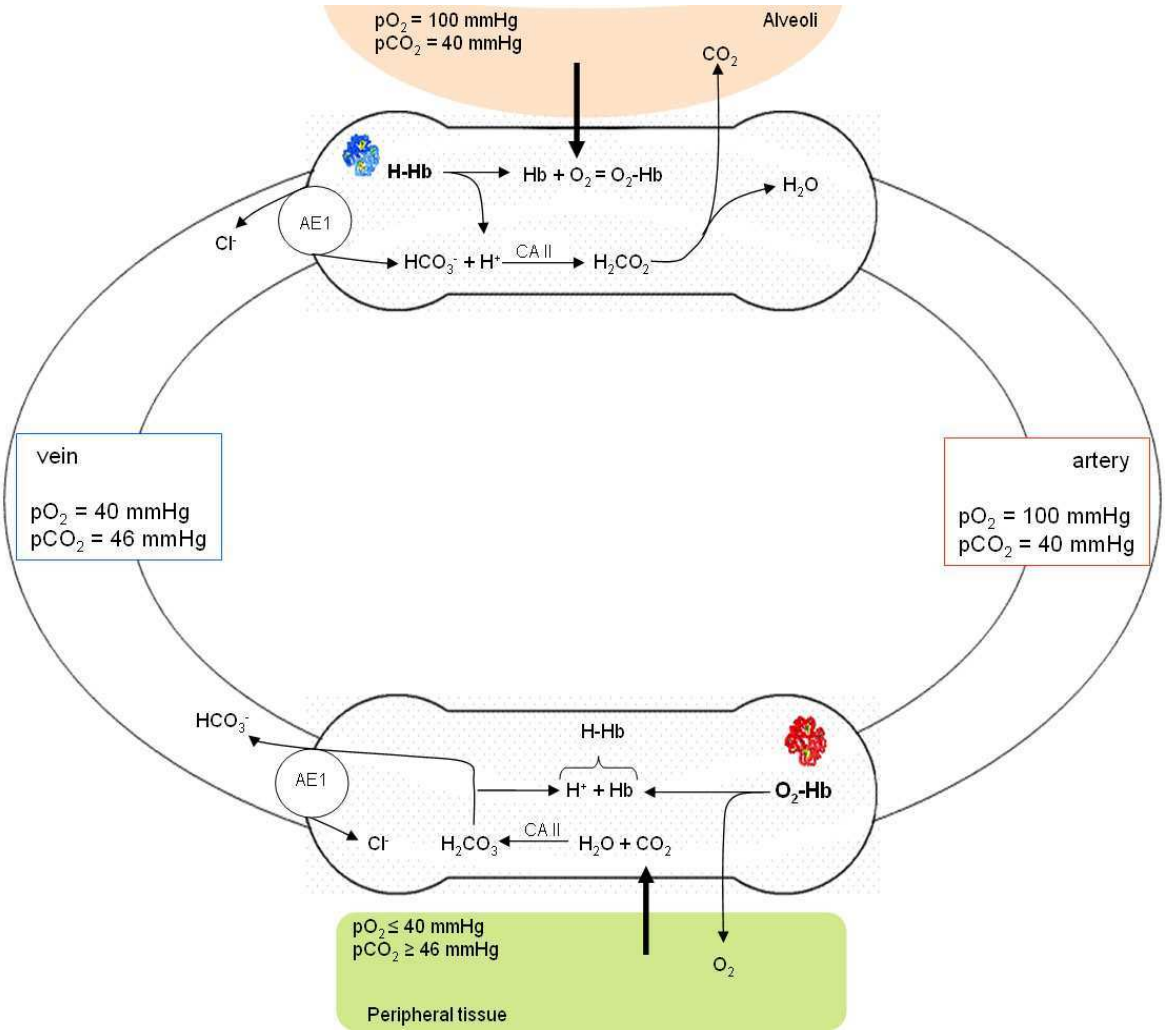

Annex #1. The Jacobs-Stewart cycle. In the peripheral tissues oxygenated RBCs (oxy-RBCs) release O_2 carried by the haemoglobin (O_2-Hb) and uptake the CO_2. O_2/CO_2 exchange is possible because gases freely diffuse across the biological membranes. Their movement is triggered by the change in the partial pressures of O_2 and CO_2 (pO_2 and pCO_2, respectively) encounter in the metabolically active tissues. CO_2 once in the red cell cytosol reacts with water yielding carbonic acid (H_2CO_3). The reaction is catalyzed by carbonic anhydrase II (CA II). The acid then dissociates into a proton and bicarbonate (HCO^-_3). The proton is buffered by haemoglobin (H-Hb) and HCO_3^- leaves the cell undergoing a rapid electroneutral exchange with Cl^- which is mediated by anion exchanger (AE1) – an effect known as a Bohr effect. Production of HCO^-_3 by RBCs minimizes acidification of venous blood and increases its carbon dioxide caring capacity.

In the lungs deoxy-RBCs gain O_2 in exchange for CO_2. It is a reverse process to describe for oxy-RBCs/deoxy-RBCs transition in peripheral tissue.

ANNEX #2.

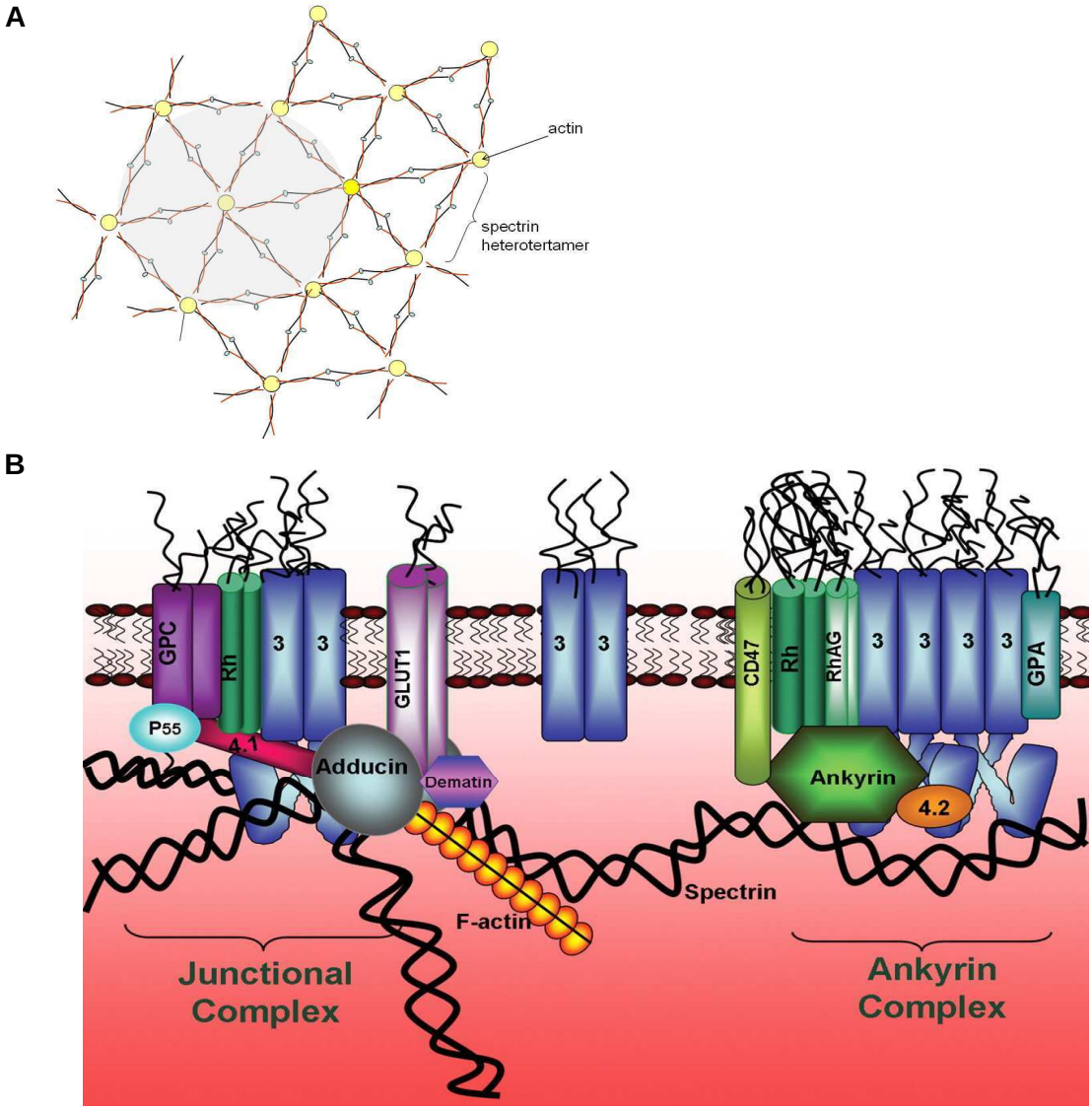

Annex #2. Cytoskeleton. (A) The actin-spectrin lattice. Spectrins are extended flexible molecules ~(200 – 260) nm in length. Spectrins are comprised of α- and β-subunits, which are both related to actin. The α- and β-subunits are associated laterally to form antiparallel heterodimers, and heterodimers are assembled head-head to form heterotetramers. Polygonal spectrin-actin connection is shaded. **(B)** (Fig. 7 from the paper of Anong et al). The relationships between phospholipid bilayer and underlying cytoskeleton in human RBC. “In this model, two major membrane protein complexes serve to anchor the spectrin-actin cytoskeleton to the phospholipid bilayer: (1) an ankyrin-bridged complex that contains membrane-spanning proteins band 3, glycophorin A, Rh complex proteins, and CD47, in addition to the peripheral proteins ankyrin, protein 4.2, and a variety of glycolytic enzymes, and (2) a junctional complex that contains the membrane-spanning proteins band 3, glycophorin C, Rh complex proteins, and a glucose transporter, in addition to peripheral proteins actin, tropomyosin, tropomodulin, adducin, dematin, p55, protein 4.1, protein 4.2, and a variety of glycolytic enzymes.” (Anong et al. 2009)

ANNEX #3.

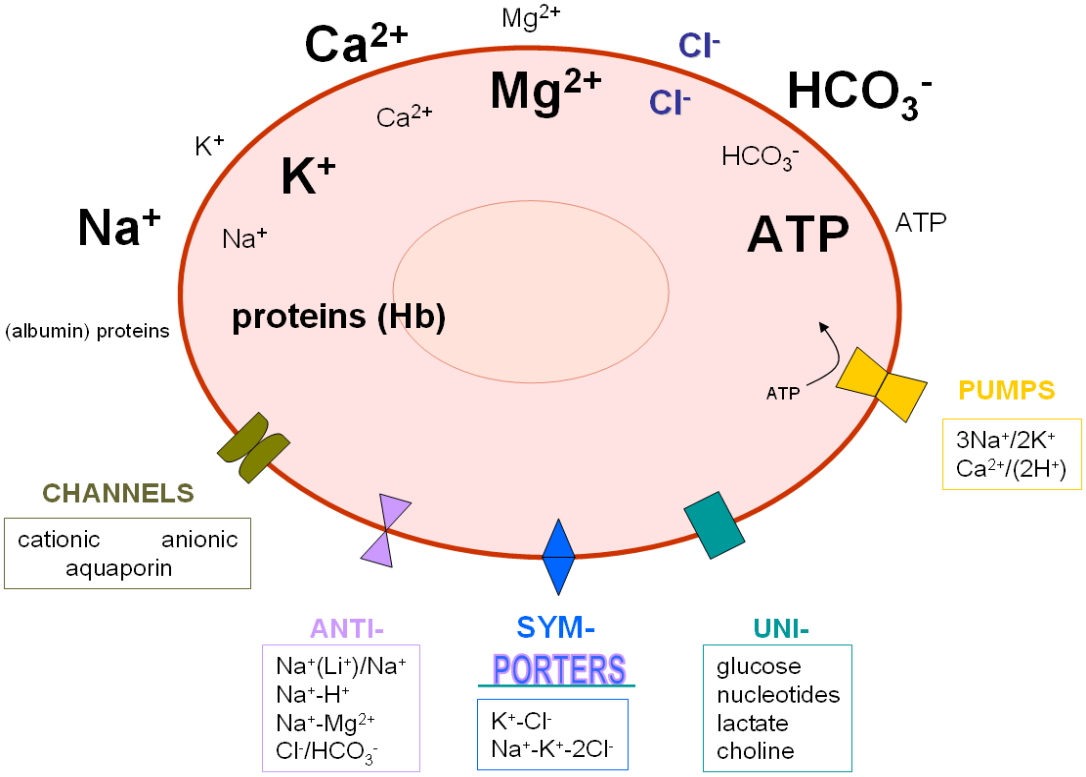

Annex #3. Transporters in the human RBC membrane. "The cell membrane is a major barrier to ion movement, and specific proteins – the ion channels, transporters and pumps – have evolved to transport ions across it. Ion channels are gated pores that permit the passive flow of ions down their electrochemical gradients. Ion pumps, by contrast, use the energy of ATP hydrolysis to transport ions against their electrochemical gradient. In between are the coupled transporters (antiporters and symporters), in which movement of one ion species against its electrochemical gradient is powered by the downhill movement of another." (Ashcroft 2006) In spontaneous process of facilitated diffusion mediated by transmembrane proteins, ions or molecules cross the phospholipid bilayer also downhill their concentration gradient.

Two types of channel are present in the human RBC membrane: cationic and anionic but only cationic has been well characterized so far: Ca^{2+}-gated potassium channel (also known as a Gardos channel, KCa 3.1) and non-selective cationic (NSC) channel.

Ca^{2+}-ATPase (pump) preserves low intracellular Ca^{2+} level. According to some authors Ca^{2+} extruding could be accompanied by the opposite-directed movement of one or two protons.

By the fond size the concentration gradient across the membrane is qualitatively shown. In the parenthesis the most abundant intracellular (Hb, haemoglobin) and extracellular (albumin) proteins are pointed out.

ANNEX #4.

Activators and modulators of Gardos channel. ↓, ↑ = down, up regulation, respectively, (γ) conductance of the channel, (γ_X) conductance of ion X, (P_o) open probability, (P_X) permeability of the ion X, (τ_c) mean duration of closing burst of the channel (τ_o) mean duration of opening burst of the channel.

Activator/ Modulator	Effect	Reference
1	2	3
1-EBIO	activator	(Maher and Kuchel 2003)
2-CMNQ	inhibitor – if the channel is activated by A23187 or Pb^{2+}; additional stimulator of K^+ efflux – when the channel is activated by ATP depletion and/or V^{5+}	(Fuhrmann et al. 1985)
2,3-CMNQ	inhibitor	(Fuhrmann et al. 1985)
7-CMNQ	inhibitor	(Fuhrmann et al. 1985)
A23187	inhibitor	(Fehlau et al. 1989)
atebrin	inhibitor – alters channel gating	(Fehlau et al. 1989)
ATP	$\uparrow\gamma$ in presence of Mg^{2+} and at depolarizing potential	(Romero and Rojas 1992)
Ba^{2+}	inhibitor ($\downarrow$amplitude and $\uparrow\tau_c$); the degree of inhibition $\uparrow$ when $\uparrow[Ba^{2+}]_o$ together with more negative potential	(Grygorczyk and Schwarz 1985; Dunn 1998)
Ca^{2+}	concentration-dependent: below threshold – no effect, above threshold – saturation at (5 – 10) μM	(Grygorczyk and Schwarz 1983; Schwarz and Passow 1983; Grygorczyk et al. 1984; Grygorczyk and Schwarz 1985; Fehlau et al. 1989; Leinders et al. 1992)
Cd^{2+}	concentration-dependent: lower dose stimulates, higher – inhibits the channel	(Leinders et al. 1992)
cetiedil	inhibitor ($\downarrow P_o$)	(Dunn 1998)
CLT	inhibitor (reduces of burst duration)	(Dunn 1998; Maher and Kuchel 2003)
ChTX	channel blocker	(Maher and Kuchel 2003)
Co^{2+}	concentration-dependent: lower dose stimulates, higher – inhibits the channel	(Leinders et al. 1992)
Cs^+	$P_{Cs} << P_K$. $\gamma_{Cs} << \gamma_K$ (the degree of conductance reduction $\uparrow$ when $\uparrow[Cs^+]_o$)	(Grygorczyk and Schwarz 1985; Christophersen 1991)
enflurane	inhibitor	(Maher and Kuchel 2003)
Fe^{2+}	no action or inhibitor when the channel already active	(Leinders et al. 1992)
forskoline	activator	(Maher and Kuchel 2003)

1	2	3
halothane	inhibitor	(Maher and Kuchel 2003)
IBMX	activator	(Maher and Kuchel 2003)
isoflurane	inhibitor	(Maher and Kuchel 2003)
K^+	concentration-dependent: inhibition of K^+ efflux when incubated in K^+ free solution or above 25 mM, maximal channel activation at (3 – 5) mM, saturation 10 mM	(Grygorczyk and Schwarz 1983; Schwarz and Passow 1983)
Li^+	$P_{Li} << P_K$. $\gamma_{Li} << \gamma_K$	(Christophersen 1991)
menadione	influence on P_o:↑ if the channel is activated by A23187, Pb^{2+} or V^{5+}; ↓ if the channel is activated by ATP depletion	(Fuhrmann et al. 1985; Fehlau et al. 1989)
Mg^{2+}	no influx or if ↑$[Mg^{2+}]_i$ it is necessary to ↑$[Ca^{2+}]_i$ to produce the same single channel activity	(Grygorczyk and Schwarz 1985; Shields et al. 1985; Leinders et al. 1992)
Na^+	$P_{Na} < P_K$. $\gamma_{Na} << \gamma_K$ (the degree of inhibition ↑ when ↑$[Na^+]_o$. High $[Na^+]_i$ inhibits the channel.)	(Grygorczyk and Schwarz 1983; Schwarz and Passow 1983; Grygorczyk et al. 1984; Grygorczyk and Schwarz 1985; Christophersen 1991)
NH_4^+	$P_{NM+4} < P_K$. $\gamma_{NH+4} < \gamma_K$	(Bennekou and Christophersen 1990; Christophersen 1991)
nitredipine	channel blocker	(Maher and Kuchel 2003)
NS309	increases sensitivity of the channel to Ca^{2+}	
Pb^{2+}	concentration-dependent: lower dose stimulates, higher – inhibits the channel	(Grygorczyk and Schwarz 1983; Schwarz and Passow 1983; Shields et al. 1985; Fehlau et al. 1989; Leinders et al. 1992)
PGE2	activator	(Maher and Kuchel 2003)
PKA	up-regulation – ↑P_o and ↑ sensitivity of the channel to Ca^{2+}	(Pellegrino and Pellegrini 1998)
PTH	induces a significant influx of Ca^{2+}	(Maher and Kuchel 2003)
propanolol	↑ channel sensitivity to Ca^{2+}. Its action is concentration-dependent: at low dose stimulates K^+ efflux, at high – inhibits it.	(Schwarz et al. 1989; Varecka and Peterajová 1990)

1	2	3
quinine	Inhibitor ($\uparrow\tau_c$) – outward current is more potently block by internal quinine and inward by external. The degree of inhibition depends on V_m and trans concentration of K^+.	(Grygorczyk and Schwarz 1985)
Rb^+	$P_{Rb} < P_K$ or $P_{Rb} > P_K$ $\gamma_{Rb} < \gamma_K$	(Schwarz and Passow 1983; Grygorczyk et al. 1984; Grygorczyk and Schwarz 1985; Bennekou and Christophersen 1990; Christophersen 1991)
sevoflurane	inhibitor	(Maher and Kuchel 2003)
temperature	$\downarrow T = \downarrow\gamma$ but $\uparrow P_o$	(Grygorczyk 1987; Varecka and Peterajová 1990)
TEA	blocks inward current from the outside and vice versa; inhibits single–channel conductance but not kinetics	(Grygorczyk and Schwarz 1985)
Tl^+	$\gamma_{Tl} \leq \gamma_K$	(Christophersen 1991)
TRAM-34	inhibitor, more specific than CLT	(Maher and Kuchel 2003)
V^{5+}	activator (blocks PMCA)	(Varecka and Peterajová 1990)
volatile	inhibitor	(Maher and Kuchel 2003)

ANNEX #5.

Formulation of RPMI medium 1640, liquid (after http://www.invitrogen.com/site/us/en/home/support/Product-Technical-Resources/media_formulation.188.html). It contains L-glutamine and 25mM HEPES. RPMI (Roswell Park Memorial Institute) Media 1640 are enriched formulations with extensive applications for mammalian cells. They were originally formulated for suspension cultures or monolayer cultures of human leukemia cells.

Catalog Number(s): 52400017 ,52400025.

COMPONENTS	Molecular Weight	Concentration (mg/L)	mM
1	2	3	4
Amino Acids			
Glycine	**75**	**10**	**0.133**
L-Arginine	**174**	**200**	**1.15**
L-Asparagine	**132**	**50**	**0.379**
L-Aspartic acid	**133**	**20**	**0.15**
L-Cystine	**240**	**20**	**0.0833**
L-Glutamic Acid	**147**	**20**	**0.136**
L-Glutamine	**146**	**300**	**2.05**
L-Histidine	**155**	**15**	**0.0968**
L-Hydroxyproline	**131**	**20**	**0.153**
L-Isoleucine	**131**	**50**	**0.382**
L-Leucine	**131**	**50**	**0.382**
L-Lysine hydrochloride	**146**	**40**	**0.274**
L-Methionine	**149**	**15**	**0.101**
L-Phenylalanine	**165**	**15**	**0.0909**
L-Proline	**115**	**20**	**0.174**
L-Serine	**105**	**30**	**0.286**
L-Threonine	**119**	**20**	**0.168**
L-Tryptophan	**204**	**5**	**0.0245**
L-Tyrosine	**181**	**20**	**0.11**
L-Valine	**117**	**20**	**0.171**
Vitamins			
Biotin	**244**	**0.2**	**0.00082**
Choline chloride	**140**	**3**	**0.0214**
D-Calcium pantothenate	**477**	**0.25**	**0.000524**
Folic Acid	**441**	**1**	**0.00227**
Niacinamide	**122**	**1**	**0.0082**
Para-Aminobenzoic Acid	**137**	**1**	**0.0073**

1	2	3	4
Pyridoxine hydrochloride	**206**	**1**	**0.00485**
Riboflavin	**376**	**0.2**	**0.000532**
Thiamine hydrochloride	**337**	**1**	**0.00297**
Vitamin B12	**1355**	**0.005**	**0.0000037**
i-Inositol	**180**	**35**	**0.194**
Inorganic Salts			
Calcium nitrate (Ca(NO3)2 4H2O)	**236**	**100**	**0.424**
Magnesium Sulfate (MgSO4-7H2O)	**246**	**100**	**0.407**
Potassium Chloride (KCl)	**75**	**400**	**5.33**
Sodium Bicarbonate (NaHCO3)	**84**	**2000**	**23.81**
Sodium Chloride (NaCl)	**58**	**5500**	**94.83**
Sodium Phosphate dibasic (Na2HPO4) anhydrous	**142**	**800**	**5.63**
Other Components			
D-Glucose (Dextrose)	**180**	**2000**	**11.11**
Glutathione (reduced)	**307**	**1**	**0.00326**
HEPES	**238**	**5958**	**25.03**
Phenol Red	**376.4**	**5**	**0.0133**

REFERENCES.

Abraham, E., B. Shrivastav, et al. (2001). "Cellular and biophysical evidence for interactions between adenosine triphosphate and P-glycoprotein substrates: functional implications for adenosine triphosphate/drug cotransport in P-glycoprotein overexpressing tumor cells and in P-glycoprotein low - level expressing erythrocytes." Blood Cells Mol Dis **27**(1): 181-200.

Abraham, E., K. Sterling, et al. (2001). "Erythrocyte membrane ATP binding cassette (ABC) proteins: MRP1 and CFTR as well as CD39 (ecto - apyrase) involved in RBC ATP transport and elevated blood plasma ATP of cystic fibrosis." Blood Cells, Molecules, and Diseases **27**(1): 165-180.

Al-Awqati, Q. (1995). "Regulation of ion channels by ABC transporters that secrete ATP." Science **269**(5225): 805-806.

Allan, D., P. Thomas, et al. (1980). "The isolation and characterization of 60 nm vesicles ('nanovesicles') produced during ionophore A23187-induced budding of human erythrocytes." Biochem J **188**(3): 881–887.

Alper, S. (2009). "Molecular physiology and genetics of Na(+) - independent SLC4 anion exchangers." J Exp Biol **212**(11): 1672-1683.

Alper, S., D. Vandorpe, et al. (2008). "Reduced DIDS - sensitive chloride conductance in Ae1-/- mouse erythrocytes." Blood Cells, Molecules, and Diseases **41**(1): 22-34.

Alvarez, J. and J. Garcia-Sancho (1987). "An estimate of the number of Ca2 (+) - dependent K(+) channels in the human red cell." Biochim Biophys Acta **903**(3): 543-546.

Alvarez, J., M. Montero, et al. (1992). "High affinity inhibition of Ca2(+) - dependent K(+) channels by cytochrome P-450 inhibitors." Journal of Biological Chemistry **267**(17): 11789-11793.

Anong, W., T. Franco, et al. (2009). "Adducin forms a bridge between the erythrocyte membrane and its cytoskeleton and regulates membrane cohesion." Blood **114**(9): 1904-1912.

Ashcroft, F. (2006). "From molecule to malady." Nature **440**(7083): 440-447.

Bao, L., S. Locovei, et al. (2004). "Pannexin membrane channels are mechanosensitive conduits for ATP." FEBS Lett **572**(1-3): 65-68.

Baunbaek, M. and P. Bennekou (2008). "Evidence for a random entry of Ca2(+) into human red cells." Bioelectrochemistry **73**(2): 145-150.

Bennekou, P. (1993). "The voltage - gated non - selective cation channel from human red cells is sensitive to acetylcholine." Biochemica et Biophysica Acta **1147**: 165-167.

Bennekou, P. (1993). "The voltage - gated non - selective cation channel from human red cells is sensitive to acetylcholine." Biochim Biophys Acta **1147**(1): 165-167.

Bennekou, P. and P. Christophersen (1990). "The gating of human red cell Ca2(+) - activated K(+) - channels is strongly affected by the permeant cation species." Biochim Biophys Acta **1030**(1): 183-187.

Bennekou, P., L. de Franceschi, et al. (2001). "Treatment with NS3623, a novel Cl - conductance blocker, ameliorates erythrocyte dehydration in transgenic SAD mice: a possible new therapeutic approach for sickle cell disease." Blood **97**(5): 1451-1457.

Bernhardt, I. and C. Ellory (2003). Red Cell Membrane Transport in Health and Diseease. Heidelberg, Springer**:** 748.

Bookchin, R., Z. Etzion, et al. (2000). "Identification and characterization of a newly recognized population of high - Na(+), low - K(+), low - density sickle and normal red cells." Proceedings of the National Academy of Sciences of the United States of America **97**(14): 8045-8050.

Borgers, M., F. Thone, et al. (1983). "Localization of calcium in red blood cells." J. Histochem. Cytochem. **31**(9): 1109-1116.

Bouyer, G., S. Egee, et al. (2006). "Three types of spontaneously active anionic channels in malaria - infected human red blood cells." Blood Cells, Molecules, and Diseases **36**(2): 248-254.

Bouyer, G., S. Egee, et al. (2007). "Toward a unifying model of malaria - induced channel activity." Proceedings of the National Academy of Sciences **104**(26): 11044-11049.

Brain, M., C. Pihl, et al. (2004). "Evidence for a mechanosensitive calcium influx into red cells." Blood Cells, Molecules, and Diseases **32**: 349-352.

Brakemeier, S., A. Kersten, et al. (2003). "Shear stress - induced up - regulation of the intermediate - conductance Ca2(+) - activated K(+) channel in human endothelium." Cardiovasc Res **60**(3): 488-496.

Browning, J. and R. Wilkins (2003). Water permeability. Red Cell Membrane Transport in Health and Diseease. I. Bernhardt and C. Ellory. Heidelberg, Springer**:** 476-488.

Bruce, L. and M. Tanner (1999). "Erythroid band 3 variants and disease." Best Practice & Research Clinical Haematology **12**(4): 637-654.

Brugnara, C., B. Gee, et al. (1996). "Therapy with oral clotrimazole induces inhibition of the Gardos channel and reduction of erythrocyte dehydration in patients with sickle cell disease." The Journal of Clinical Investigation **97**(5): 1227-1234.

Bureau, M. and R. Banerjee (1976). "Structure - volume relationships in hemoglobin. A densitometric and dilatometric study of the oxy leads to deoxy transformation." Biochimie **58**(4): 403-407.

Cabantchik, Z. and A. Rothstein (1972). "The nature of the membrane sites controlling anion permeability of human red blood cells as determined by studies with disulfonic stilbene derivatives." J Membr Biol **10**(3): 311-330.

Cantiello, H. (2001). "Electrodiffusional ATP movement through CFTR and other ABC transporters." Pflugers Arch **443 suppl1**: S22-S27.

Cassady, G., D. Crouse, et al. (1989). "A randomized, controlled trial of very early prophylactic ligation of the ductus arteriosus in babies who weighed 1000 g or less at birth." N Engl Med **320**(23): 1511-1516.

Chien, S. (1987). "Red cell deformability and its relevance to blood flow." Annual Review of Physiology **49**(1): 177-192.

Christophersen, P. (1991). "Ca2(+) - activated K(+) channel from human erythrocyte membranes: single channel rectification and selectivity." J Membr Biol **119**(1): 75-83.

Christophersen, P. and P. Bennekou (1991). "Evidence for a voltage - gated, non - selective cation channel in the human red cell membrane." Biochim Biophys Acta **1065**(1): 103-106.

Cordero, J. and P. Romero (2002). "Caffeine activates a mechanosensitive Ca2(+) channel in human red cells." Cell Calcium **31**(5): 189-200.

Coupry, I., C. Armsby, et al. (1996). "Clotrimazole and efaroxan inhibit red cell Gardos channel independently of imidazoline I1 and I2 binding sites." European Journal of Pharmacology **295**(1): 109-112.

Dagher, G. and V. L. Lew (1988). "Maximal calcium extrusion capacity and stoichiometry of the human red cell calcium pump." J Physiol **407**(1): 569-586.

Dawson, D., S. Smith, et al. (1999). "CFTR: mechanism of anion conduction." Physiol. Rev. **79**(1): 47-75.

Decherf, G., G. Bouyer, et al. (2007). "Chloride channels in normal and cystic fibrosis human erythrocyte membrane." Blood Cells, Molecules, and Diseases **39**(1): 24-34.

Decherf, G., S. Egee, et al. (2004). "Anionic channels in malaria - infected human red blood cells." Blood Cells Mol Dis **32**(3): 366-371.

Del Carlo, B., M. Pellegrini, et al. (2003). "Modulation of Ca2(+) - activated K(+) channels of human erythrocytes by endogenous protein kinase C." Biochimica et Biophysica Acta (BBA) - Biomembranes **1612**(1): 107-116.

Denker, B., B. Smith, et al. (1988). "Identification, purification, and partial characterization of a novel Mr 28,000 integral membrane protein from erythrocytes and renal tubules." Journal of Biological Chemistry **263**(30): 15634-15642.

Desai, S., S. Bezrukov, et al. (2000). "A voltage - dependent channel involved in nutrient uptake by red blood cells infected with the malaria parasite." Nature **406**(6799): 1001-1005.

Discher, D. and N. Mohandas (1996). "Kinematics of red cell aspiration by fluorescence - imaged microdeformation." Biophysical Journal **71**(4): 1680-1694.

Drew, C., F. Lapaix, et al. (2002). "Age - dependent changes in cation transport in the chicken erythrocyte." Comp Biochem Physiol A Mol Integr Physiol **133**(1): 169.

Dunn, P. (1998). "The action of blocking agents applied to the inner face of Ca2(+) - activated K(+) channels from human erythrocytes." J Membr Biol **1998**(165): 133-143.

Duranton, C., S. Huber, et al. (2002). "Oxidation induces a Cl(-) - dependent cation conductance in human red blood cells." J Physiol **539**(Pt 3): 847-855.

Duranton, C., V. Tanneur, et al. (2008). "A high specificity and affinity interaction with serum albumin stimulates an anion conductance in malaria - infected erythrocytes." Cell Physiol Biochem **22**(5-6): 395-404.

Egee, S., F. Lapaix, et al. (2002). "A stretch - activated anion channel is up - regulated by the malaria parasite Plasmodium falciparum." J Physiol **542**(Pt 3): 795-801.

Egee, S., O. Mignen, et al. (1998). "Chloride and non - selective cation channel in unstimulated trout red blood cells." J Physiol **15**(511): 213-224.

Ellory, J., H. Robinson, et al. (2007). "Abnormal permeability pathways in human red blood cells." Blood Cells, Molecules, and Diseases **39**(1): 1-6.

Esposito, A., T. Tiffert, et al. (2008). "FRET Imaging of hemoglobin concentration in Plasmodium falciparum-infected red cells." PLoS ONE **3**(11): e3780.

Fanger, C., S. Ghanshani, et al. (1999). "Calmodulin mediates calcium - dependent activation of the intermediate conductance KCa channel, IKCa1." J Biol Chem **274**(9): 5746-5754.

Fehlau, R., R. Grygorczyk, et al. (1989). "Modulation of the Ca2(+) - or Pb2(+) - activated K(+) - selective channels in human red cells. II. Parallelisms to modulation of the activity of a membrane - bound oxidoreductase." Biochim Biophys Acta **978**(1): 37-42.

Fröhlich, O., C. Leibson, et al. (1983). "Chloride net efflux from intact erythrocytes under slippage conditions. Evidence for a positive charge on the anion binding/transport site." J Gen Physiol **81**(1): 127-152.

Fuhrmann, G., W. Schwarz, et al. (1985). "Effects of vanadate, menadione and menadione analogs on the Ca2(+) - activated K(+) channels in human red cells. Possible relations to membrane - bound oxidoreductase activity." Biochim Biophys Acta **820**(2): 223-234.

Garcia-Sancho, J. and V. Lew (1988). "Detection and separation of human red cells with different calcium contents following uniform calcium permeabilization." The Journal of Physiology **407**(1): 505-522.

Gardos, G. (1958). "The function of calcium in the potassium permeability of human erythrocytes." Biochemica et Biophysica Acta **30**: 653-654.

Ginsburg, H. (1994). "Transport pathways in the malaria - infected erythrocyte. Their characterization and their use as potential targets for chemotherapy." Biochem Pharmacol **48**(10): 1847-1856.

Ginsburg, H., M. Krugliak, et al. (1983). "New permeability pathways induced in membranes of Plasmodium falciparum infected erythrocytes." Mol Biochem Parasitol **8**(2): 177-190.

Glomski, C. and J. Tamburlin (1989). "The phylogenetic odyssey of the erythrocyte. I. Hemoglobin: the universal respiratory pigment." Histology and Histopathology **4**: 509-514.

Glomski, C. and J. Tamburlin (1990). "The phylogenetic odyssey of the erythrocyte. II. The early or invertebrate prototypes." Histology and Histopathology **5**: 513-525.

Grygorczyk, R. (1987). "Temperature dependence of Ca2(+) - activated K(+) currents in the membrane of human erythrocytes." Biochim Biophys Acta **902**(2): 159-168.

Grygorczyk, R. and W. Schwarz (1983). "Properties of the Ca2(+) - activated K(+) conductance of human red cells as revealed by the patch - clamp technique." Cell Calcium **4**(5-6): 499-510.

Grygorczyk, R. and W. Schwarz (1985). "Ca2(+) - activated K(+) permeability in human erythrocytes: modulation of single - channel events." Eur Biophys J **12**(2): 57-65.

Grygorczyk, R., W. Schwarz, et al. (1984). "Ca2(+) - activated K(+) channels in human red cells. Comparison of single - channel currents with ion fluxes." Biophys J. **45**(4): 693–698.

Hamill, O. (1981). "Potassium channel currents in human red blood cells." Physiological Society.

Hamill, O. (1983). Potassium and chloride channels in red blood cells. Single - channel recording. E. Neher and B. Sackmann. New York, Plenum Press**:** 451-471.

Hamill, O. (2006). "Twenty odd years of stretch - sensitive channels." Pflugers Arch **453**(3): 333-351.

Hamill, O., A. Marty, et al. (1981). "Improved patch - clamp techniques for high - resolution current recording from cells and cell - free membrane patches." Pflugers Arch **391**(2): 85-100.

Hardy, S., H. Goodfellow, et al. (1995). "Protein kinase C - mediated phosphorylation of the human multidrug resistance P - glycoprotein regulates cell volume - activated chloride channels." Embo J **14**(1): 68-75.

Harris, E. and B. Pressman (1967). "Obligate cation exchanges in red cells." Nature **216**(5118): 918-920.

Hoffman, J., A. Dodson, et al. (2004). "Tetrodotoxin - sensitive Na(+) channels and muscarinic and purinergic receptors identified in human erythroid progenitor cells and red blood cell ghosts." Proc Natl Acad Sci U S A **101**(33): 12370-12374.

Hoffman, J., W. Joiner, et al. (2003). "The hSK4 (KCNN4) isoform is the Ca2(+) - activated K(+) channel (Gardos channel) in human red blood cells." PNAS **100**(12): 7366-7371.

Hoffman, J. and P. Laris (1974). "Determination of membrane potentials in human and Amphiuma red blood cells by means of a fluorescent probe." The Journal of Physiology **239**(3): 519-552.

Huber, S., C. Duranton, et al. (2004). "Plasmodium induces swelling - activated ClC-2 anion channels in the host erythrocyte." J Biol Chem **279**(40): 41444-41452.

Huber, S., C. Duranton, et al. (2005). "Patch - clamp analysis of the "new permeability pathways" in malaria - infected erythrocytes." Int Rev Cytol **246**: 59-134.

Huber, S., C. Lang, et al. (2008). "Organic osmolyte channels in malaria - infected erythrocytes." Biochemical and Biophysical Research Communications **376**(3): 514-518.

Huber, S., A. Uhlemann, et al. (2002). "Plasmodium falciparum activates endogenous Cl(-) channels of human erythrocytes by membrane oxidation." Embo J **21**(1_2): 22-30.

Huber, S. M., N. Gamper, et al. (2001). Chloride conductance and volume-regulatory nonselective cation conductance in human red blood cell ghosts. Pflugers Arch. **441:** 551-558.

Huber, S. M., N. Gamper, et al. (2001). "Chloride conductance and volume-regulatory nonselective cation conductance in human red blood cell ghosts." Pflugers Arch **441**(4): 551-558.

Hunter, M. (1971). "A quantitative estimate of the non - exchange - restricted chloride permeability of the human red cell." J Physiol **218**(1): 49P-50P.

Hunter, M. (1977). "Human erythrocyte anion permeabilities measured under conditions of net charge transfer." The Journal of Physiology **268**(1): 35-49.

Jiang, H., A. Zhu, et al. (2007). "Stimulation of rat erythrocyte P2X7 receptor induces the release of epoxyeicosatrienoic acids." British Journal of Pharmacology **151**: 1033-1040.

Johnson, R. (1994). "Membrane stress increases cation permeability in red cells." Biophys J **67**(5): 1876-1881.

Johnson, R. and S. Gannon (1990). "Erythrocyte cation permeability induced by mechanical stress: a model for sickle cell cation loss." Am J Physiol **259**(5 Pt 1): C746-751.

Johnson, R. and K. Tang (1992). "Induction of a Ca2(+) - activated K(+) channel in human erythrocytes by mechanical stress." Biochim Biophys Acta **1107**(2): 314-318.

Joiner, C. H. (1993). "Cation transport and volume regulation in sickle red blood cells." Am J Physiol Cell Physiol **264**(2): C251-270.

Kaestner, L. and I. Bernhardt (2002). "Ion channels in the human red blood cell membrane: their further investigation and physiological relevance." Bioelectrochemistry **55**(1-2): 71-74.

Kaestner, L., C. Bollensdorff, et al. (1999). "Non - selective voltage - activated cation channel in the human red blood cell membrane." Biochim Biophys Acta **1417**(1): 9-15.

Kaestner, L., W. Tabellion, et al. (2004). "Prosteglandin E2 activates channel - mediated calcium entry in human erythrocytes: an indication for a blood clot formation supporting process." Thromb Haemost **92**(6): 1269-1272.

Kikuchi, Y. (1992). "Transient increase in deformability of stressed red blood cells and role of plasma proteins." The Japanese Journal of Physiology **42**(3): 431-441.

Kirk, K. (2001). "Membrane transport in the malaria-infected erythrocyte." Physiol Rev **81**(2): 495-537.

Kirk, K. and H. A. Horner (1995). Novel anion dependence of induced cation transport in malaria-infected erythrocytes. J Biol Chem. **270:** 24270-24275.

Knauf, P., F. Law, et al. (1983). "Relationship of net chloride flow across the human erythrocyte membrane to the anion exchange mechanism." J Gen Physiol **81**(1): 95-126.

Kohn, D., J. Nolta, et al. (2006). Hematopoietic stem cells. Encyclopedia of Life Science, John Wiley & Sons, Ltd: Chichester.

Lang, K., P. Lang, et al. (2005). "Mechanisms of suicidal erythrocyte death." Cell Physiol Biochem **15**(5): 195-202.

Lang, K. S., S. Myssina, et al. (2003). "Inhibition of erythrocyte cation channels and apoptosis by ethylisopropylamiloride." Naunyn Schmiedebergs Arch Pharmacol **367**(4): 391-396.

Lapaix, F., G. Bouyer, et al. (2008). "Further characterization of cation channels present in the chicken red blood cell membrane." Bioelectrochemistry **73**(2): 129-136.

Lapaix, F., S. Egee, et al. (2002). "ATP - sensitive K(+) and Ca2(+)-activated K(+) channels in lamprey (Petromyzon marinus) red blood cell membrane." Pflugers Arch **445**(1): 152-160.

Larsen, F., S. Katz, et al. (1981). "Physiological shear stress enhance the Ca2(+) permeability of human erythrocyte." Nature **294**: 667-668.

Lassen, U., L. Pape, et al. (1974). "Calcium - related hyperpolarization of the Amphiuma red cell membrane following micropuncture." J Membr Biol **18**(2): 125-144.

Lassen, U. and O. Sten-Knudsen (1968). "Direct measurements of membrane potential and membrane resistance of human red cells." The Journal of Physiology **195**(3): 681-696.

Leinders, T., R. van Kleef, et al. (1992). "Distinc metal ion binding sites on Ca2(+) - activated K(+) channels in inside - out mode patches of human erythrocytes." Biochemica et Biophysica Acta **1112**(1992): 75-82.

Leinders, T., R. van Kleef, et al. (1992). "Single Ca2(+) - activated K(+) channels in human erythrocytes: Ca2(+) dependence of opening frequency but not of open lifetimes." Biochim Biophys Acta **1112**(1): 67-74.

Lew, V. and R. Bookchin (1986). "Volume, pH, and ion - content regulation in human red cells: analysis of transient behavior with an integrated model." J Membr Biol **92**(1): 57-74.

Lew, V. and R. Bookchin (2005). "Ion transport pathology in the mechanism of sickle cell dehydration." Physiol Rev **85**(1): 179-200.

Lew, V., N. Daw, et al. (2007). "Effects of age - dependent membrane transport changes on the homeostasis of senescent human red blood cells." Blood **110**(4): 1334-1342.

Lew, V., Z. Etzion, et al. (2002). "Dehydration response of sickle cells to sickling-induced Ca2(+) permeabilization." Blood **99**(7): 2578-2585.

Lew, V., C. Freeman, et al. (1991). "A mathematical model of the volume, pH, and ion content regulation in reticulocytes. Application to the pathophysiology of sickle cell dehydration." The Journal of Clinical Investigation **87**(1): 100-112.

Lew, V., L. Macdonald, et al. (2004). "Excess haemoglobin digestion by malaria parasites: a strategy to prevent premature host cell lysis." Blood Cells Mol Dis **32**(3): 353-359.

Lew, V., S. Muallem, et al. (1982). "Properties of the Ca2(+) - activated K(+) channel in one - step inside - out vesicles from human red cell membranes." Nature **296**: 742-744.

Lew, V., J. Raftos, et al. (1995). "Generation of normal human red cell volume, hemoglobin content, and membrane area distributions by "birth" or regulation?" Blood **86**(1): 334-341.

Lew, V., T. Tiffert, et al. (2003). "Excess hemoglobin digestion and the osmotic stability of Plasmodium falciparum - infected red blood cells." Blood **101**(10): 4189-4194.

Lew, V. L. and H. Ferreira (1978). Calcium transport and the properties of a calcium - activated potassium channel in red cell membranes. Current Topics in Membranes and Transport. A. Kleizeller and F. Bronner. New York, Academic Press. **10:** 217-277.

Lew, V. L., T. Tiffert, et al. (2005). "Distribution of dehydration rates generated by maximal Gardos-channel activation in normal and sickle red blood cells." Blood **105**(1): 361-367.

Locovei, S., L. Bao, et al. (2006). "Pannexin 1 in erythrocytes: function without a gap." PNAS **103**(20): 7655-7659.

Loukopoulos, D. (2002). Heamoglobinopathies. Encyclopedia of Life and Sciences, John Wiley & Sons, Ltd: Chichester.

Low, F., M. Hampton, et al. (2008). "Peroxiredoxin 2 and peroxide metabolism in the erythrocyte." Antioxidants & Redox Signaling **10**(9): 1621-1630.

Lutz, H., S. Liu, et al. (1977). "Release of spectrin - free vesicles from human erythrocytes during ATP depletion: 1. characterization of spectrin - free vesicles." J. Cell Biol. **73**(3): 548-560.

Maher, A. and P. Kuchel (2003). "The Gardos channel: a review of the Ca2(+) - activated K(+) channel in human erythrocytes." The International Journal of Biochemistry & Cell Biology **35**(8): 1182-1197.

Mason, M., A. Simpson, et al. (2005). "The interpretation of current - clamp recordings in the cell - attached patch - clamp configuration." Biophysical Journal **88**(1): 739-750.

Mauritz, J., A. Esposito, et al. (2009). "The homeostasis of *Plasmodium falciparum* - infected red blood cells." PLoS Comput Biol **5**(4): e1000339.

McGoron, A., C. Joiner, et al. (2000). "Dehydration of mature and immature sickle red blood cells during fast oxygenation/deoxygenation cycles: role of KCl cotransport and extracellular calcium." Blood **95**(6): 2164-2168.

Merckx, A., G. Bouyer, et al. (2009). "Anion channels in Plasmodium - falciparum - infected erythrocytes and protein kinase A." Trends in Parasitology **25**(3): 139-144.

Merckx, A., M.-P. Nivez, et al. (2008). "Plasmodium falciparum regulatory subunit of cAMP - dependent PKA and anion channel conductance." PLoS Pathogens **4**(2): e19.

Mignen, O., S. Egee, et al. (2000). "Basolateral outward rectifier chloride channel in isolated crypts of mouse colon." Am J Physiol Gastrointest Liver Physiol **279**(2): G277-287.

Ney, P., M. Christopher, et al. (1990). "Synergistic effects of oxidation and deformation on erythrocyte monovalent cation leak." Blood **75**(5): 1192-1198.

Oyewole, O., S. Malomo, et al. (2008). "Comperative studies on antisickling properties of thiocyanate, tellurite and hydroxyurea." Pak J Med Sci **24**(1): 18-22.

Parker, J. (1983). "Hemolytic action of potassium salts on dog red blood cells." Am J Physiol **244**(5): C313-317.

Pellegrino, M. and M. Pellegrini (1998). "Modulation of Ca2(+) - activated K(+) channels of human erythrocytes by endogenous cAMP - dependent protein kinase." Pflugers Arch **436**(5): 749-756.

Pellegrino, M., M. Pellegrini, et al. (1998). "Properties of Ca2(+) - activated K(+) channels in erythrocytes from patients with myotonic muscular dystrophy." Muscle Nerve **21**(11): 1465-1472.

Ponder, E. (1948). Hemolysis and related phenomena. New York, Grune & Stratton.

Raftos, J., R. Bookchin, et al. (1996). "Distribution of chloride permeabilities in normal human red cells." J Physiol **491**(Pt_3): 773-777.

Ribeiro, M., N. Alloisio, et al. (2000). "Severe hereditary spherocytosis and distal renal tubular acidosis associated with the total absence of band 3." Blood **96**(4): 1602-1604.

Rodighiero, S., A. De Simoni, et al. (2004). "The voltage - dependent nonselective cation current in human red blood cells studied by means of whole - cell and nystatin - perforated patch - clamp techniques." Biochem Biophys Acta **1660**(1-2): 164-170.

Romero, P. and L. Rojas (1992). "The effect of ATP on Ca2(+) - dependent K(+) channels of human red cells." Acta Cient Venez **43**(1): 19-25.

Scarpa, A., A. Cecchetto, et al. (1970). "The mechanism of anion translocation and pH equilibration in erythrocytes." Biochem Biophys Acta **219**(1): 179-188.

Schillers, H. (2008). "Imaging CFTR in its native environment." Pflügers Archiv European Journal of Physiology **456**(1): 163-177.

Schmid-Schönbein, H. and P. Gaehtgens (1981). "What is red cell deformability?" Scan J Clin Lab Invest **41**(156): 13-26.

Schmidt-Schonbein, H. and R. Wells (1969). "Fluid drop - like transition of erythrocytes under shear." Science **165**(890): 288-291.

Schwarz, W., R. Grygorczyk, et al. (1989). Recording single - channel currents from human red cells. Biomembranes Part T. S. F. a. B. Fleischer, Academic Press**:** 112-121.

Schwarz, W., H. Keim, et al. (1989). "Modulation of the Ca2(+) - or Pb2(+) - activated K(+) - selective channels in human red cells. I. Effects of propranolol." Biochim Biophys Acta **978**(1): 32-36.

Schwarz, W. and H. Passow (1983). "Ca2(+) - activated K(+) channels in erythrocytes and excitable cells." Annu Rev Physiol **45**: 359-374.

Schwiebert, E., D. Benos, et al. (1999). "CFTR is a conductance regulator as well as a chloride channel." Physiol Rev **79**(1 Suppl): S145-166.

Scott, R. (1966). "Comparative hematology: the phylogeny of the erythrocyte." Blut **XII**: 340-351.

Shields, M., R. Grygorczyk, et al. (1985). "Lead - induced activation and inhibition of potassium - selective channels in the human red blood cell." Biochim Biophys Acta **815**(2): 2232-2232.

Shindo, M., Y. Imai, et al. (2000). "A novel type of ATP block on a Ca2(+) - activated K(+) channel from bullfrog erythrocytes." Biophys J **79**(1): 287-297.

Skalak, R. and P. Branemark (1969). "Deformation of red blood cells in capillaries." Science **164**(2): 717-719.

Smith, B. and P. Agre (1991). "Erythrocyte Mr 28,000 transmembrane protein exists as a multisubunit oligomer similar to channel proteins." Journal of Biological Chemistry **266**(10): 6407-6415.

Southgate, C., A. Chisht, et al. (1996). "Targeted disruption of the murine erythroid band 3 gene results in spherocytosis and severe haemolytic anaemia despite a normal membrane skeleton." Nat Genet **14**(2): 227-230.

Sprague, R., M. Ellsworth, et al. (1998). "Deformation - induced ATP release from red blood cells requires CFTR activity." Am J Physiol **275**(5 Pt 2): H1726-H1732.

Sprague, R., M. Ellsworth, et al. (2001). "Participation of cAMP in a signal - transduction pathway relating erythrocyte deformation to ATP release." Am J Physiol Cell Physiol **281**(4): C1158-1164.

Staines, H. M., T. Powell, et al. (2003). "Modulation of whole-cell currents in Plasmodium falciparum-infected human red blood cells by holding potential and serum." J Physiol **552**(Pt 1): 177-183.

Stampe, P. and B. Vestergaard-Bogind (1985). "The Ca2(+) - sensitive K(+) - conductance of the human red cell membrane is strongly dependent on cellular pH." Biochim Biophys Acta **815**(2): 313-321.

Strobaek, D., L. Teuber, et al. (2004). "Activation of human IK and SK Ca2(+) - activated K(+) channels by NS309 (6,7 - dichloro - 1H - indole - 2,3 - dione 3 - oxime)." Biochimica et Biophysica Acta (BBA) - Biomembranes **1665**(1-2): 1-5.

Svetina, S. (1982). "Relations among variations in human red cell volume, density, membrane area, hemoglobin content and cation content." Journal of Theoretical Biology **95**(1): 123-134.

Svetina, S., D. Kuzman, et al. (2004). "The cooperative role of membrane skeleton and bilayer in the mechanical behaviour of red blood cells." Bioelectrochemistry **62**(2): 107-113.

Tharp, D. and D. Bowles (2009). "The intermediate - conductance Ca2(+) - activated K(+) channel (KCa3.1) in vascular disease." Cardiovascular & Hematological Agents in Medicinal Chemistry **7**(1): 1-11.

Thomas, S. and S. Egee (1998). "Fish red blood cells: characteristics and physiological role of the membrane ion transporters." Comp Biochem Physiol A Mol Integr Physiol **119**(1): 79-86.

Thomas, S. and V. Lew (2004). "Plasmodium falciparum and the permeation pathway of the host red blood cell." Trends Parasitol **20**(3): 122-125.

Tiffert, T., N. Daw, et al. (2001). "A fast and simple screening test to search for specific inhibitors of the plasma membrane calcium pump." J Lab Clin Med **137**(3): 199-207.

Tiffert, T., V. Lew, et al. (2005). "The hydration state of human red blood cells and their susceptibility to invasion by Plasmodium falciparum." Blood **105**(12): 4853-4860.

Tosteson, D. and J. Hoffman (1960). "Regulation of cell volume by active cation transport in high and low potassium sheep red cells." J Gen Physiol **44**: 169-194.

van Bavel, E. (2003). "Shear stress and intermediate - conductance calcium - activated potassium channels." Cardiovasc Res **60**(3): 457-459.

Vandorpe, D., B. Shmukler, et al. (1998). "cDNA cloning and functional characterization of the mouse Ca2(+) - gated K(+) channel, mIK1." Journal of Biological Chemistry **273**(34): 21542-21553.

Varecka, L. and E. Peterajová (1990). "Activation of red cell Ca2(+) - activated K(+) channel by Ca2(+) involves a temperature - dependent step." FEBS Letters **276**(1-2): 169-171.

Verloo, P., C. Kocken, et al. (2004). "Plasmodium falciparum - activated chloride channels are defective in erythrocytes from cystic fibrosis patients." J Biol Chem **279**(11): 10316-10322.

Wiley, J. and K. McCulloch (1982). "Calcium ions, drug action and the red cell membrane." Pharmacology & Therapeutics **18**: 271-292.

Wolosin, J., H. Ginsburg, et al. (1977). "Functional characterization of anion transport system isolated from human erythrocyte membranes." J. Biol. Chem. **252**(7): 2419-2427.

VU :

Le Directeur de Thèse
Serge THOMAS

VU :

Le Responsable de l'École Doctorale
Yvan LAGADEUC

VU pour autorisation de soutenance
Rennes, le

Le Président de l'Université de Rennes 1

Guy CATHELINEAU

VU après soutenance pour autorisation de publication :
Le Président de Jury,

”**Dynamiczne zachowanie kanałów jonowych w błonie czerwonych komórek krwi”.**

Erytrocyty są najczęściej wykorzystywanymi komórkami do badań nad transportem błonowym. Jednakże po dzień dzisiejszy struktura molekularna oraz fizjologiczna rola kanałów jonowych w błonie czerwonych komórek krwi (RBCs) nie jest jednoznacznie określona.

W niniejszej pracy, przy pomocy techniki patch clampu oraz badań biofizycznych, zostały rozpatrzone następujące zagadnienia z zakresu fizjologii RBCs: 1/ objętość komórki a jej podatność osmotyczna; 2/ czynniki aktywujące kanały jonowe i 3/ opis (charakterystyka elektrofizjologiczna oraz molekularna) kanałów anionowych.

1/ Zbadano czy korelacja pomiędzy wrażliwością osmotyczną a objętością komórki obowiązuje również dla izoosmotyczne odwodnionych erytrocytów i czy oczekiwany powrót to początkowego stanu uwodnienia jest wynikiem aktywacji kanałów jonowych. Wyniki badań okazały się być w opozycji do powszechnie obowiązującej wiedzy. Jednakże interesującym jest, że wzrost wrażliwości osmotycznej nie jest wynikiem napływu wody do komórki, a jest ścisle związany ze wzrostem stężenia wewnątrzkomórkowego wapnia.

2/ Elektrofizjologiczne wyniki doświadczeń wykazały, iż deformacja błony, która ma miejsce podczas tworzenia się seala w technice patch clamp, aktywuje kanały potasowe wapniowo zależne i że to zjawisko zachodzi jedynie poprzez (skończony) wpływ Ca^{2+} do komórki. Równocześnie zauważono, że aktywacji kanałów Gardosa towarzyszy aktywacja kanałów anionowych.

3/ Kanały anionowe dotychczas opisane w zdrowych ludzkich RBCs, jak również w tych zakażonych malarią, wydają się odpowiadać jednemu maxi kanałowi anionowemu, którego zachowanie (kinetyka, bramkowanie i konduktacja) zależy od warunków eksperymentu.

Słowa kluczowe: erytrocyt, kanały jonowe, oporność osmotyczna, elektrofizjologia, technika patch clamp

„Dynamical behaviour of human red blood cell ionic channels."

Erythrocytes are one of the most frequently cellular models used so far to decipher the physiology of membrane transport. However, if pumps, antiporters and cotransporters are now well defined, the molecular identity and the physiological role of the conductive pathways present in the membrane of blood cell (RBC) is still elusive albeit the growing evidences of their role in physiological and pathological conditions.

The present work, using the patch clamp technique and biophysical studies, show that:

1) The changes in osmotic fragility observed after Gardos channel dependent dehydration is mainly not due to rehydration of the cell via membrane transporters but rather due to change in membrane properties elicited by the Ca^{2+} loading and must reflect a specific calcium-induced lytic vulnerability of the membrane causing rupture before the cells attain their maximal spherical volumes.

2) The Gardos channel can be transiently activated when seal formation induces membrane deformation. This phenomenon can result only from activation of a permeability pathway with a finite Ca^{2+} conductance. This transient activity generates secondary transient anionic channel activity that has been studied further.

3) The diversity of anionic channel activities recorded in normal human RBCs, as well as in P. falciparum-infected RBCs, corresponds to different kinetic modalities of a unique type of maxi anion channel with multiple conductance levels, gating properties and pharmacology.

Finally, the present work contributes to the understanding of the role of ion channels in RBCs and opens questions on the contribution of ion channel in the rheological properties of RBCs.

Keywords: erythrocyte, ionic channels, osmotic fragility, patch clamp

« Etude du comportement dynamique des canaux ioniques de la membrane du globule rouge humain. »

Les érythrocytes sont un des modèles pour l'étude des voies de transport membranaire. Si les pompes, les antiports et les cotransports sont bien définies, l'identité moléculaire et le rôle physiologique des voies de conductances du globule rouge restent méconnus. Le présent travail réalisé à l'aide des techniques de patch-clamp montre que :

1) Les changements de fragilité osmotique observés lors d'une déhydratation des cellules après stimulation du canal Gardos, ne sont pas dus à une réhydration des cellules *via* l'activation de transporteurs, mais à des changements de propriétés de la membrane liées à l'augmentation du $[Ca^{2+}]_i$. Elle reflète une vulnérabilité spécifique de la membrane au Ca^{2+}, induisant la rupture de la membrane avant que la cellule n'ait atteint son volume critique.

2) Le canal Gardos peut-être activé transitoirement lors d'épisode de déformation de la membrane. Ce phénomène ne peut-être que le résultat de l'activation d'une voie de perméabilité au Ca^{2+} ayant une conductance déterminée.

3) L'activité transitoire du canal Gardos active secondairement une voie de conductance anionique. La diversité des canaux anioniques précédemment décrites dans la membrane des érythrocytes humains correspond à l'activité d'un unique canal anionique de type maxi-chlorure ayant des modalités d'activation et de fonctionnement (état d'ouverture multiple, cinétique, pharmacologie…) différentes en fonction des conditions expérimentales.

Ce travail contribue à une meilleure compréhension des canaux ioniques présents dans la membrane du globule rouge et permet d'envisager la participation de ces canaux dans la régulation des propriétés rhéologiques des globules rouges.

Mots clés: érythrocyte, canaux ioniques, fragilité osmotique, patch-clamp